Modeling the Hydrologic Performance of Bioretention and Permeable Pavement Stormwater Controls in Northern Ohio using DRAINMOD: Calibration, Validation, Sensitivity Analysis, and Future Climate Scenarios

Prepared for:

Chagrin River Watershed Partners, Inc. under NOAA award No. NA09NOS4190153

Prepared by:

Alessandra P. Smolek, PhD Student, Biological & Agricultural Engineering, North Carolina State University*

Ryan J. Winston, PhD Candidate, P.E., Biological & Agricultural Engineering, North Carolina State University*

Jay D. Dorsey, PhD, P.E., Water Resources Engineer, Ohio Department of Natural Resources, Division of Soil and Water Resources

William F. Hunt, PhD, P.E., William Neal Reynolds Professor, Extension Specialist, and University Faculty Scholar, Biological & Agricultural Engineering, North Carolina State University

*These authors contributed equally to this work

June 30, 2015

This material is based upon work supported by the University of New Hampshire under Cooperative Agreement No. NA09NOS4190153 (CFDA No. 11.419) from the National Oceanic and Atmospheric Association. Financial assistance was also provided under award number DNRFP038 from the National Oceanic and Atmospheric Administration, U.S. Department of Commerce through the Old Woman Creek National Estuarine Research Reserve, administered by the Ohio Department of Natural Resources, Division of Wildlife. The Old Woman Creek National Estuarine Research Reserve is part of the National Estuarine Research Reserve System, (NERRS), established by Section 315 of the Coastal Zone Management Act, as amended. Additional information about the system can be obtained from the Estuarine Reserves Division, Office of Ocean and Coastal Resource Management, National Oceanic and Atmospheric Administration, US Department of Commerce, 1305 East West Highway – N/ORM5, Silver Spring, MD 20910.Any opinions, findings, and conclusions or recommendations expressed in this publication are those of the author(s) and do not necessarily reflect the views of the University of New Hampshire or the National Oceanic and Atmospheric Association.

This work was completed as part of a NERRS Science Collaborative project led by Old Woman Creek NERR, Chagrin River Watershed Partners, Inc., Ohio Department of Natural Resources- Division of Soil and Water Resources, North Carolina State University, Erie Soil and Water Conservation District, and Consensus Building Institute. The "Implementing Credits and Incentives for Innovative Stormwater Management" project promoted the implementation of low impact development (LID) stormwater control measures (SCMs) that reduce the impacts of stormwater runoff on Ohio's coastal communities and Lake Erie and worked to improve state and local stormwater policies. A Collaborative Learning Group of municipal and consulting engineers, stormwater utilities, and regulators provided feedback on this project.

TABLE OF CONTENTS

FIGURES

TABLES

LIST OF ACRONYMS

ASTM – American Society for Testing and Materials
BRC – bioretention cell
ET - evapotranspiration
HA – Holden Arboretum
HLR – hydraulic loading ratio
HSG – Hydrologic Soil Group
IWS – internal water storage
PC – pervious concrete
PICP – permeable interlocking concrete pavement
PP – permeable pavement
PT – Perkins Township
RCP – Representative Concentration Pathway
SCM – stormwater control measure
SWMM – Storm Water Management Model
UC – Ursuline College
USEPA – United States Environmental Protection Agency
TMDL – Total Maximum Daily Load
WH – Willoughby Hills

1 EXECUTIVE SUMMARY

Engineers and regulators in Ohio are currently limited to a “one size fits all” approach for the design of permeable pavements and bioretention cells. To propagate a more flexible design and crediting mechanism for these systems, long-term models are needed to simulate the hydrologic performance of bioretention and permeable pavement stormwater control measures (SCMs) under varying design parameters. In this work, DRAINMOD, a widely accepted agricultural drainage and water balance model, was adapted for use in modeling urban stormwater practices. The model was calibrated and validated against field-collected hydrologic data from three bioretention cells and three permeable pavement applications in northern Ohio.

The measured and modeled results for both SCMs were in good to excellent agreement during the calibration and validation periods; Nash-Sutcliffe efficiencies for runoff, drainage, overflow and exfiltration/evapotranspiration commonly exceeded 0.80, suggesting excellent model agreement. Over the course of data collection, the difference between the modeled and monitored percentage of drainage, overflow, and exfiltration/evapotranspiration was within 3% for the bioretention cells and 4% for the permeable pavements, suggesting that DRAINMOD could be applied as a tool for analysis of long-term bioretention and permeable pavement hydrology.

Sensitivity analyses were conducted in DRAINMOD by singularly modifying design parameters including hydraulic loading ratio (HLR), internal water storage (IWS) zone depth, media/aggregate depth, underlying soil infiltration rate, *et cetera*. Both SCMs were most sensitive to HLR and IWS zone depth, with wide variations in performance dependent on underlying soil type; the models were less sensitive to other parameters. The results from the sensitivity analyses could be used to create a “sliding scale” crediting system for both

bioretention cells and permeable pavements in Ohio based on the fractions of treated drainage and volume reduction through exfiltration and ET.

Rainfall and temperature data derived from dynamically downscaled future climate data were used in DRAINMOD to assess the change in hydrologic performance from existing (2001-2004) and future (2055-2059) climate scenarios for northern Ohio. Generally, future climate scenarios suggested lower annual average rainfall depths, longer dry periods, and hotter temperatures for northern Ohio. Compared to existing climate scenarios, the volume reductions provided by the SCMs changed from current conditions by a -7% to 8% range under future climate conditions. In most cases, however, the fraction of untreated overflow did increase under climate change scenarios. Results from this future climate analysis suggest that current designs may need to be only marginally modified to be resilient to climate change along the Ohio Lake Erie shoreline.

KEYWORDS

Bioretention, permeable pavement, urban stormwater, modeling, DRAINMOD, hydrology, long-term, simulation, climate change

2 DRAINMOD MODEL DESCRIPTION

2.1 Background and Introduction

2.1.1 Modeling Bioretention in DRAINMOD

Increased land development augments the rate and volume of stormwater runoff during wet-weather events, which is one of the major causes for impairment of surface waters in the U.S. (USEPA 2007). Increased runoff leads to stream channel incision, loss of habitat and real estate, and increased pollutant transport (Wang et al. 2001; Dietz and Clausen 2008). To mitigate these deleterious impacts, pre-development rate, volume, and duration of flow are mimicked to the maximum extent practicable using Low Impact Development strategies (Page et al. 2015). Chief in the LID strategy are infiltration-based stormwater control measures (SCMs), which augment groundwater recharge and spur evaporation and transpiration (DeBusk et al. 2010; Denich and Bradford 2010). Two such SCMs, bioretention and permeable pavement, aid in restoration of the natural hydrology of a site and reduce the negative effects caused from increased impervious areas in urbanized watersheds (Hunt et al. 2012; Wardynski et al. 2012). These are two of the most commonly-used and effective LID practices.

Intensive research and installation experience have assisted in the evolution of bioretention design recommendations (Hunt et al. 2012). A large variation in hydrologic performance exists based on a number of design characteristics, the underlying soils, the local climate, and the vegetation present in the SCM (Hunt et al. 2006; Bratieres et al. 2008; Hunt et al. 2008; Davis 2008; Passeport et al. 2009; Hatt et al. 2009; Li et al. 2009; Brown and Hunt 2011a; Luell et al. 2011). Deeper media depth increased exfiltration and reduced outflow volume and frequency (Li et al. 2009; Brown and Hunt 2011a). Also, as the ratio of bioretention surface area to drainage area increased, outflow volume was reduced (Hatt et al. 2009; Jones and Hunt 2009).

Bioretention cells located over sandy soils exfiltrated a greater fraction of the water balance when compared to those located over tighter clay soils (Brown and Hunt 2011a, 2011b; Passeport et al. 2009). Much previous research exists on the effects of the internal water storage (IWS) design feature, which promotes denitrification and provides greater pollutant load mitigation through enhanced exfiltration in both sandy and clayey soils (Dietz and Clausen 2006; Hunt et al. 2008; Brown and Hunt 2011b; Li et al. 2009; Passeport et al. 2009; Winston et al. 2015). While significant field research has been undertaken on bioretention, it is difficult to determine volume reduction and pollutant load reduction without modeling various design configurations, underlying soil types, and climatic factors that influence SCM performance (Brown et al. 2013).

The water balance for a bioretention cell can perhaps be best evaluated using a long-term model calibrated to field-collected data. One such model is DRAINMOD, a long term, continuous simulation drainage model first developed in the 1970s at North Carolina State University. DRAINMOD is typically used to simulate water movement in parallel tile or ditch-drained agricultural fields. It has been used to model controlled drainage, subirrigation, wetland hydrology, nitrogen dynamics and losses from drained soils, impacts of drainage system and irrigation management on soil salinity in irrigated arid soils, on-site wastewater treatment, forest hydrology, and other applications (Skaggs 1978, 1982, 1999; Youssef et al. 2005). Bioretention and permeable pavement modeling are two of its latest applications (Brown et al. 2013).

A model is needed to predict long-term bioretention hydrology so that predictions of bioretention function under various design scenarios can be made with greater confidence. Instead of the current “one-size-fits-all” technique used across the country, crediting of under- and over-sized bioretention cells (relative to the current sizing guidance in Ohio – filter bed area should be at minimum 5% of the impervious drainage area; ODNR 2006) could be underpinned by a sensitivity analysis performed using calibrated models. Two drivers for developing flexible design and crediting mechanisms are: (1) retrofits often must be undersized due to the constraints of the site, and (2) hydrologic performance of bioretention systems vary widely, based mainly on underlying soil type, presence or absence of an IWS zone, hydraulic loading, and bowl storage depth.

Long-term models calculate the water balance using rainfall and temperature (as well as bioretention design characteristics) to parameterize the model. Groundwater recharge (exfiltration), treated outflow (drainage), untreated bypass (overflow), and volume reduction through exfiltration and evapotranspiration (ET) can be enumerated using this type of model. The water balance also allows for estimation of pollutant loads to meet Total Maximum Daily Load (TMDL) requirements. Finally, the long-term volume mitigation can be used to estimate whether a site meets the pre-development hydrologic condition.

No widely accepted long-term model exists for bioretention. Currently available bioretention models either: (1) are single-storm models, (2) use unsubstantiated estimation methodologies to calculate drainage, (3) do not account for the variations in the volumetric water content in the media, and/or (4) cannot model the IWS configuration.

Initial modeling studies of bioretention systems were bioinfiltration devices (i.e. no underdrain), simplifying the modeling substantially (Brander et al. 2004; Dussaillant et al. 2004, 2005; Heasom et al. 2006). Brander et al. (2004) and Heasom et al. (2006) used single-event models to predict overflow from bioinfiltration systems during design events; the drawback of these models is that they do not account for antecedent soil moisture conditions, which could cause over- or under-estimation of system performance. Single-event models assume the bioretention cell is dry prior to the start of the storm, which rarely happens in reality; long-term models are better able to predict the variability in performance under the varying soil moisture conditions that occur under real world conditions.

Dussaillant et al. (2004) developed a long-term, continuous simulation, numerical model that was based on the mixed formulation of the one-dimensional Richards equation (RECHARGE). Dussaillant et al. (2005) also created a simplified numerical model, RECARGA, based on the Green-Ampt infiltration equation; it compared well against the more complex RECHARGE model. At the time, neither modeled underdrain flow. The newest version of RECARGA (V2.3) models underdrain flow using the orifice equation, which may not represent drain flow properly.

He and Davis (2011) recently developed a two-dimensional variable saturated flow model based on the Richards equation; it could model a variety of bioretention input parameters, but it is a single-event model, and only was able to evaluate one or two underdrains. Palhegyi (2010) developed a computational bioretention hydrology model based on the soil moisture calculation procedure in Hydrologic Engineering Center Hydrologic Modeling System (HEC-HMS) (USACE 2000). It calculates water movement through the soil due to ET, exfiltration, and drainage until the water content recedes to field capacity. Between field capacity and the wilting point, the model predicts ET is the only potential hydrologic fate. Underdrain flow is modeled using Bernoulli’s equation. The model was calibrated to a biofiltration cell in Villanova, PA; however, its ability to model drainage was not evaluated. Lucas (2010) modeled a bioretention planter system for a design storm using HydroCAD and for continuous data using SWMM 5.0.014. Both models used orifice control to throttle inflow to the media and Darcy’s Law to model flow under saturated conditions. Neither model was calibrated to field-collected data, but both gave similar results for design storm event model runs.

Storm Water Management Model (SWMM) 5.0, Windows-based Source Loading and Management Model (WinSLAMM) 9.4, and Model for Urban Stormwater Improvement Conceptualism (MUSIC) 3.1 can be used to model bioretention hydrology under continuous, long-term simulations. However, the methodology of the models for soil water movement and flow to the drains are not state-of-the-science. DRAINMOD calculates drainage rates as a function of soil properties and drainage configuration based on field-verified agricultural drainage principles. The previously described bioretention models either calculate water storage capacity as the difference between total porosity and field capacity or use a void ratio of the media. In reality, water table depth affects the water storage in the media profile.

DRAINMOD requires inputs for the soil-water characteristic curve and related functions to account for the variation in volumetric water content as a function of water table depth, providing an accurate representation of the water present in the media. Using field capacity to calculate the amount of water stored in the profile is scientifically valid only when the water table is far from the soil surface (Smith and Warwick 2007); however, in bioretention systems, the water table can be at the soil surface during large events. As an example, the volume of water drained based on the water table depth in the media was calculated per the soil-water characteristic curve and by subtracting the field capacity (volumetric water content at a suction of -3 ft) from the saturated volumetric water content (Table 1). Results are given for three examples of bioretention media from Ohio subsequently used in the calibration of DRAINMOD. All three examples of bioretention media met the Ohio filter media specifications for particle size distribution and organic matter content (ODNR 2006). Table 1 shows that the largest errors occur when the water table is closest to the surface, with greater than 3000% error when the water table is at a 0.3 ft depth. The Ursuline media had a higher fraction of organic matter than the Holden Arboretum media, so it held more water in the media at larger suctions (Winston et al. 2015). The percent error in volume drained was calculated to compare the use of the soil water characteristics versus the difference between saturation and field capacity (Table 1). For a bioretention cell with a water table 2 ft below the soil surface, the error associated with neglecting the soil water characteristic curve was at minimum 101 percent. This is an inherent error in most models for bioretention and permeable pavement, which have shallow water tables during and following runoff events. This concept is especially important for modeling bioretention cells employing an IWS zone because the water level may remain within the profile for the entire inter-event period. An illustration of this concept is presented in Figure 1.

Table 1. Comparison of calculating volume of water drained from media based on water level distance from soil surface by using soil-water characteristic curve versus subtracting field capacity from saturated volumetric water content.

Water level distance from soil surface (ft)	Volume drained: soil water characteristic curve (ft^3/ft^2)			Volume drained: saturation minus field capacity (ft^3/ft^2)			Percent difference (%)		
	Ursuline media (ft)	Holden North media (ft)	Holden South media (ft)	Ursuline media (ft)	Holden North media (ft)	Holden South media (ft)	Ursuline media	Holden North media	Holden South media
0.3	0.001	0.002	0.002	0.043	0.071	0.083	-3304	-3390	-5400
1	0.035	0.051	0.046	0.128	0.212	0.249	-268	-319	-447
2	0.127	0.189	0.198	0.256	0.424	0.498	-101	-125	-151
3	0.316	0.389	0.430	0.384	0.637	0.747	-21	-64	-74

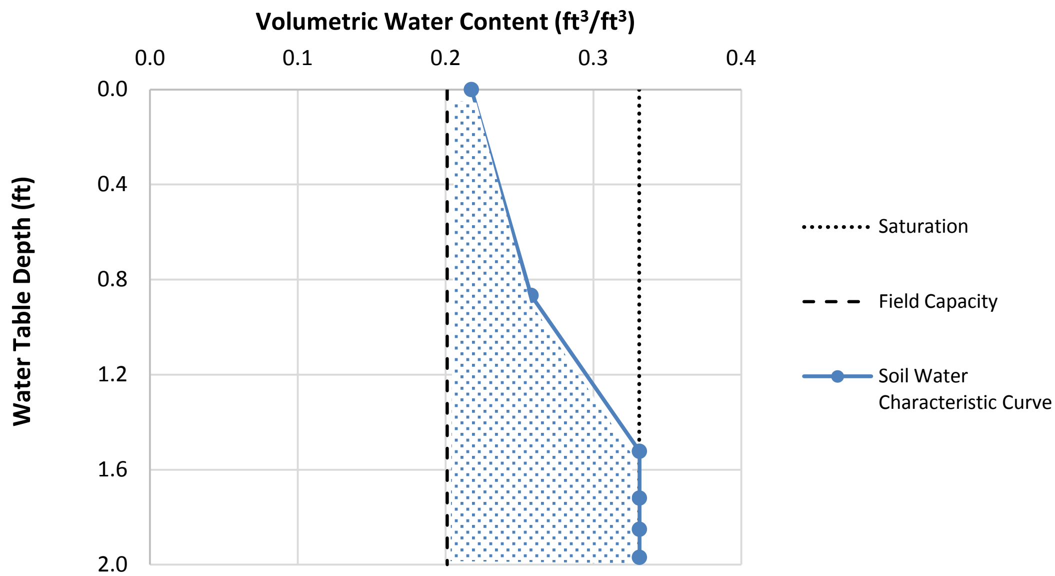

Figure 1. Volumetric water content present in profile for the Ursuline media when the water table depth is 2 ft., using a soil-water characteristic (solid line) and field capacity (long dashes) methods. The hatched area is the difference in volume drained between the two methods.

With the large variation in hydrologic performance from bioretention cells, a continuous, long-term model such as DRAINMOD can be used to evaluate the performance of the many possible design configurations. A calibrated and validated DRAINMOD model can be used to conduct a sensitivity analysis to predict performance of design configurations that have not been field-tested and help identify best design methodologies for fill media depth, fill media composition, ponding depth, and underdrain configuration across Ohio's poorly draining hydrologic soil group (HSG) C and D soils (Davis et al. 2009; Hunt et al. 2012). Since DRAINMOD can accept long-term data sets, it also can be used to evaluate the performance of these stormwater control measures (SCMs) under future-climate projections (Hathaway et al. 2014). All these applications will help the engineering community to move away from a "one-size-fits-all" bioretention design.

2.1.2 Modeling Permeable Pavement in DRAINMOD

Permeable pavement is another widely implemented SCM. Design variables that affect the hydrologic performance of permeable pavement include surface infiltration rate, aggregate depth, native soil type, contributing watershed area and drainage configuration. When permeable pavements are well-maintained (and therefore retain high surface infiltration rates), studies have shown they consistently reduce surface runoff by more than 99% compared to traditional asphalt (i.e. all rainfall infiltrates the pavement surface; Bean et al. 2007b; Booth and Leavitt 1999; Collins et al. 2008; Fassman and Blackbourn 2010). Similar to bioretention, runoff volume reduction via exfiltration to the subsoil is largely dependent upon the infiltration capacity of the native soil. Permeable pavements implemented over Hydrologic Soil Group (HSG) A and B soils have produced runoff volume reductions of over 50% (Bean et al. 2007b; Dreelin et al. 2006; Wardynski et al. 2012); permeable pavements constructed over HSG C and D soils exhibit lower volume reductions, with reported runoff volume reductions from 3-43% from a conventionally-drained practice (Collins et al. 2008; Drake et al. 2013, Roseen et al. 2012, Fassman and Blackbourn 2010). The drainage configuration [presence/lack of an underdrain, or inclusion of internal water storage (IWS)] also affects the hydrologic performance of a permeable pavement. Inclusion of an IWS zone via an elevated or upturned underdrain increased volume reduction by 23% compared to a conventionally drained system; deeper IWS zones tend to augment exfiltration (Wardynski et al. 2012). Winston et al. (2015) reported volume reductions ranging from 13-47% for three permeable pavements with 6 inches of IWS; without IWS, volume reduction would have been minimal due to the underlying HSG D soils (Winston et al. 2015).

Given the site-by-site variability of hydrologic performance among practices and the lack of funds to field-test every design configuration, a long-term hydrologic model is needed to better understand the influence of these design variations on the annual hydrologic performance of permeable pavements. Current permeable pavement design standards in Ohio limit the ratio of impervious watershed area to permeable pavement area to 2:1, and do not provide guidance on the inclusion of an IWS zone (ODNR 2006). Results from a field-calibrated, long-term model could be used to develop a more flexible design and crediting mechanism that incorporates design variations beyond the current "one-size-fits-all" approach. Additionally, retrofits often must be constructed within the constraints of the existing site; therefore, designs may deviate from the current design guidance. Understanding the expected performance of retrofitted systems is another driver for development of a long-term permeable pavement model specific to Ohio.

Past research has shown DRAINMOD can be calibrated to accurately predict the hydrology of bioretention cells with and without IWS zones (Brown et al. 2013). Given that bioretention and permeable pavement employ infiltration and drainage as primary hydrologic mechanisms, it is hypothesized DRAINMOD also could be calibrated to predict the water balance for permeable pavement.

Currently, no widely implemented model exists for permeable pavement. Permeable pavement models presently available either: (1) are unable to run continuous simulations, (2) do not accurately model underdrain flow, (3) do not properly account for evaporation within the aggregate profile, or (4) are unable to model an internal water storage zone.

Many of the models applied to permeable pavements are broad, infiltration-based models that do not include underdrains (Brander et al. 2004, Browne et al. 2008, Lee et al. 2015, Martin and Kaye 2015, Schlüter et al. 2007). Exfiltration from a storage-based infiltration system is best analyzed with Richards' equation (Richards 1931), but the complexity and lengthy run time associated with soil moisture flow models developed based on Richards' equation (e.g.

HYDRUS; SEEP/W; Thomson 1990; Browne et al. 2008) have limited their widespread application in stormwater design.

Simplified models based on Darcy's law (Darcy 1856) or the Green-Ampt infiltration equation (Green and Ampt 1911) have demonstrated success in modeling exfiltration when developed for both 1D-vertical (Braga et al. 2007; Schlüter et al. 2007) and 2D-vertical and horizontal flow (Emerson et al. 2010; Lee et al. 2015). However, of these models, Lee et al. (2015) is the only one to calibrate to field-collected hydrologic data for a permeable pavement; all other models were typically developed for infiltration basins, infiltration trenches, or bioinfiltration devices. Lee and colleagues (2015) developed a continuous unit process model which could simulate infiltration through the permeable pavement, vertical and horizontal exfiltration from the subbase, and clogging impacts at the pavement surface and interface with the underlying soil. While the model was calibrated to a field data with high accuracy, it lacked the capability to model an underdrain. Martin and Kaye (2015) created a p model to predict the initial abstraction from permeable pavement, but it was also developed for undrained systems and was not calibrated. Given most of Ohio has poorly-draining soils that require the use of underdrains, the aforementioned models are not representative of the typical permeable pavement design in Ohio.

Few modeling efforts specific to underdrained permeable pavement systems exist. Schluter and Jefferies (2002) field-calibrated the hydrologic model Erwin 3.0 (AWS 1998) to predict outflow from permeable pavements with underdrains, but it did not predict the full hydrologic balance (e.g., exfiltration and evaporation). More recently, Zhang and Guo (2014) developed an analytical equation to predict long-term average runoff volume reductions of permeable pavements both with and without underdrains. While the analytical equation produced average runoff volume reductions in good agreement with results from the continuous simulation of the permeable pavement LID module in Storm Water Management Model (SWMM) 5.0, none of the simulations were calibrated to field-collected data. Additionally, the model did not consider evaporation from the permeable pavement, which has been measured to be 16% higher than evaporation from traditional asphalt (Starke et al. 2010), and up to 8% of the water balance from a lined permeable pavement (Brown and Borst 2015).

Other models with continuous simulation capabilities currently available to designers include: Storm Water Management Model (SWMM) 5.0, Windows-based Source Loading and Management Model (WinSLAMM) 9.4, and Model for Urban Stormwater Improvement Conceptualism (MUSIC) 3.1. Of the available models, only SWMM includes an option to create an elevated underdrain outlet in the aggregate subbase. Additionally, the processes used by these models to model water movement through the aggregate and into the drains are not as comprehensive as those in DRAINMOD. The previously described models do not take into account evaporation that occurs after the aggregate has reached field capacity. Current models also either calculate water storage capacity as the difference between total porosity and field capacity or use a void ratio of the aggregate. As described in Section 2.1.1, the soil-water characteristic curve (or for the case of aggregate, the water retention curve) provides a better estimate when the water table is close to the surface. Though the percent difference between the two methods is not as pronounced for aggregate as it is for a bioretention media, the difference is over 35% when the water table is within 4 inches of the pavement surface (Table 2, Figure 2). The soil-water characteristic curve always produces a more conservative value; other models tend to over-predict the amount of water drained from the aggregate.

Table 2. Calculating volume drained from aggregate by (1) distance from the underlying soil by using the water retention curve and (2) subtracting field capacity from saturated volumetric water content.

Water level distance from pavement surface (ft)	Volume drained: water retention curve (ft^3/ft^2)	Volume drained: saturation minus field capacity (ft^3/ft^2)	Percent difference (%)
	Aggregate media (ft)	Aggregate media (ft)	Aggregate Media
0.3	0.062	0.084	-36.3
1.0	0.226	0.252	-11.7
2.0	0.476	0.504	-5.8
3.0	0.728	0.756	-3.8

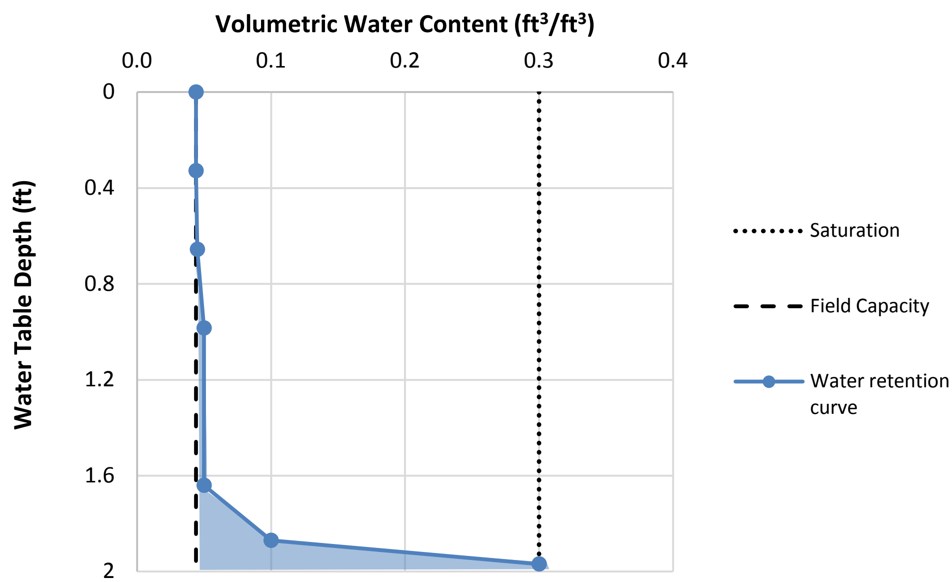

Figure 2. Volumetric water content present in profile for an aggregate when the water table depth is 2 ft, using a water retention curve developed for aggregate (solid line) and field capacity (long dashes) methods. The difference between the two methods is shaded.

Given the limitations of existing permeable pavement models, a more powerful, comprehensive model is needed to predict the annual water balance. A continuous, long-term model such as DRAINMOD could help stormwater engineers and regulators evaluate the performance of many different permeable pavement design configurations, and subsequently identify the best design specifications for aggregate depth, underdrain configuration and drainage area to permeable pavement area ratio specific to Ohio. Results from this new application of DRAINMOD have the potential to advance permeable pavement design in Ohio via the development of a more flexible design and crediting guidance. Additionally, DRAINMOD can also be used as a tool to predict long-term performance under future-climate scenarios (Hathaway et al. 2014).

2.2 MODEL DESCRIPTION AND APPLICATION

2.2.1 Description of DRAINMOD

As presented by Skaggs (1978, 1982, 1999), the governing equations for DRAINMOD are based on two water balances: (1) in the soil profile (Equation 1) and (2) at the soil surface (Equation 2). In the soil profile, the water balance is computed for a section of soil of unit surface area, located at the midpoint between adjacent drains, and extending from the impermeable layer (i.e. the interface between the bottom of the practice and the *in situ* soil) to the soil surface:

$$\Delta V_a = D + ET + DS - F \qquad (1)$$

where ΔV_a = change in the air volume, D = lateral drainage from the section, ET = evapotranspiration, DS = deep seepage, and F = infiltration entering the section in Δt (time increment). DRAINMOD uses the Green and Ampt equation to calculate the rate of infiltration. The water balance at the surface is computed per unit surface area by:

$$P = F + \Delta S + RO \qquad (2)$$

where P = precipitation, F = infiltration, ΔS = change in volume of water stored on the surface, and RO = runoff during time period Δt.

DRAINMOD computes each water balance for a time increment Δt, with all units expressed in terms of depth (cm). The time increment is normally 1 hour; however, when the rainfall rate exceeds the infiltration capacity, Δt decreases to 0.05 hours or less. When there is no rainfall and the drainage rate is rapid, Δt is increased to 2 hours, and when the drainage and ET rates are slow, Δt is further increased to daily. To solve for the losses via drainage, DRAINMOD uses Hooghoudt's equation (Equation 3) to compute drainage flux when the water table is below the surface. The flux is evaluated in terms of the water table at the midway point between the drains and the hydraulic head in the drains:

$$q = \frac{8Kd_e m + 4Km^2}{L^2} \tag{3}$$

where K = effective lateral hydraulic conductivity, L = drain spacing, m = water table height above the drains at the midpoint, and d_e = equivalent drain depth. To correct for convergence near the drain, an equivalent depth is calculated using equations developed in Moody (1967). For typical bioretention installations, the drain depth to drain spacing ratio will likely be less than 0.3, so Equation 4 is used to calculate the equivalent depth:

$$d_e = \frac{d}{1+\frac{d}{L}\left[\frac{8}{\pi}\ln(\frac{d}{r})-(3.55-\frac{1.6d}{L}+2\left(\frac{2}{L}\right)^2)\right]} \tag{4}$$

where r = drain radius and d = drain depth. If the depth to spacing ratio exceeds 0.3, a different equation is used. When the surface is ponded and the profile is saturated, drainage rate is calculated with the Kirkham equation (Equation 5) (Kirkham 1957):

$$q = \frac{4\pi K(t+d-r)}{GL} \tag{5}$$

where t = ponding depth and G is a term dependent on drain depth and spacing and depth of the profile. It is called Kirkham's coefficient G in DRAINMOD and is defined in Equation 6:

$$G = 2\ln\left[\frac{\tan(\frac{\pi(2d-r)}{4h})}{\tan(\frac{\pi r}{4h})}\right] + 2\sum_{m=1}^{\infty}\ln\left[\frac{\cosh\left(\frac{\pi mL}{2h}\right)+\cos(\frac{\pi r}{2h})}{\cosh(\frac{\pi mL}{2h})-\cos(\frac{\pi r}{2h})}\cdot\frac{\cosh(\frac{\pi mL}{2h})-\cos(\pi(2d-r)/2h}{\cosh(\frac{\pi mL}{2h})+\cos(\pi(2d-r)/2h}\right] \quad (6)$$

where h = depth of profile. If the drainage rate is limited by pipe size, valves or other structural features, a user-specified drainage coefficient is used by DRAINMOD to limit the maximum drainage flux from the system.

There are multiple ways to calculate potential evapotranspiration (PET), with some methods requiring more meteorological data than others. Under the most basic application, DRAINMOD uses the Thornthwaite method (with monthly correction factors) to calculate daily PET (Thornthwaite 1948). PET is distributed daily for the 12 hours between 6:00 a.m. and 6:00 p.m, and PET is set equal to zero when rainfall occurs. ET is calculated based on the soil water conditions. If the conditions are not limiting, ET is equal to PET.

However, as the soil water conditions become limiting (dry zone depth exceeds root depth), ET is set equal to the upward flux from the water table. More detailed information about DRAINMOD's governing equations, model components, how various model utilities function, and ways to measure model input parameters are provided in Skaggs (1999) and in the DRAINMOD Reference Report (Skaggs 1980).

A general description of the modeling in DRAINMOD is given below. First, the runoff from the urban catchment must be simulated; the model input parameters are varied to match surface conditions and runoff created by impermeable surfaces: wide drain spacing, shallow surface storage, and low infiltration rate. The contributing area runoff file is created from this initial simulation, and is included in the overall bioretention or permeable pavement simulation. The model is parameterized based on as-built conditions, underlying soil parameters, and watershed characteristics for the SCM of interest. While the authors believe DRAINMOD can be utilized to effectively predict long-term hydrologic fate of stormwater in bioretention and permeable pavement, some of the drawbacks of DRAINMOD are: (1) the model must be "tricked" to model inflow from a highly impervious watershed by changing the Green-Ampt infiltration parameters of the watershed, (2) it only predicts total volume of drainage, exfiltration, ET, and overflow, and does not predict peak flow rates, (3) the highest resolution DRAINMOD will accept for weather files (temperature and rainfall) is hourly, (4) DRAINMOD will only provide outputs in daily, monthly, or yearly format, (5) it does not predict changes in single storm hydrographs due to the addition of an infiltration-based SCM and (6) all inputs are held constant for the entire period of the simulation. Emerson and Traver (2008) and Braga et al. (2007) have shown seasonal variation in performance of infiltration SCMs occurred because of temperature-related variation in infiltration rates; this cannot be effectively simulated by DRAINMOD. Additionally, surface clogging in permeable pavements results in temporal and spatial changes to surface infiltration rates which cannot be simulated using DRAINMOD (Bean et al. 2007a).

2.2.2 Comparison of Permeable Pavement and Bioretention Design Specifications to DRAINMOD Inputs

The concepts of water movement in bioretention cells when installed with underdrains are very similar to agricultural fields drained by tiles. Additionally, while permeable pavements utilize aggregate to support the paving course (instead of the soil media present in bioretention), the underlying principles of flow to an underdrain beneath permeable pavement are similar to those in a bioretention cell. Because of the similarities, many DRAINMOD inputs correspond directly to bioretention cell and permeable pavement design specifications. A comparison of these inputs is presented in Table 3. DRAINMOD is unique as a bioretention and permeable pavement model because an option exists to create an elevated underdrain outlet through the model input for controlled drainage, and it can simulate multiple drains of various spacing distances and diameters. Other models to date have been unable to simulate these types of drainage configurations. DRAINMOD can also simulate varying outlet controls throughout the year and throttling of outflow using valves or orifice plates. In Table 4, examples of DRAINMOD outputs are related to bioretention cell and permeable pavement applications.

Table 3. DRAINMOD inputs compared to typical bioretention and permeable pavement design parameters.

Bioretention Design Parameters	**Permeable Pavement Design Parameters**	**DRAINMOD Inputs**
Drain depth	Drain depth	Depth (in downward direction) from soil surface to drain (B)
Underdrain radius	Underdrain radius	Effective radius of the drain (Re)
Drain spacing	Drain spacing	Spacing between drains (L)
Average surface storage depth	Average surface storage depth (assumed zero)	Maximum surface storage (Sm)
Depth from media surface to in situ soil	Depth from pavement surface to in situ soil	Distance from soil surface to impermeable layer (H)
Drainage coefficient	Drainage coefficient	Drainage rate (limited by hydraulic capacity of the underdrains and outlet structure)
Gravel/mulch/media characteristics and depths	Pavement and aggregate characteristics and depths	Soil water characteristics curve and saturated hydraulic conductivity for each layer
Drainage configuration (inclusion of IWS zone)	Drainage configuration (inclusion of IWS zone)	Weir setting for controlled drainage
Drainage area to bioretention surface area ratio	Drainage area to permeable pavement surface area ratio	Field ratio of contributing drainage area
Root depth	Not applicable (set to minimum of 1 cm)	Vegetation root depth
Exfiltration rate of subsoil	Exfiltration rate of subsoil	Vertical or deep seepage parameters
Weather conditions	Weather conditions	Rainfall and temperature files
Evapotranspiration	Evaporation (no transpiration due to lack of plants)	Either use of Thornthwaite method (with or without monthly correction factors) or enter calculated PET data

Table 4. Relating DRAINMOD outputs to analogous bioretention and permeable pavement processes.

DRAINMOD Outputs	Bioretention or Permeable Pavement Factor
ET	Evapotranspiration (volume eliminated)
Drainage	Underdrain flow (volume treated)
Runoff	Overflow or bypass (untreated volume)
Seepage	Exfiltration (volume eliminated)
Wet stress	Vegetation stress indicator (bioretention only)
Dry stress	Vegetation stress indicator (bioretention only)
Rank files for above outputs	Quantify impact of infrequent ARI events

2.3 References

Abertay Waste Solutions (AWS). (1998). *Erwin user guide version 3.0, English*, Urban Water Technology Center, Univ. of Abertay, Dundee, U.K.

Bean, E.Z., Hunt, W.F., and Bidelspach, D.A. (2007a). "Field survey of permeable pavement surface infiltration rates." *Journal of Irrigation and Drainage Engineering*. 133(3), 249-255.

Bean, E. Z., Hunt, W. F. and Bidelspach, D. A. (2007b). Evaluation of Four Permeable Pavement Sites in Eastern North Carolina for Runoff Reduction and Water Quality Impacts. *Journal of Irrigation and Drainage Engineering*, 133(6), 583-592.

Booth, D. and Leavitt, J. (1999). "Field evaluation of permeable pavement systems for improved stormwater management." *Journal of the American Planning Association,* 65(3), 314-325.

Braga, A., Horst, M., and Traver, R.G. (2007). "Temperature effects on the infiltration rate through an infiltration basin BMP." *Journal of Irrigation and Drainage Engineering*, 133(6), 593-601.

Brander, K. E., Owen, K. E., and Potter, K. W. (2004). "Modeled impacts of development type on runoff volume and infiltration performance." *Journal of the American Water Resources Association*, 40(4), 961-969.

Bratieres, K., Fletcher, T. D., Deletic, A., and Zinger, Y. (2008). "Nutrient and sediment removal by stormwater biofilters: A large-scale design optimisation study." *Water Research*. 42(14), 3930-3940.

Brown, R. A., and Borst, M. (2015). "Quantifying evaporation in a permeable pavement system." *Hydrological Processes*, 29(9), 2100-2011.

Brown, R.A. and Hunt, W.F. (2011a). "Impacts of media depth on effluent water quality and hydrologic performance of under-sized bioretention cells." *Journal of Irrigation and Drainage Engineering.* 137(3), 132-143.

Brown, R. A. and Hunt, W. F. (2011b). "Underdrain configuration to enhance bioretention exfiltration to reduce pollutant loads." *Journal of Environmental Engineering*. 137(11), 1082-1091.

Brown, R.A., R.W. Skaggs, and W.F. Hunt. (2013). "Calibration and validation of DRAINMOD to model bioretention hydrology." *Journal of Hydrology*. 486, 430-442.

Browne, D., Deletic, A., Mudd, G.M., and Fletcher, T.D. (2008). "A new saturated/unsaturated model for stormwater infiltration systems." *Hydrological Processes*. 22(25), 4838–4849.

Collins, K. A., Hunt, W. F. and Hathaway, J. M. (2008). "Hydrologic comparison of four types of permeable pavement and standard asphalt in Eastern North Carolina." *Journal Hydrologic Engineering*, 13(12), 1146-1157.

Darcy, H. (1856). *The public fountains of the City of Dijon*, Victor Dalmont, Paris.

Davis, A.P. (2008). "Field performance of bioretention: Hydrology impacts." *Journal of Hydrologic Engineering*. 13(2), 90-95.

Davis, A.P., Hunt, W. F., Traver, R.G., and Clar, M. (2009). "Bioretention technology: Overview of current practice and future needs." *Journal of Environmental Engineering,* 135(3), 109-117.

DeBusk, K. M., Hunt, W.F., & Line, D.E. (2010). "Bioretention outflow: Does it mimic nonurban watershed shallow interflow?" *Journal of Hydrologic Engineering*. 16(3), 274-279.

Denich, C., and Bradford, A. (2010). "Estimation of evapotranspiration from bioretention areas using weighing lysimeters." *Journal of Hydrologic Engineering*. 15(6), 522-530.

Dietz, M.E. and Clausen, J.C. (2006). "Saturation to improve pollutant retention in a rain garden." *Environmental Science and Technology.* 40(4), 1335-1340.

Dietz, M.E., and Clausen, J.C. (2008). "Stormwater runoff and export changes with development in a traditional and low impact subdivision." *Journal of Environmental Management*. 87(4), 560-566.

Drake, J., Bradford, A., and Van Seters, T. (2013). "Hydrologic performance of three partial infiltration permeable pavements in a cold climate over low permeability soil." *Journal of Hydrologic Engineering*, 19(9), 1-9.

Dreelin, E., Fowler, L. and Carroll, C. (2006). "A test of porous pavement effectiveness on clay soils during natural storm events." *Water Research,* 40(4), 799-805.

Dussaillant, A.R., Wu, C.H., and Potter, K.W. (2004). "Richards equation model of a rain garden." *Journal of Hydrologic Engineering*, 9(3), 219-225.

Dussaillant, A.R., Cuevas, A., and Potter, K.W. (2005). "Raingardens for stormwater infiltration and focused groundwater recharge: Simulations for different world climates." *Water Science and Technology: Water Supply*, 5(3-4), 173-179.

Emerson, C.H., and Traver, R.G. (2008). "Multiyear and seasonal variation of infiltration from storm-water best management practices." *Journal of Irrigation and Drainage Engineering*, 134(5), 598-605.

Emerson, C. H., Wadzuk, B. M., and Traver, R. G. (2010). “Hydraulic evolution and total suspended solids capture of an infiltration trench.” *Hydrologic Processes,* 24(8), 1008–1014.

Fassman, E. A. and Blackbourn, S. D. (2010). “Urban runoff mitigation by a permeable pavement system over impermeable soils.” *Journal of Hydrologic Engineering,* 15(6), 475-485.

Green,W. H., and Ampt, G. A. (1911). “Studies on soil physics. I. The flow of air and water through soil.” *Journal of Agricultural Science,* 4(01), 1–24.

Hathaway, J.M., Brown, R.A., Fu, J.S., and Hunt, W.F. (2014). “Bioretention function under climate change scenarios in North Carolina, USA.” *Journal of Hydrology*, *519*, 503-511.

Hatt, B.E., Fletcher, T.D., and Deletic, A. (2009). “Hydrologic and pollutant removal performance of stormwater biofiltration systems at the field scale.” *Journal of Hydrology*, *365*(3), 310-321.

He, Z., and Davis, A.P. (2011). “Process modeling of stormwater flow in a bioretention cell.” *Journal of Irrigation and Drainage Engineering*, 137(3), 121-131.

Heasom, W., Traver, R.G., and Welker, A. (2006). “Hydrologic modeling of a bioinfiltration best management practice.” *Journal of the American Water Resources Association*, 42(5), 1329-1347.

Hunt, W. F., Jarrett, A. R., Smith, J. T., and Sharkey, L. J. (2006). “Evaluating bioretention hydrology and nutrient removal at three field sites in North Carolina.” *Journal of Irrigation and Drainage Engineering*. 132(6), 600–608.

Hunt, W. F., Smith, J. T., Jadlocki, S. J., Hathaway, J. M., and Eubanks, P. R. (2008). “Pollutant removal and peak flow mitigation by a bioretention cell in urban Charlotte, NC.” *Journal of Environmental Engineering*. 134(5), 403-408.

Hunt, W.F., Davis, A.P., and Traver, R.G. (2012). “Meeting hydrologic and water quality goals through targeted bioretention design.” *Journal of Environmental Engineering*. 138(6), 698-707.

HYDRUS [Computer software]. Prague, Czech Republic, PC-Progress s.r.o.

Jones, M.P., and Hunt, W.F. (2009). “Bioretention impact on runoff temperature in trout sensitive waters.” *Journal of Environmental Engineering*. 135(8), 577-585.

Kirkham, D. (1957). “Theory of land drainage.” *Drainage of Agricultural Lands: Agronomy Monograph No. 7*, J. N. Luthin, ed., American Society of Agronomy, Madison, Wisc., 139-181.

Lee, J. G., Borst, M., Brown, R. A., Rossman, L., & Simon, M. A. (2015). Modeling the Hydrologic Processes of a Permeable Pavement System. *Journal of Hydrologic Engineering*, 20(5), 1-9.

Li, H., Sharkey, L.J., Hunt, W.F., & Davis, A.P. (2009). "Mitigation of impervious surface hydrology using bioretention in North Carolina and Maryland." *Journal of Hydrologic Engineering*. 14(4), 407-415.

Lucas, W.C. (2010). "Design of integrated biofiltration-detention urban retrofits with design storm and continuous simulation methods." *Journal of Hydrologic Engineering*, 15(6), 486-498.

Luell, S.K., Hunt, W.F., & Winston, R.J. (2011). "Evaluation of undersized bioretention stormwater control measures for treatment of highway bridge deck runoff." *Water Science & Technology*. 64(4), 974-979.

Martin III, W. D., and Kaye, N. B. (2015). "Characterization of undrained porous pavement systems using a broken-line model." *Journal of Hydrologic Engineering*, *20*(2), 1-8.

Moody, W. T. (1967). "Nonlinear differential equation of drain spacing." *Journal of Irrigation and Drainage Division*, ASCE, 92(IR2), 1-9.

Ohio Department of Natural Resources (ODNR), Division of Soil and Water Conservation. (2006). *Rainwater and land development: Ohio's standards for stormwater management, low impact development, and urban stream protection*. 3rd edition. Ed: John Mathews.

Page, J.L., Winston, R.J., Mayes, D.B., Perrin, C., Hunt, W.F. (2015). "Hydrologic mitigation of impervious cover in the municipal right-of-way through innovative stormwater control measures." *Journal of Hydrology*. Accepted.

Palhegyi, G. E. (2010). "Modeling and sizing bioretention using flow duration control." *Journal of Hydrologic Engineering*, 15(6), 417-425.

Passeport, E., Hunt, W.F., Line, D.E., Smith, R.A., and Brown, R.A. (2009). "Field study of the ability of two grassed bioretention basins to reduce storm-water runoff pollution." *Journal of Irrigation and Drainage Engineering.* 135(4), 505-510.

Richards, L. A. (1931). "Capillary conduction through porous mediums." Physics, 1(5), 318–333.

Roseen, R. M., Ballestero, T. P., Houle, J. J., Briggs, J. F., and Houle, K. M. (2012). "Water quality and hydrologic performance of a porous asphalt pavement as a storm-water treatment strategy in a cold climate." *Journal of Environmental Engineering*, 138(1), 81-89.

Schlüter, W., Jefferies, C., and Zhang, X. X. (2007). "Modelling of flow through gravel-filled trenches." *Urban Water Journal*, 4(4), 241–251.

SEEP/W [Computer software]. Calgary, Canada, GEO-SLOPE International.

Schluter, W., and Jeffries, C. (2002). “Modelling the outflow from a porous pavement.” *Urban Water*, 4(3), 245-253.

Skaggs, R.W. (1978). “A water management model for shallow water table soils.” *Technical Report No. 134*, Water Resources Research Institute of the University of North Carolina, N.C. State University, Raleigh, N.C., 1-128.

Skaggs, R.W. (1980). “DRAINMOD: Reference report - Methods for design and evaluation of drainage-water management systems for soils with high water tables.” U.S. Department of Agriculture – Soil Conservation Service, Fort Worth, TX.

Skaggs, R.W. (1982). “Field evaluation of a water management simulation model.” *Transactions of the ASAE*, 25(3), 666-674.

Skaggs, R.W. (1999). “Drainage simulation models.” *Agricultural drainage: Monograph No. 38*, R. W. Skaggs and J. van Schilfgaarde, eds., American Society of Agronomy, Madison, Wisc., 469-500.

Smith, R.E., and Warwick, A.W. (2007). “Soil water relationships.” *Design and operation of farm irrigation systems*. Chapter 6, 2nd edition, American Society of Agricultural and Biological Engineers (ASABE), St. Joseph, Michigan, USA.

Starke, P., Göbel, P., and Coldewey, W.G. (2010). “Urban evaporation rates from water-permeable pavements.” *Water Science and Technology*, 62(5), 1161-1169.

Thomson, N. R. (1990). 2DUSAT: User’s guide and documentation, Univ.of Waterloo, Waterloo, Canada.

Thornthwaite, C.W. (1948). “An approach toward a rational classification of climate.” *The Geographical Review*, 38(1), 55-94.

U.S. Army Corps of Engineers (USACE). (2000). “Hydrologic modeling system HEC-HMS technical reference manual.” USACE, Hydrologic Engineering Center, Davis, Calif.

U.S. Environmental Protection Agency (USEPA). (2007). “National water quality inventory: Report to Congress—2002 reporting cycle.” *Rep. No. EPA 841-R-07-001*, USEPA, Washington, D.C.

Wang, L., Lyons, J., Kanehl, P., and Bannerman, R. (2001). “Impacts of urbanization on stream habitat and fish across multiple spatial scales.” *Journal of Environmental Planning and Management*, 28(2), 255–266.

Wardynski, B.J., Winston, R.J., and Hunt, W.F. (2012). “Internal water storage enhances exfiltration and thermal load reduction from permeable pavement in the North Carolina mountains.” *Journal of Environmental Engineering*, 139(2), 187-195.

Winston, R.J., Dorsey, J.D. and Hunt, W.F. (2015). *Monitoring the performance of bioretention and permeable pavement stormwater controls in Northern Ohio: Hydrology, water quality, and maintenance needs*. Final Report Submitted to the University of New Hampshire and the Chagrin River Watershed Partners. In Fulfilment of NOAA Award number NA09NOS4190153.

Youssef, M.A., Skaggs, R.W., Chescheir, G.M., and Gilliam, J.W. (2005). “The nitrogen simulation model, DRAINMOD-N II.” *Transactions of the ASAE*. 48(2), 611-626.

Zhang, S., and Guo, Y. (2014). “Analytical equation for estimating the stormwater capture efficiency of permeable pavement systems.” *Journal of Irrigation and Drainage Engineering*, 141(4), 1-9.

3 BIORETENTION HYDROLOGIC MODELING USING DRAINMOD

The agricultural water balance model DRAINMOD was utilized to simulate long-term bioretention performance for three field-monitored bioretention cells in northeast Ohio. The model was calibrated and validated against the field collected data using separate DRAINMOD models for each site. The models were parameterized using as-built design variables and laboratory-measured soil parameters. Sensitivity analyses were completed to determine the response of the water balance to the many different design configurations possible in a bioretention cell. Finally, future climate data for the mid-twenty-first century were used to model bioretention performance under predicted changing temperature and rainfall patterns in northeast Ohio.

3.1 Methods

3.1.1 Site Description and Monitoring Methods

DRAINMOD was calibrated and validated for three bioretention cells in northeast Ohio: two at Holden Arboretum and one on the campus of Ursuline College. These monitoring sites and the methods utilized to obtain field data are described in detail in Winston et al. (2015). Approximately one year of data was collected at each site, with the exception of the winter, when freezing temperatures precluded stormwater monitoring. The surface area of the bioretention cells at Holden Arboretum were sized to be 5% of the impervious drainage area. The Ursuline College cell was slightly over-sized at 6.5% of the impervious drainage area. The Holden Arboretum cells employed 2.75-3 ft of media, while the Ursuline College cell had 2 ft of media. All three cells employed internal water storage (IWS) zones of varying depth: 15 inches at Holden South, 18 inches at Holden North, and 24 inches at Ursuline. Each cell had a total of 18 inches of aggregate and/or sand layers beneath the media. The average bowl storage depth at

Ursuline was 11.7 inches. At Holden Arboretum, the South and North cells had 15.3 inch to 15.9 inch average bowl storage depths, respectively, due to a slight construction mishap. Therefore, all three cells were over-sized for water quality volume capture, and effectively designed to store the 1.16, 1.78, and 1.76 inch events at Ursuline, Holden South, and Holden North, respectively. Thus, the bioretention cells had variability in IWS zone depth, surface storage volume, underlying soil type, media depth, and media characteristics.

The hydrologic monitoring methods are described for each site in detail in Winston et al. (2015). In general, runoff, drainage, and overflow volumes were measured or estimated for each bioretention monitoring site. Because runoff entered each bioretention cell in a diffuse manner, runoff was estimated using the discrete Curve Number (CN) method offset by an antecedent moisture correction (NRCS 1986). At the Ursuline site, overflow and drainage were measured together using a sharp crested 60° v-notch weir. Flow depth was measured on a 2-minute interval using a Hobo U-20 logger offset by barometric pressure measured on site. In order to separate drainage from overflow, the system was modeled in USEPA SWMM 5.1 using a pipe flow equation; the drainage output from SWMM was compared against the measured outflow hydrograph. Overflow was then separated as all flow above the modeled drainage hydrograph. At the Holden Arboretum south cell, drainage was measured with a sharp-crested 45° v-notch weir and a pressure transducer. The storm sewer from the south cell drained through the north cell catch basin, where a 60° v-notch weir measured combined outflow from the north and south cells. Data were post-processed to subtract flow rates on each two minute interval from the south cell monitoring point, so the north cell outflow could be isolated. Overflow was estimated for the Holden Arboretum bioretention cells through hydrograph separation. Drain flow had a relatively constant peak flow rate, and varied as a function of head within the media; overflow occurred as peaks in the outflow hydrograph above this near-constant rate. Overflow and drainage volumes were determined by separation of the respective hydrographs.

The sum of exfiltration and ET was estimated by using a Hobo U20 pressure transducer housed inside a well installed in each bioretention cell to measure the water table depth on a 2-minute interval within the media with time; a second Hobo U20 pressure transducer was used to offset the pressure reading in the well by barometric pressure that was measured on site. Drawdown was calculated during inter-event periods as the change in water table depth over time, and was only considered from the invert of the underdrain until the IWS zone was completely drained. Above the invert of the underdrain, drainage affected the drawdown rate, and negated the validity of this calculation. The drawdown rate was then offset by soil media (0.30) or aggregate (0.40) effective drainable porosity to calculate the exfiltration rate. Average measured exfiltration rates of 0.083 in/hr, 0.065 in/hr, and 0.17 in/hr were used in the Holden South, Holden North, and Ursuline College DRAINMOD models, respectively (Winston et al. 2015). Exfiltration rates were non-linear, and varied as a function of water depth in the IWS zone. This was presumably due to the effects on lateral exfiltration into the soil making up the side walls of the bioretention cell (Browne et al. 2008).

At each site, the drainage area, bioretention cell area, average surface storage zone depth, media depth, drain depth, and depth to drain outlet (for IWS designs) were determined from as-built surveys and construction notes. The model was parameterized using survey data and measurements of the media soil-water characteristic curves, saturated hydraulic conductivities, and infiltration and exfiltration rates. Since a single underdrain was used at all three sites, an effective drain spacing for each application was estimated by dividing the bioretention surface area by the total length of the underdrain (Brown 2011). Once these properties were determined, they were entered into DRAINMOD to simulate the hydrologic response of the systems (Figure 3).

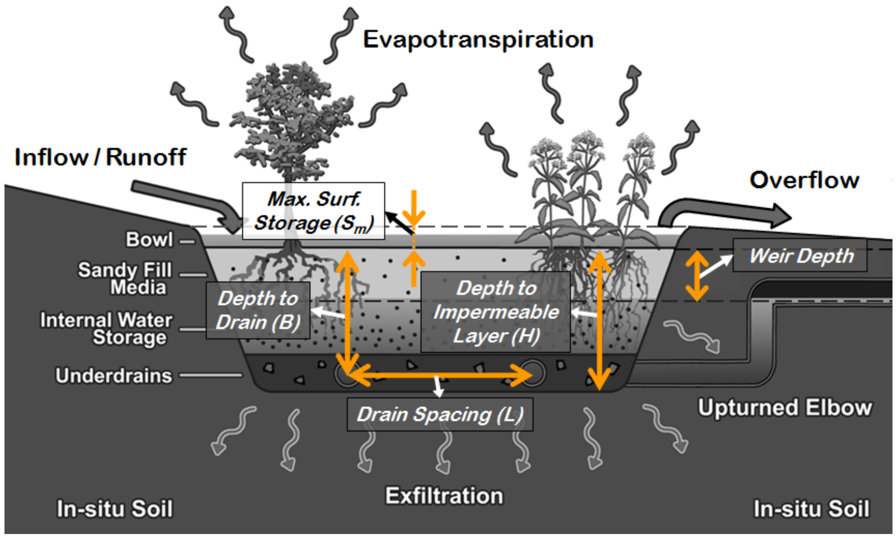

Figure 3. Model inputs for DRAINMOD and corresponding design parameters for bioretention cells.

3.1.2 Drainage Coefficient

The drainage coefficient sets a maximum hydraulic limit on the amount of drainage that can occur in a day (cm/day). This is typically limited by the diameter of the drain, the number and type of perforations, the drainage configuration, and any restrictions to flow in the drain (e.g. orifice plate or valve). The Kirkham equation calculates the flux to the drain when the surface storage is fully ponded and the media is saturated. When the drainage coefficient exceeds this flux, the drainage rate is set by the Kirkham equation; otherwise, the maximum drainage rate predicted by the model is set equal to the drainage coefficient. The drainage coefficient was determined by examining the maximum drainage rate from the largest events from each monitoring period. The largest events were selected because it was likely the entire profile would be saturated and the surface storage zone would be full. Based on the maximum observed drainage rates from the cells at Holden Arboretum, the drainage coefficients were set to 50 cm/day and 45 cm/day for the south and north cells, respectively. Based on the maximum observed drainage rate at Ursuline College, the drainage coefficient was set to 120 cm/day.

3.1.3 Soil Inputs

In order to model soil water movement in DRAINMOD, two input parameters are required: (1) the saturated hydraulic conductivity of media and (2) the soil water characteristic curve. To determine these inputs, three 3 inch diameter soil cores were obtained from the bioretention media at Ursuline College, Holden South, and Holden North bioretention cells. The samples were obtained from the upper 12 in of media. The soil water characteristic curve was measured in the laboratory on a pressure plate apparatus which measures the volume of water drained from an initially saturated soil core under various suction pressures (Klute 1986). The average volumetric water contents at various pressures are presented for the three media types in Table 5. Saturated hydraulic conductivity was measured using a constant head permeability test, as described in Klute and Dirksen (1986).

Table 5. Soil water characteristic curves for Ursuline, Holden South, and Holden North bioretention cells.

Pressure Head (ft)	Volumetric Water Content (ft^3/ft^3)		
	Ursuline	Holden North	Holden South
0.000	0.331	0.312	0.387
-0.001	0.331	0.290	0.380
-0.003	0.331	0.290	0.375
-0.010	0.258	0.206	0.271
-0.020	0.217	0.112	0.156
-0.033	0.201	0.096	0.135
-0.066	0.190	0.090	0.123
-0.098	0.179	0.093	0.113
-0.131	0.174	0.082	0.110

Soil samples were collected during construction and analyzed in two laboratories for particle size distribution to confirm that the media mixes met the Ohio standards (ODNR 2006). The standard mix design has a minimum of 80% sand and maximum 10% clay in the mineral fraction, and 3-5% organic matter by weight (8-20% by volume). Soil particle size distribution was measured using a sieve analysis and followed the procedure in Gee and Bauder (1986). The Holden North and South soil media were classified as loamy sand (88% sand, 2% silt, 10% clay) and the Ursuline College media was also a loamy sand (87% sand, 4% silt, and 9% clay).

3.1.4 Climatic Inputs

3.1.4.1 Temperature

Maximum and minimum daily air temperatures are climate inputs for DRAINMOD. Air temperature was measured using an on-site Onset U-30 weather station at each monitoring site; the weather station was located at most 500 ft from the bioretention cells, and measured air temperature on a 1-minute interval. These temperatures were converted to daily minimum and maximum values using a script in R statistical software (R Core Team 2015).

3.1.4.2 Precipitation

Rainfall was measured at each bioretention monitoring site using an automated tipping bucket rain gauge (Davis Instruments). Each tip represented 0.01 inches of rainfall and was recorded as a sum over each 1-minute interval on the data logger for the Onset U-30 weather station for later retrieval. Because DRAINMOD accepts rainfall data on an hourly or daily time step, rainfall data were transformed to hourly sums using R statistical software (R Core Team 2015).

3.1.4.3 Potential Evapotranspiration (PET)

Potential evapotranspiration can be incorporated into the DRAINMOD model using any method the user chooses by creating a simple input file of daily PET. If PET is not calculated outside the model, DRAINMOD will calculate PET using the Thornthwaite method, which is based on the daily maximum and minimum air temperatures. The Thornthwaite method is not as precise as other methods, as it requires only the mean monthly temperature to calculate PET (Amatya et al. 1995). DRAINMOD has an option to include PET correction factors, which were utilized but were not specific to northern Ohio. The mean monthly air temperature is used to calculate the heat index from the site. The calculation of heat index (I) is described in equation 3.1, where T_i is the mean monthly temperature in degrees Celsius. Based on mean monthly air temperatures for 1983-2012 reported for Cleveland Hopkins airport (NOAA 2015), the calculated heat index was 50. The calculated heat index and daily temperatures are then used to calculate daily PET.

$$I = \sum_{i=1}^{12} \left(\frac{T_i}{5}\right)^{1.514} \quad (3.1)$$

3.1.4 Data Analysis

To calibrate and validate DRAINMOD, the measured/estimated water table depths, inflow, drainage, and overflow+ET data were split into two separate data sets. To account for seasonality in bioretention performance (Emerson and Traver 2008; Muthanna et al. 2008), storm events that occurred during even months of the year (April, June, etc.) were used for model calibration. Data collected during odd months of the year (May, July, etc.) were extracted for model validation. Field monitoring methods were consistent during the calibration and validation periods. A separate model was created for each bioretention cell, and the models were parameterized with measured or estimated inputs which remained constant during the calibration and validation periods. Model parameters that could not be measured, such as piezometric head of the contributing aquifer and thickness of the restricting layer, were modified to maximize the values of the goodness of fit tests presented below.

Enumeration methods were used to determine the quality of model fit to the calibration and validation data sets. These included calculating percent error of runoff (inflow to the bioretention cell), drainage, overflow, and combined exfiltration and ET. Additionally, the measured and predicted depths of each of the aforementioned outputs were compared (in inches per bioretention surface area). Finally, Nash-Sutcliffe coefficients and coefficients of determination (R^2) were calculated. Nash-Sutcliffe coefficients were calculated on an event-basis using equation 3.2.

$$NSE = 1 - \frac{\sum_{i=1}^{N}(Q_{i,measured} - Q_{i,predicted})^2}{\sum_{i=1}^{N}(Q_{i,measured} - Q_{average})^2} \quad (3.2)$$

where, $Q_{i,measured}$ = measured volume for event i, $Q_{i,predicted}$ = predicted volume for event i, $Q_{average}$ = average measured volume for N events, N = total number of events for the monitoring period, and NSE = Nash-Sutcliffe coefficient (Nash and Sutcliffe 1970).

3.1.5 Sensitivity Analyses

Once each DRAINMOD model was successfully calibrated and validated, the baseline model that matched all as-built characteristics was used as the basis for a sensitivity analysis. The Ursuline and Holden South models were utilized for the sensitivity analysis. Holden North had similar design characteristics to the South cell and hydrologic data complicated by the pass-through of flow from the South cell, and therefore this system was not utilized for the sensitivity analysis. Long-term climatic data sets were obtained from the NOAA National Climatic Data Center (NOAA 2015). These included hourly temperature and rainfall data measured at the Cleveland Hopkins Airport between 1983-2012. These data were used as inputs for the sensitivity analysis to determine long-term bioretention cell performance. Design variables were modified one-at-a-time to determine model sensitivity to: media depth, IWS zone depth, bowl depth, and hydraulic loading ratio. Four base models were created to represent varying exfiltration rates: 0.5 in/hr, 0.2 in/hr, 0.05 in/hr, and 0.02 in/hr. Levels of each design characteristic modeled are presented in Table 6. This resulted in a total of 64 modeling runs for each of the two sensitivity analyses.

For each model run, yearly output files were exported from DRAINMOD. Total inflow, drainage, overflow, exfiltration, and ET (all reported in inches per bioretention surface area) were each summed over the 30-year simulations. For each simulation, the percentage of inflow represented by drainage, overflow, exfiltration, and ET were reported. Comparisons were made with regards to bioretention performance with varying underlying soil types and design scenarios.

Table 6. Levels of each design variable modeled in the sensitivity analysis.

Design Characteristics	Baseline Ursuline	Baseline Holden South	Other Model Runs				
Media Depth (in)	24	33	24	36	48		
IWS zone (in)	24	15	0	6	12	18	24
Loading Ratio (imp:BRC)	15:1	20:1	10:1	20:1	35:1	50:1	
Rooting Depth (in)	12	12	24				
Bowl Depth (in)	10.7	15	9	12	18	24	

3.1.6 Future Climate Modeling

For climate change predictions, site specific data were gleaned from Gao et al. (2012) who generated climate projection data for the eastern United States at high resolution by performing dynamic downscaling using the Weather Research and Forecasting (WRF) model. Modeling was performed on a 4 km x 4 km high resolution scale with the Community Earth System Model version 1.0 (CESM v1.0) serving to establish boundary conditions for the WRF model. Dynamic downscaling requires a number of surface and three-dimensional variables, which were extracted from Community Atmosphere Component Version 4 (CAM4) and Community Land Model (CLM4) output taken from CESM v1.0. The WRF pre-processing system was used to horizontally interpolate surface variables from CESM v1.0 output to the WRF domains. A full description of the dynamical downscaling methodology is available in Gao et al. (2012).

Three climate scenarios were utilized for this work, each containing 4 or 5 years of data. The base model case was for 2001-2004 climate data, and data were obtained from Cleveland Hopkins airport for this time period (NOAA 2015). This location, approximately 39 miles from Holden Arboretum and 25 miles from Ursuline College, was chosen for its long-term climatic record and was also used for the sensitivity analysis. The base case was then utilized to compare measured to modeled climate data under existing climate conditions, similar to the approach taken in Gao et al. (2012). For the base scenario, the average annual rainfall for 2001-2004 was 39.7 inches (range 34.8-44.0) at Ursuline and 39.6 inches (range 33.6-50.1) at Holden. During the same time period, Cleveland Hopkins airport experienced on average 34.5 inches (range 32.1-38.1) of rainfall per year (NOAA 2015).

The high spatial resolution provided by dynamic downscaling allows an analysis of climate change impacts on a highly resolved regional basis. Additionally, this methodology has advantages over statistical downscaling techniques as stationary relationships between present weather observations and those in the future based on emission projections need not be assumed. To ensure the WRF model performed adequately for this specific location, modeling was performed for the Base data period for Ursuline College and Holden Arboretum and compared to the 2001–2004 data observed at Cleveland Hopkins Airport (NOAA 2015), the nearest reliable weather data source. The model overestimated average yearly rainfall for the two sites by 3.4 and 3.3 inches when compared to the observed data, but had comparable median and 90th percentile rainfall. Similarly, the median and 90th percentile consecutive dry days were similar between the modeled and observed data.

Data from two of the Intergovernmental Panel on Climate Change (IPCC) Representative Concentration Pathways (RCP 4.5 and RCP 8.5) were utilized in this study. Bioretention performance was analyzed under two fossil fuel usage scenarios, one moderate (RCP 4.5) and one intensive (RCP 8.5). Predictions from 2055 to 2059 (5 years) were used for both climate change scenarios. Differences among performance of bioretention under the two climate scenarios will not be the focus of this work. Rather, the focus was differences in performance noted between the base case and both climate change scenarios. Due to the uncertainty surrounding climate projections and future fossil fuel usage, utilizing two RCPs allowed a more robust analysis of climate change impacts.

3.2 Results and Discussion

3.2.1 Contributing Area Runoff

The contributing runoff to each bioretention cell was the first parameter to be calibrated. Since all of the three watersheds were at minimum 20% pervious, methods for estimating inflow were modified from those in Brown et al. (2013). Inflow calibration was improved by splitting the impervious and pervious fractions into separate modeled sub-watersheds, parameterizing each with measured values, and then varying Green-Ampt infiltration characteristics and drain spacing to affect the amount of surface runoff (i.e. inflow to the bioretention cell). Modeled inflow to each bioretention cell was set equal to the sum of modeled surface runoff from the pervious and impervious catchments. Estimated and modeled inflow for the Ursuline College, Holden South, and Holden North sites were compared in Figure 3, Figure 4, and Figure 5, respectively. Coefficients of determination for the relationship between modeled and estimated inflow were 0.98-0.99, suggesting the inflow was well calibrated. Nash-Sutcliffe efficiencies during the calibration period for inflow were 0.99 for all modeled sites. During the validation period, the model fit the estimated inflow very well, with Nash-Sutcliffe efficiencies of 0.99, 0.96, and 0.96, respectively. The slightly lower NSEs for the Holden watersheds likely were due to the smaller impervious fractions in these watersheds. Modeling of runoff processes from soil surface is more tenuous than from an impervious surface due to variations in predicted runoff as a function of soil moisture and vegetative cover type.

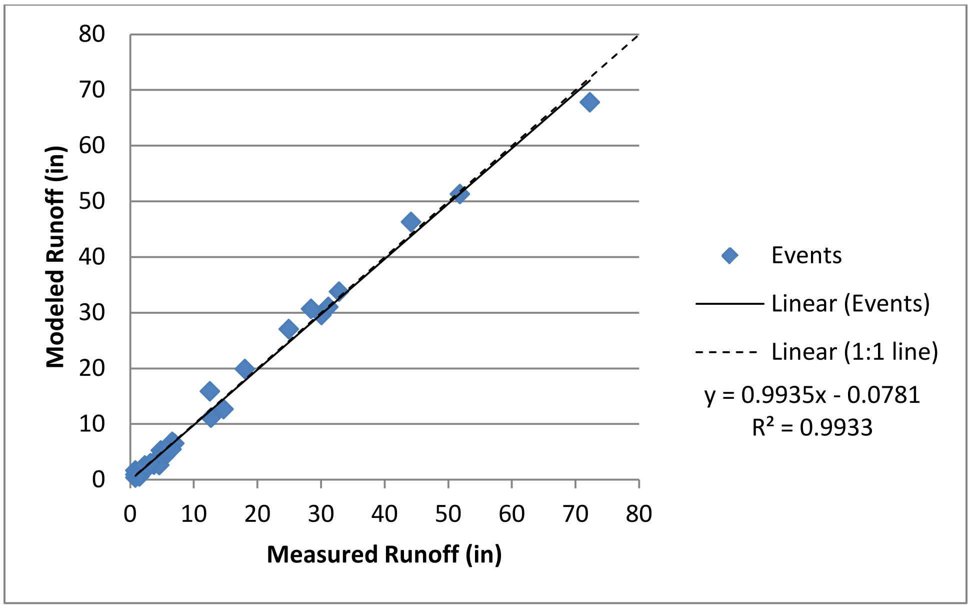

Figure 4. Modeled (predicted) vs. estimated runoff volume from the Ursuline College watershed for all 49 monitored storm events. Also presented are the linear trendline with equation, Coefficient of Determination (R^2), and the 1:1 line. All units are in inches per bioretention surface area.

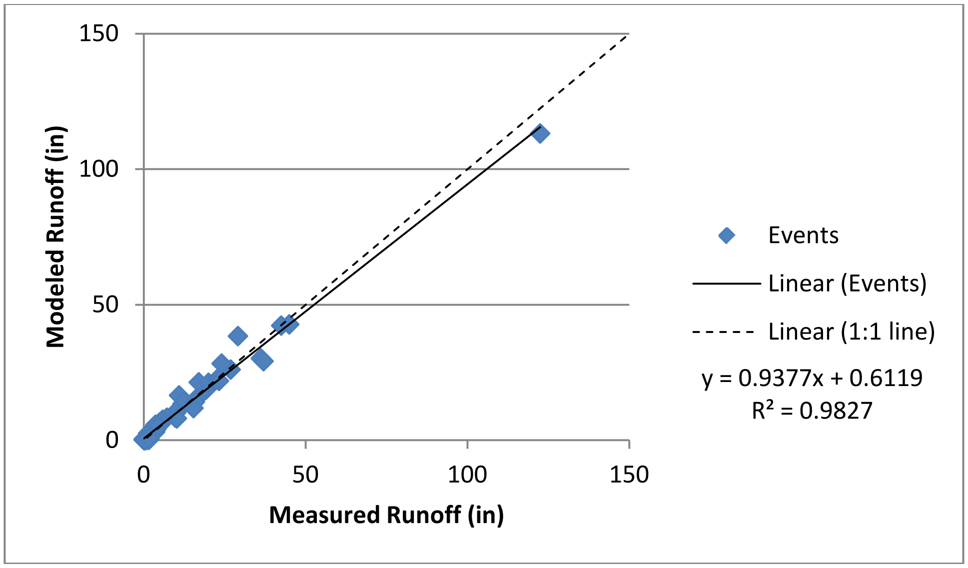

Figure 5. Modeled (predicted) vs. estimated runoff volume from the Holden South watershed for all 86 monitored storm events. Also presented are the linear trendline with equation, Coefficient of Determination (R^2), and the 1:1 line. All units are in inches per bioretention surface area.

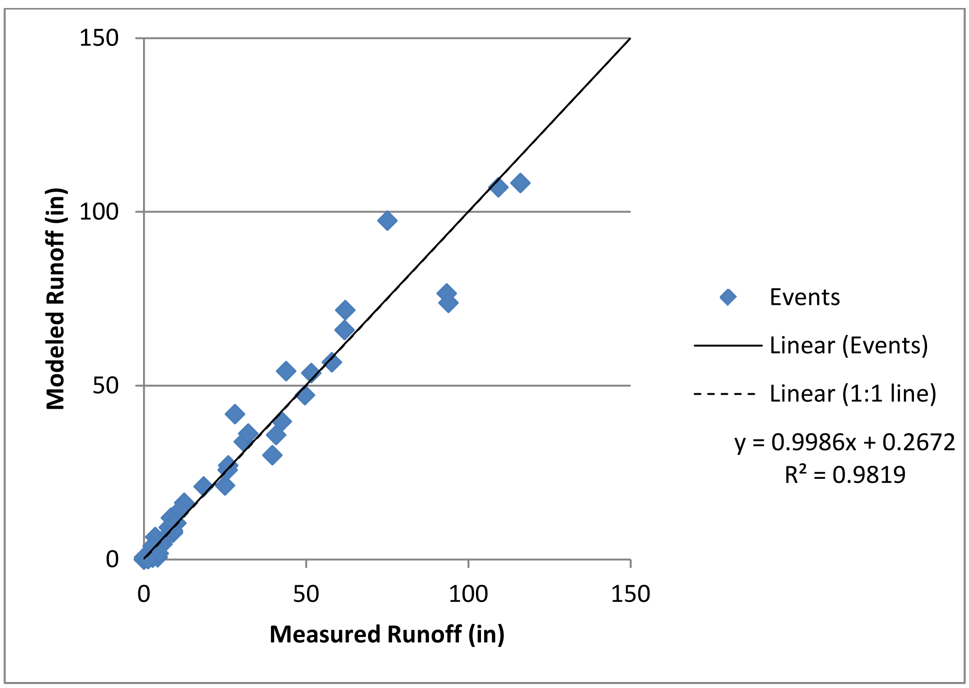

Figure 6. Modeled (predicted) vs. estimated runoff volume from the Holden North watershed for all 86 monitored storm events. Also presented are the linear trendline with equation, Coefficient of Determination (R^2), and the 1:1 line. All units are in inches per bioretention surface area.

3.2.2 DRAINMOD Calibration and Validation

At the Ursuline College site, DRAINMOD was calibrated to the field collected data over the 6 month monitoring period (Figure 7). The model reliably predicted the fraction of drainage, overflow, and exfiltration/ET on an event-by-event basis, and percent error between modeled and measured hydrologic fates was within 6% during the calibration period (Table 7). Nash-Sutcliffe coefficients of 0.94, 0.97, and 0.95 were determined for drainage, overflow, and exfiltration/ET; coefficients of determination for these parameters were all greater than 0.95, suggesting DRAINMOD was well calibrated against the hydrologic data from the even-numbered months of the monitoring period. Nash-Sutcliffe coefficients were 0.98 and 0.95 for drainage and exfiltration/ET during the validation period with R^2 greater than 0.96 for these parameters. However, the NSE for overflow was 0.73 (R^2 of 0.85), with a 35% difference between modeled and measured overflow volume. This error may be because only 4 of 28 events produced overflow during the validation period which compounds any errors in the modeled overflow volumes. Overall model performance was still quite robust, with measured drainage, overflow, and exfiltration/ET representing 33.1%, 8.9%, and 57.9% of estimated inflow; the DRAINMOD output suggested these parameters represented 30.6%, 11.9%, and 57.4% of the inflow. While percent error was large for overflow, the overall error during the validation period was only 3% when considering the entire water balance.

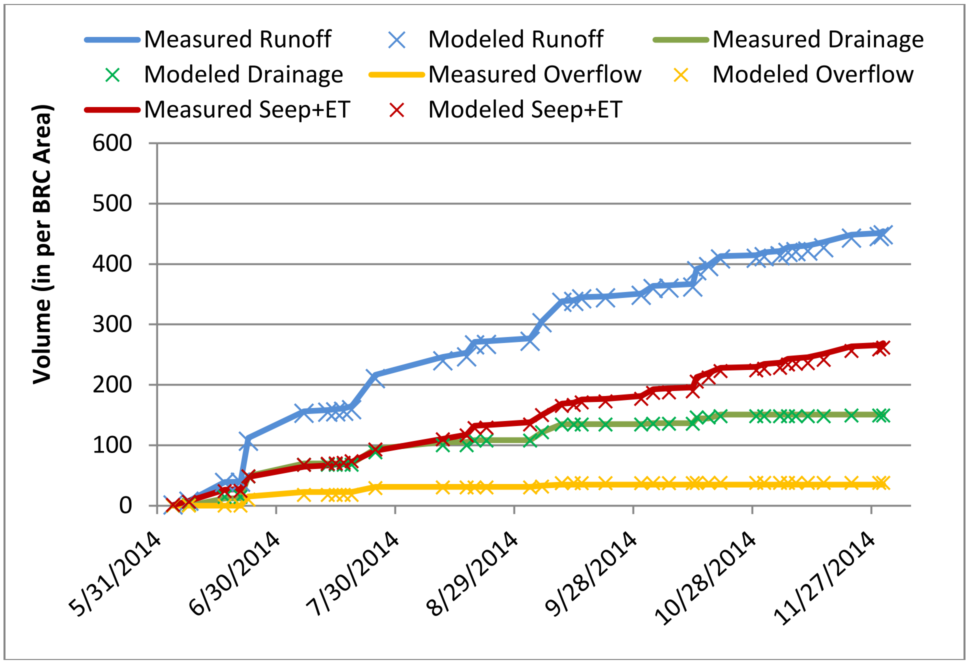

Figure 7. Cumulative fate of runoff for the Ursuline College bioretention cell, with field-measured depths shown as lines and modeled depth shown as symbols.

Table 7. Comparison of measured/estimated and modeled results for the Ursuline College bioretention cell.

Monitoring Period	Method of Comparison	Fate of Runoff: (inches per bioretention surface area over the monitoring period [percent of annual runoff])			
		Runoff	Drainage	Overflow	Exfiltration/ET
Calibration (June, August, October 2014)	Measured/estimated volume	236	82.1	11.5	142.7
			[34.8]	[4.9]	[60.4]
	Modeled volume	227	81.4	11.4	134.5
			[35.8]	[5]	[59.2]
	Difference between modeled and measured	-9	-1	0	-8
	Percent difference between modeled and measured	-4%	-0.9%	-1.5%	-5.7%
	Nash-Sutcliffe Coefficient	0.99	0.94	0.97	0.95
	Coefficient of Determination (r^2)	0.99	0.95	0.99	0.95
Monitoring Period	**Method of Comparison**	**Fate of Runoff**: (inches per bioretention surface area over the monitoring period [percent of annual runoff])			
		Runoff	Drainage	Overflow	Exfiltration/ET
Validation (May, July, September, November 2014)	Measured/estimated volume	218	72.1	19.5	126.3
			[33.1]	[8.9]	[57.9]
	Modeled volume	221	67.8	26.3	127.1
			[30.6]	[11.9]	[57.4]
	Difference between modeled and measured	-3.1	4.3	-6.8	-0.8
	Percent difference between modeled and measured	1.4%	-6.0%	34.7%	0.6%
	Nash-Sutcliffe Coefficient	0.99	0.98	0.73	0.95
	Coefficient of Determination (R^2)	1.00	0.99	0.89	0.96

For the Holden Arboretum bioretention cells, the duration of the monitoring period was 10 months, with the even months used for calibration and the odd months for validation (Table 8 and Table 9). Average rainfall depths were larger during the calibration period (0.60 inches) than in the validation period (0.43 inches), meaning about two-thirds of the inflow occurred during the calibration period. Both the Holden South and Holden North DRAINMOD models predicted the long-term fractions of drainage, overflow, and exfiltration/ET reliably (Figure 7 and Figure 8). Reliable monitoring data were not able to be collected during the winter months, due to snowfall and below freezing temperatures. Therefore, data from the beginning of December to the end of March were excluded from the modeling.

For the Holden South bioretention cell, the model was well calibrated against the field measured data, with Nash-Sutcliffe coefficients of 0.95, 0.87, and 0.77 for drainage, overflow, and exfiltration/ET, respectively. Corresponding coefficients of determination were 0.96, 1.0, and 0.80. Nash-Sutcliffe coefficients during the validation period were 0.95, 0.71, and 0.75 for drainage, overflow, and exfiltration/ET volume. Only 3 overflow events occurred during the monitoring period (2 during the calibration period and 1 during validation), resulting in large percentage errors during the calibration and validation periods. However, as a function of overall inflow volume, overflow was predicted to within 3.3% and 1.5% of the measured value during the calibration and validation periods, respectively. Coefficient of determination tended to be larger than Nash-Sutcliffe efficiency for overflow, since the calculation of R^2 takes into account storm events with zero overflow, while these events make very little difference in the calculation of the Nash-Sutcliffe coefficient. Modeled drainage and exfiltration/ET volumes were within 2% of the corresponding measured values, suggesting that DRAINMOD provided reliable long-term water balance predictions.

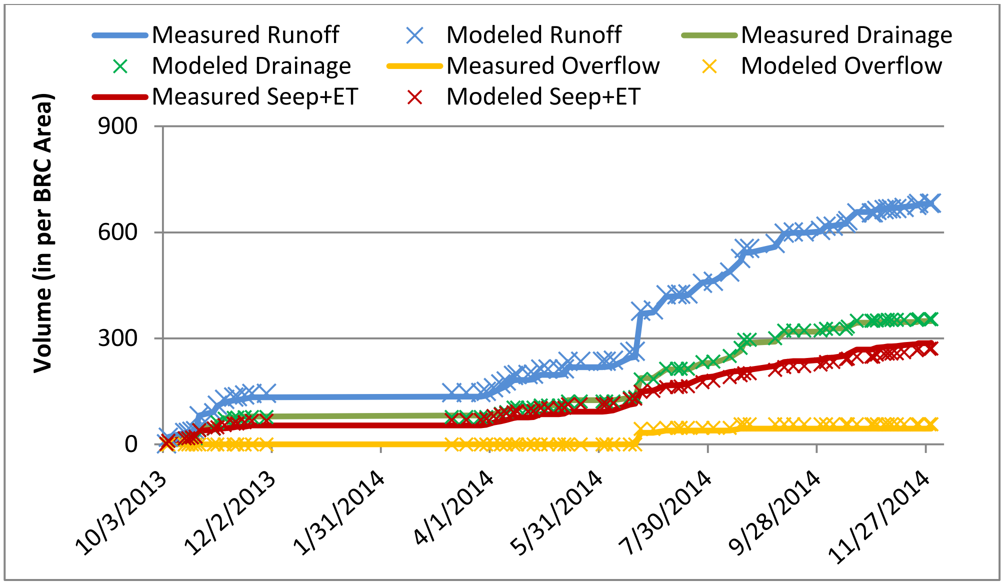

Figure 8. Cumulative fate of runoff for the Holden South bioretention cell, with field-measured depths shown as lines and modeled depth shown as symbols.

Table 8. Comparison of measured/estimated and modeled results for the Holden South bioretention cell.

Monitoring Period	Method of Comparison	Fate of Runoff: (inches per bioretention surface area over the monitoring period [percent of annual runoff])			
		Runoff	Drainage	Overflow	Exfiltration/ET
Calibration (Even Months)	Measured/estimated volume	452	226	39	188
			[49.9]	[8.6]	[41.5]
	Modeled volume	453	232	54	167
			[51.2]	[11.9]	[36.9]
	Difference between modeled and measured	1	6	15	-21
	Percent difference between modeled and measured	0.1%	2.8%	39.2%	-11.1%
	Nash-Sutcliffe Coefficient	0.99	0.96	0.87	0.76
	Coefficient of Determination (r^2)	0.99	0.96	1.00	0.80
Monitoring Period	**Method of Comparison**	**Fate of Runoff**: (inches per bioretention surface area over the monitoring period [percent of annual runoff])			
		Runoff	Drainage	Overflow	Exfiltration/ET
Validation (Odd Months)	Measured/estimated volume	224	121	6	97
			[53.8]	[2.8]	[43.4]
	Modeled volume	224	122	3	99
			[54.6]	[1.3]	[44.1]
	Difference between modeled and measured	0	-2	3	-1
	Percent difference between modeled and measured	-0.1%	1.4%	-52.9%	1.5%
	Nash-Sutcliffe Coefficient	0.96	0.95	0.71	0.75
	Coefficient of Determination (r^2)	0.97	0.96	1.00	0.76

The Holden North bioretention cell hydrologic data had the most inherent monitoring error, since the drainage and overflow from the South cell passed over the weir which measured outflow hydrology for the North cell (Winston et al. 2015). Thus, error inherent in monitoring the South cell was compounded in the North cell data, as drainage and overflow rate from the South cell were subtracted out of those measured at the North cell weir on a two-minute interval. Because of this additional error, and because design considerations were similar for the North and South cell, the North cell DRAINMOD model was not used for the sensitivity analysis that follows in section 3.2.3.

Despite this, the North cell DRAINMOD model was well calibrated against the field collected data, with excellent agreement between long-term runoff, drainage, overflow, and exfiltration/ET (Figure 8). Nash-Sutcliffe coefficients during the calibration period were 0.97, 0.87, and 0.81 for drainage, overflow, and exfiltration/ET volumes; corresponding r^2 values were all greater than 0.82. Total measured and monitored volumes of drainage and exfiltration/ET were within 4% over the calibration period. Overflow was over-predicted by about 50% during the calibration period and under-predicted by approximately the same amount during the validation period. This was probably due to the small number of overflow events (2 apiece during each modeling period). When comparing Nash-Sutcliffe coefficients during the validation period, NSEs from Holden North were the lowest of any of the modeled bioretention cells at 0.98, 0.74, and 0.76 for drainage, overflow, and exfiltration/ET, respectively. This probably was due to the additional error imparted by the monitoring scheme for this bioretention cell. Over the validation period, drainage and exfiltration/ET were each predicted to within 6% of measured volumes.

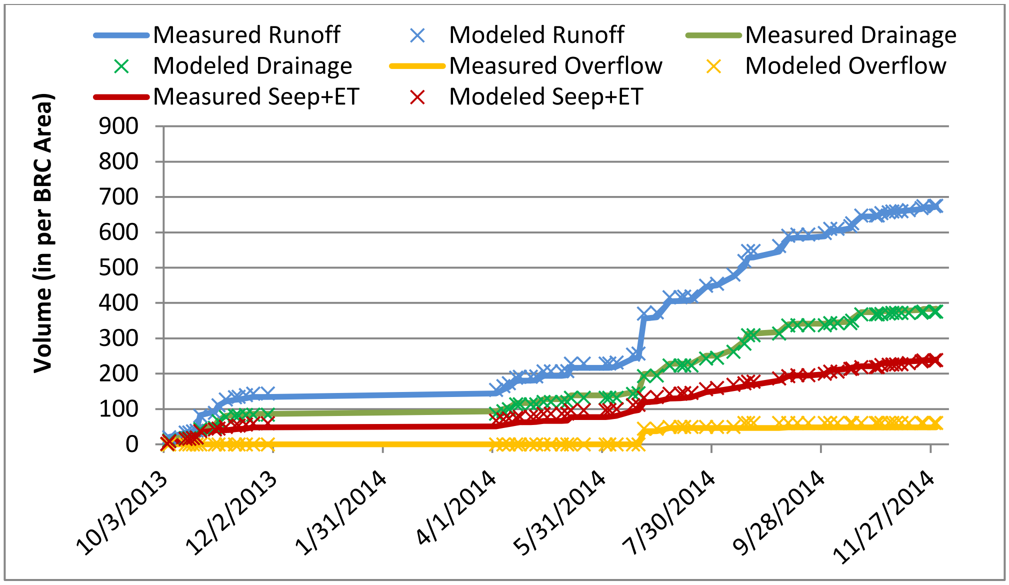

Figure 9. Cumulative fate of runoff for the Holden North bioretention cell, with field-measured depths shown as lines and modeled depth shown as symbols.

Table 9. Comparison of measured/estimated and modeled results for the Holden North bioretention cell.

Monitoring Period	Method of Comparison	Fate of Runoff: (inches per bioretention surface area over the monitoring period [percent of annual runoff])			
		Runoff	Drainage	Overflow	Exfiltration/ET
Calibration (Even Months)	Measured/estimated volume	445	254	37.3	154
			[57]	[8.4]	[34.6]
	Modeled volume	452	243	55.7	153
			[53.9]	[12.3]	[33.8]
	Difference between modeled and measured	6.9	-10.1	18.4	-1.4
	Percent difference between modeled and measured	1.5%	-4.0%	49.3%	-0.9%
	Nash-Sutcliffe Coefficient	0.99	0.97	0.87	0.81
	Coefficient of Determination (R^2)	0.99	0.97	0.94	0.82
Monitoring Period	**Method of Comparison**	**Fate of Runoff**: (inches per bioretention surface area over the monitoring period [percent of annual runoff])			
		Runoff	Drainage	Overflow	Exfiltration/ET
Validation (Odd Months)	Measured/estimated volume	233	129	11.4	92
			[55.5]	[4.9]	[39.5]
	Modeled volume	223	132	5.1	86
			[59.1]	[2.3]	[38.6]
	Difference between modeled and measured	9.7	-2.7	6.4	6.0
	Percent difference between modeled and measured	-4%	2%	-56%	-6%
	Nash-Sutcliffe Coefficient	0.96	0.98	0.74	0.76
	Coefficient of Determination (R^2)	0.97	0.98	0.96	0.77

The three DRAINMOD models developed for each field monitored bioretention cell in northeast Ohio were calibrated and validated, with reliable agreement between measured and modeled data. The lowest NSE and R^2 values were 0.71 and 0.76 for any combination of bioretention cell and modeling period. Following the work of Brown et al. (2013), this showed DRAINMOD is an excellent long-term, mechanistic model for prediction of bioretention performance. This is further supported by the measured versus modeled hydrology in Table 10, which shows excellent agreement for the percentage of the water balance (monitored versus modeled) over the entire monitoring period for each bioretention cell. At most, a 3% difference existed between monitored and modeled drainage, overflow, or exfiltration/ET. Because monitored hydrology from the Holden South and Ursuline monitoring sites were reliably predicted by DRAINMOD, these two models will be used as the basis for sensitivity analyses.

Table 10. Monitored versus modeled percentage of the water balance over the entire monitoring period for each of the bioretention cells in northeast Ohio.

Type of Data	Hydrologic Fate	Ursuline	Holden North	Holden South
Monitored	Drainage	33	57	51
Modeled		33	56	52
Monitored	Overflow	8	7	7
Modeled		9	9	8
Monitored	Exfiltration/ET	59	36	42
Modeled		58	35	40

3.2.3 Sensitivity Analysis

Calibrated models for Ursuline and Holden South were used as the basis for a sensitivity analysis. Base models were not modified from the design parameters determined from as-built surveys and laboratory measurements (Table 6). The one exception was underlying soil infiltration rate, which was set at four levels (0.5, 0.2, 0.05, and 0.02 in/hr) to create four base models. For each sensitivity analysis, one design variable was modified at a time and all other design variables held constant at their base case levels to reduce modeling error (Saltelli 2002). Design variables modified during the sensitivity analysis included: media depth, IWS zone depth, rooting depth, bowl storage depth, and hydraulic loading ratio (the ratio of watershed area to bioretention surface area). For each modeled case, the total inflow, drainage, overflow, exfiltration, and ET were cataloged and the percentage of each fate over the 30-yr weather record calculated.

Baseline model runs were utilized to develop benchmark long-term water balances for each of the underlying soil infiltration rates for both Ursuline and Holden South (Figure 9 and Figure 10). Because the two cells had slightly different design cross-sections and exfiltration rates (Table 6), the models produced slightly divergent results for the water balance over the long-term, with the fraction of drainage and exfiltration for the two cells within 15% of one another for all base case scenarios. The deeper ponding depth at the Holden South site may have been offset by a deeper IWS zone and a higher average exfiltration rate at the Ursuline site. Overflow decreased with increasing underlying soil infiltration rate, with at maximum 7% overflow in the 0.02 in/hr underlying soil infiltration rate case. In each case DRAINMOD predicted ET represented 5.5% or less of the water balance. For all base case scenarios, a minimum of 93% of the stormwater infiltrated the filter media, meaning that it either evapotranspired, exfiltrated, or left the system as treated drainage. Thus, designing to treat the 80th percentile event in Ohio (0.75 inches) results in treatment of the vast majority of the stormwater over the long-term.

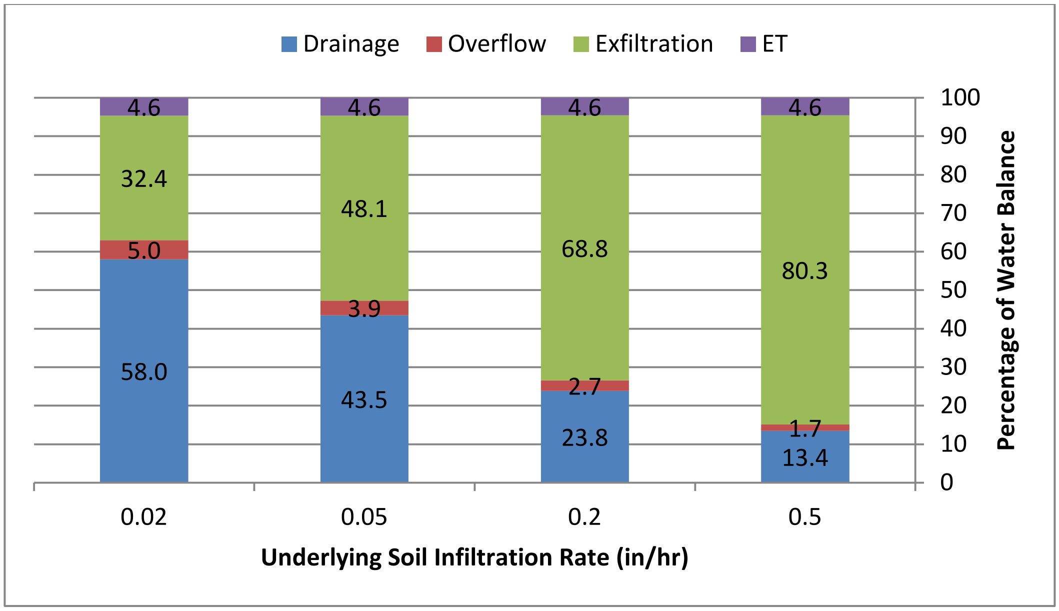

Figure 10. Base case model results for the Ursuline College bioretention cell.

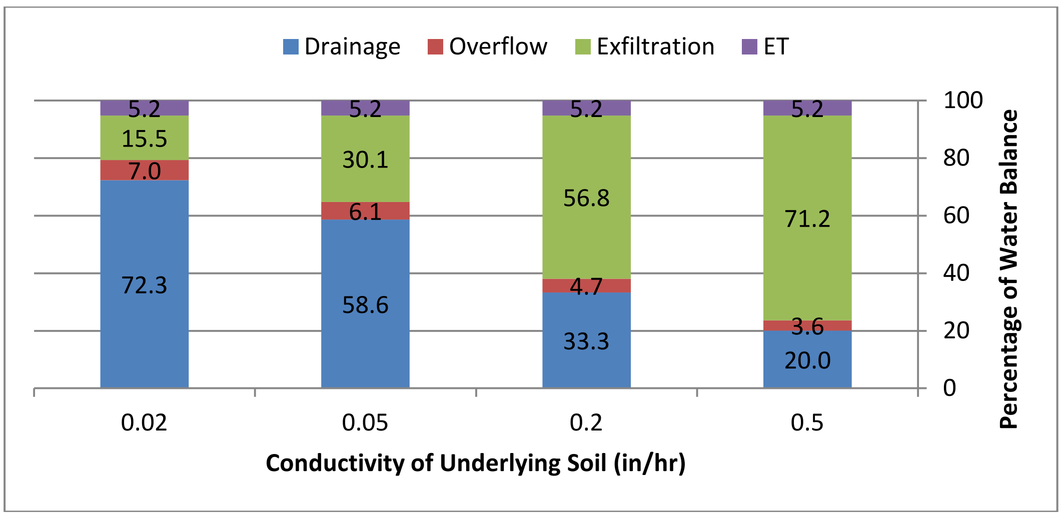

Figure 11. Base case model results for the Holden South bioretention cell.

3.2.3.1 Media Depth

To determine the effect of media depth on long-term bioretention hydrologic performance, the media depth was varied within the DRAINMOD soil file among commonly-used media depths of 2, 3, and 4 ft (Hunt et al. 2012). Beneath the media, 3 inches of clean sand, 3 inches of pea gravel, and 12 inches of #57 stone was modeled, as in the base case. The depth to the underdrain and the depth to the top of the IWS zone were also modified to keep a consistent IWS zone depth of 24 inches (Ursuline) or 15 inches (Holden South) based on the base case scenarios (Table 6). Results of each of the modeling runs are presented in Table 11 and Table 12, with total volume and percent of annual runoff shown.

As media depth increased, drainage tended to decrease (albeit modestly), especially in higher underlying soil infiltration rate scenarios. Media depth had very little impact on percentage exfiltration, with a 0-3% increase in exfiltration for each additional foot of media depth. Media depth had the greatest impact on the volume of overflow; for each additional foot of media depth, overflow decreased by 1-1.5% for underlying soil infiltration rate. Increasing media depth had no discernable effect on evapotranspiration. It should be noted that concomitant increases in rooting depth were not modeled, which may have augmented the evapotranspiration from the bioretention cells. While the modeled effects of media depth on long-term hydrology were modest, deeper media depths provide additional hydraulic retention time for treatment of nutrients (LeFevre et al. 2014) and dissipation of thermal load (Jones and Hunt 2009). These results are in contrast to past field monitoring results (Brown et al. 2011a; Davis et al. 2012) and recommendations for bioretention design published in the literature (Hunt et al. 2012), which claim media depth is a critical factor in bioretention hydrologic functionality. Since increases in media depth add significantly to construction costs, additional research is merited.

Table 11. Effect of media depth at Ursuline College for different underlying soil infiltration rates. Internal water storage depth was kept at 24 inches and the loading ratio at 20:1.

Media Depth (ft)	Underlying Soil Infiltration Rate (in/hr)	Annual Fate of Runoff: (in per bioretention surface area per year [percent of annual runoff])				
		Runoff	*Drainage*	*Overflow*	*Exfiltration*	*ET*
2	0.02	583	344 [58]	30 [5]	192 [32.4]	27 [4.6]
3	0.02	583	337 [56.8]	21 [3.6]	206 [34.8]	28 [4.7]
4	0.02	583	342 [57.8]	18 [3]	205 [34.6]	27 [4.6]
2	0.05	583	257 [43.5]	23 [3.9]	285 [48.1]	27 [4.6]
3	0.05	583	247 [41.7]	17 [2.9]	301 [50.8]	28 [4.7]
4	0.05	583	251 [42.4]	14 [2.4]	299 [50.5]	27 [4.6]
2	0.2	583	141 [23.8]	16 [2.7]	408 [68.8]	27 [4.6]
3	0.2	583	130 [21.9]	12 [2]	423 [71.5]	27 [4.6]
4	0.2	583	130 [21.9]	10 [1.7]	425 [71.8]	27 [4.6]
2	0.5	583	79 [13.4]	10 [1.7]	475 [80.3]	27 [4.6]
3	0.5	583	70 [11.9]	8 [1.3]	487 [82.2]	27 [4.6]
4	0.5	583	69 [11.7]	6 [1.1]	490 [82.7]	27 [4.6]

Table 12. Effect of media depth at Holden South for different underlying soil infiltration rates. Internal water storage depth was kept at 15 inches and the loading ratio at 20:1.

Media Depth (ft)	Underlying Soil Infiltration Rate (in/hr)	Annual Fate of Runoff: (in per bioretention surface area per year [percent of annual runoff])				
		Runoff	*Drainage*	*Overflow*	*Exfiltration*	*ET*
2	0.02	522	371 [71.1]	44 [8.4]	80 [15.3]	27 [5.2]
3	0.02	522	378 [72.3]	36 [7]	81 [15.5]	27 [5.2]
4	0.02	522	383 [73.4]	28 [5.5]	83 [15.9]	28 [5.3]
2	0.05	522	300 [57.4]	39 [7.5]	156 [29.9]	27 [5.2]
3	0.05	522	306 [58.6]	32 [6.1]	157 [30.1]	27 [5.2]
4	0.05	522	309 [59.1]	27 [5.1]	159 [30.5]	28 [5.3]
2	0.2	522	171 [32.8]	30 [5.8]	294 [56.3]	27 [5.2]
3	0.2	522	174 [33.3]	25 [4.7]	297 [56.8]	27 [5.2]
4	0.2	522	178 [34.1]	20 [3.8]	297 [56.9]	27 [5.2]
2	0.5	522	102 [19.4]	24 [4.6]	370 [70.8]	27 [5.2]
3	0.5	522	105 [20]	19 [3.6]	372 [71.2]	27 [5.2]
4	0.5	522	107 [20.5]	15 [2.8]	374 [71.6]	27 [5.2]

3.2.3.2 Internal Water Storage Zone Depth

The effect of an IWS zone on long-term bioretention hydrology was evaluated by varying the weir depth in DRAINMOD to change the invert elevation of the underdrain. For both the Ursuline and Holden South base models, the IWS zone depth was varied to: 0 inches (i.e. standard underdrain at the bottom of the cell), 6 inches, 12 inches, 18 inches, and 24 inches (Table 13 and Table 14).

The inclusion of an IWS zone improved bioretention cell volume reduction performance, with each increase of 6 inches in IWS zone depth decreasing the fraction of drainage and increasing that of exfiltration. For all underlying soil infiltration rates, there is typically a 15-30% increase in exfiltration from a bioretention cell without IWS to a 24 inch IWS zone, regardless of underlying soil type. These results confirm those from field and lab-scale testing of the effects of IWS zones on bioretention hydrology (Li et al. 2009; Brown and Hunt 2011b; Lucas and Greenway 2011). The Holden South and Ursuline models diverge with regards to the optimal IWS zone depth: for Ursuline, an 18 inch IWS zone depth maximized exfiltration and minimized drainage; however, for Holden South, a 24 inch IWS zone depth still provided additional benefit to the hydrologic balance. This is most probably related to the exfiltration rates and media saturated hydraulic conductivity for the bioretention cells, which were used to calibrate the respective models; the average exfiltration rates were 0.17 and 0.083 in/hr, respectively, at Ursuline and Holden South. Media K_{sat} was 6.5 in/hr and 4 in/hr, respectively. The higher exfiltration rate and media K_{sat} at Ursuline produced a point of diminishing returns where the IWS zone emptied during most dry periods, maximizing storage for the following storm. Thus, increasing the IWS zone beyond this optimal depth provided minimal additional benefit. For underlying soils with higher conductivity than Ursuline, the optimal IWS zone depth will be smaller than 18 inches.

In the poorest underlying soil conditions (0.02 and 0.05 in/hr infiltration rates), increasing the IWS zone marginally increases the long-term fraction of overflow. This increase is about 1.5-3% in 0.02 in/hr conductivity soils and 1-2% in 0.05 in/hr conductivity soils. In soils with higher infiltration rates, the IWS zone dewaters more quickly, resulting in little to no increase in overflow as IWS zone depth increases. The long-term fraction of ET was not impacted by the inclusion of an IWS zone, and was between 4.5-5.5% for the two bioretention cells.

Table 13. Effect of IWS zone depth at Ursuline College for different underlying soil infiltration rates.

IWS Depth (in)	Underlying Soil Infiltration Rate (in/hr)	Annual Fate of Runoff: (in per bioretention surface area per year [percent of annual runoff])				
		Runoff	*Drainage*	*Overflow*	*Exfiltration*	*ET*
0	0.02	583	495 [83.6]	21 [3.6]	49 [8.2]	27 [4.6]
6		583	452 [76.4]	21 [3.5]	92 [15.5]	27 [4.6]
12		583	401 [67.7]	24 [4.1]	140 [23.6]	27 [4.6]
15		583	360 [60.7]	28 [4.7]	177 [29.9]	27 [4.6]
18		583	344 [58.1]	30 [5.1]	190 [32.1]	28 [4.7]
24		583	344 [58]	30 [5]	192 [32.4]	27 [4.6]
0	0.05	583	446 [75.4]	18 [3.1]	100 [16.9]	27 [4.6]
6		583	377 [63.7]	19 [3.2]	169 [28.5]	27 [4.6]
12		583	314 [53]	21 [3.5]	230 [38.9]	27 [4.6]
15		583	272 [45.9]	22 [3.7]	271 [45.8]	27 [4.6]
18		583	258 [43.6]	23 [3.8]	283 [47.9]	28 [4.7]
24		583	257 [43.5]	23 [3.9]	285 [48.1]	27 [4.6]
0	0.2	583	314 [52.9]	15 [2.5]	237 [39.9]	27 [4.6]
6		583	236 [39.8]	14 [2.4]	315 [53.2]	27 [4.6]
12		583	181 [30.6]	15 [2.5]	369 [62.3]	27 [4.6]
15		583	150 [25.3]	16 [2.7]	400 [67.5]	27 [4.6]
18		583	141 [23.8]	17 [2.8]	406 [68.6]	28 [4.7]
24		583	141 [23.8]	16 [2.7]	408 [68.8]	27 [4.6]
0	0.5	583	200 [33.8]	11 [1.8]	354 [59.8]	27 [4.6]
6		583	140 [23.6]	10 [1.7]	415 [70.1]	27 [4.6]
12		583	103 [17.5]	10 [1.7]	452 [76.2]	27 [4.6]
15		583	86 [14.5]	10 [1.7]	469 [79.2]	27 [4.6]
18		583	79 [13.4]	10 [1.8]	474 [80.1]	28 [4.7]
24		583	79 [13.4]	10 [1.7]	475 [80.3]	27 [4.6]

Table 14. Effect of IWS zone depth at Holden South for different underlying soil infiltration rates

IWS Depth (in)	Underlying Soil Infiltration Rate (in/hr)	Annual Fate of Runoff: (in per bioretention surface area per year [percent of annual runoff])				
		Runoff	*Drainage*	*Overflow*	*Exfiltration*	*ET*
0	0.02	522	435 [83.3]	28 [5.3]	32 [6.2]	27 [5.2]
6		522	414 [79.2]	29 [5.6]	52 [9.9]	27 [5.2]
12		522	391 [74.8]	34 [6.5]	71 [13.5]	27 [5.2]
15		522	378 [72.3]	36 [7]	81 [15.5]	27 [5.2]
18		522	368 [70.5]	37 [7.1]	90 [17.2]	27 [5.2]
24		522	348 [66.6]	42 [8.1]	105 [20.1]	27 [5.2]
0	0.05	522	400 [76.5]	26 [5.1]	69 [13.3]	27 [5.2]
6		522	360 [68.9]	28 [5.3]	108 [20.7]	27 [5.2]
12		522	322 [61.6]	34 [6.4]	140 [26.8]	27 [5.2]
15		522	306 [58.6]	32 [6.1]	157 [30.1]	27 [5.2]
18		522	289 [55.4]	34 [6.6]	172 [32.8]	27 [5.2]
24		522	266 [50.9]	36 [6.8]	194 [37.1]	27 [5.2]
0	0.2	522	304 [58.3]	23 [4.4]	168 [32.1]	27 [5.2]
6		522	241 [46]	22 [4.3]	232 [44.5]	27 [5.2]
12		522	195 [37.3]	24 [4.5]	277 [53]	27 [5.2]
15		522	174 [33.3]	25 [4.7]	297 [56.8]	27 [5.2]
18		522	160 [30.6]	24 [4.7]	311 [59.6]	27 [5.2]
24		522	137 [26.2]	25 [4.8]	333 [63.8]	27 [5.2]
0	0.5	522	224 [42.9]	18 [3.4]	253 [48.5]	27 [5.2]
6		522	164 [31.4]	17 [3.3]	314 [60.1]	27 [5.2]
12		522	121 [23.3]	19 [3.5]	355 [68]	27 [5.2]
15		522	105 [20]	19 [3.6]	372 [71.2]	27 [5.2]
18		522	94 [18]	18 [3.4]	383 [73.4]	27 [5.2]
24		522	78 [14.9]	18 [3.4]	399 [76.5]	27 [5.2]

3.2.3.3 Rooting Depth

To determine effects of larger plants with more vigorous roots on long-term hydrology, the rooting depth was varied in both the soil file and the crop tab in DRAINMOD. The base model assumed a 12 inch rooting depth, since plants were juvenile during the monitoring period. For each underlying soil infiltration rate, the model was also varied to a 24 inch rooting depth.

The inclusion of a deeper rooting depth modestly increased the fraction of ET over the long-term at Ursuline College (by 0.1%), but made no difference at Holden South. Deeper rooting depth did not affect the hydrologic balance much for the Holden South model. The Ursuline College model was more sensitive to rooting depth, with changes to the long-term hydrology (drainage, overflow, and exfiltration) observed for all underlying soil infiltration rates. Perhaps the deeper rooting depth case at Ursuline aided the plants in transpiring additional runoff volume, because the top of the IWS zone was 1 ft closer to the soil surface at Ursuline than at Holden South. The lower saturated hydraulic conductivity and lower exfiltration rate, coupled with the presence of an IWS zone, probably meant the roots in the Holden South cell had easier access to water during dry periods. Therefore, additional rooting depth did not change system performance.

Table 15. Effect of rooting depth for the Ursuline College bioretention cells as a function of various underlying soil infiltration rates.

Rooting Depth (in)	Underlying Soil Infiltration Rate (in/hr)	Annual Fate of Runoff: (in per bioretention surface area per year [percent of annual runoff])				
		Runoff	*Drainage*	*Overflow*	*Exfiltration*	*ET*
12	0.02	583	344 [58]	30 [5]	192 [32.4]	27 [4.6]
24		583	344 [58.1]	344 [5.1]	190 [32.1]	28 [4.7]
12	0.05	583	257 [43.5]	257 [3.9]	285 [48.1]	27 [4.6]
24		583	258 [43.6]	258 [3.8]	283 [47.9]	28 [4.7]
12	0.2	583	141 [23.8]	141 [2.7]	408 [68.8]	27 [4.6]
24		583	141 [23.8]	141 [2.8]	406 [68.6]	28 [4.7]
12	0.5	583	79 [13.4]	79 [1.7]	475 [80.3]	27 [4.6]
24		583	79 [13.4]	79 [1.8]	474 [80.1]	28 [4.7]

Table 16. Effect of rooting depth at Holden South as a function of various underlying soil infiltration rates.

Rooting Depth (in)	Underlying Soil Infiltration Rate (in/hr)	Annual Fate of Runoff: (in per bioretention surface area per year [percent of annual runoff])				
		Runoff	*Drainage*	*Overflow*	*Exfiltration*	*ET*
12	0.02	522	378 [72.3]	36 [7]	81 [15.5]	27 [5.2]
24		522	378 [72.3]	36 [7]	81 [15.5]	27 [5.2]
12	0.05	522	306 [58.6]	32 [6.1]	157 [30.1]	27 [5.2]
24		522	306 [58.6]	32 [6.1]	157 [30.1]	27 [5.2]
12	0.2	522	174 [33.3]	25 [4.7]	297 [56.8]	27 [5.2]
24		522	174 [33.3]	25 [4.7]	297 [56.8]	27 [5.2]
12	0.5	522	105 [20]	19 [3.6]	372 [71.2]	27 [5.2]
24		522	105 [20]	19 [3.6]	372 [71.2]	27 [5.2]

3.2.3.4 Bowl Storage Depth

Bowl storage depth was varied within the model to determine its effects on long-term volume capture. For each base case, ponding depth was modeled at the following levels: 9, 12, 15, 18, and 24 inches. Contributing watershed area was not modified, so the increase or decrease in ponding depth modified the size of the runoff volume that was being treated.

Increasing ponding depth augmented the fraction of water treated by the media, and decreased the volume of overflow from the bioretention cells. This was most prevalent in the poorest infiltrating soils, with a 5-7% increase in the drainage fraction from the smallest to largest ponding depth. Corresponding decreases in overflow occurred, and were of similar magnitude. For instance, for the 0.02 in/hr underlying soil case at Holden South, the overflow percentage decreased from 11% to 4% when ponding depth was increased from 9 to 24 inches. While the fraction of treated outflow increased with deeper ponding depth, the larger benefit is perhaps to peak flow mitigation (which DRAINMOD does not model), where a greater volume capture increases the likelihood the peak rainfall intensity during an event will be entirely captured (i.e. no overflow) by the bioretention cell (Heasom et al. 2006; Davis et al. 2012). It should be noted, however, deeper ponding depths can have detrimental effects on plant health, jeopardizing bioretention cell functionality (Hunt et al. 2012). Ponding depth had minor effects on long-term exfiltration (minor increases with ponding depth) and no appreciable influence on ET. However, if overly deep ponding depths killed off plants in this SCM, the fraction of long-term ET would certainly decline.

Table 17. Effect of bowl storage depth at Ursuline College on the water balance with various underlying soil infiltration rates.

Ponding Depth (in)	Underlying Soil Infiltration Rate (in/hr)	Annual Fate of Runoff: (in per bioretention surface area per year [percent of annual runoff])				
		Runoff	*Drainage*	*Overflow*	*Exfiltration*	*ET*
9	0.02	583	336 [56.7]	38 [6.3]	192 [32.3]	27 [4.6]
12		583	344 [58]	344 [5]	192 [32.4]	27 [4.6]
15		583	348 [58.7]	348 [4.3]	192 [32.4]	27 [4.6]
18		583	359 [60.6]	14 [2.4]	192 [32.4]	27 [4.6]
24		583	364 [61.5]	9 [1.5]	192 [32.5]	27 [4.6]
9	0.05	583	252 [42.5]	29 [4.9]	284 [47.9]	27 [4.6]
12		583	257 [43.5]	23 [3.9]	285 [48.1]	27 [4.6]
15		583	260 [43.9]	20 [3.4]	285 [48.1]	27 [4.6]
18		583	269 [45.4]	11 [1.8]	286 [48.2]	27 [4.6]
24		583	272 [46]	7 [1.1]	286 [48.3]	27 [4.6]
9	0.2	583	138 [23.3]	20 [3.5]	407 [68.7]	27 [4.6]
12		583	141 [23.8]	16 [2.7]	408 [68.8]	27 [4.6]
15		583	142 [24]	14 [2.4]	409 [69]	27 [4.6]
18		583	147 [24.9]	7 [1.3]	410 [69.3]	27 [4.6]
24		583	150 [25.3]	4 [0.7]	411 [69.4]	27 [4.6]
9	0.5	583	78 [13.2]	13 [2.2]	474 [80]	27 [4.6]
12		583	79 [13.4]	10 [1.7]	475 [80.3]	27 [4.6]
15		583	80 [13.6]	9 [1.5]	476 [80.3]	27 [4.6]
18		583	83 [13.9]	5 [0.8]	478 [80.7]	27 [4.6]
24		583	83 [14.1]	3 [0.5]	479 [80.8]	27 [4.6]

Table 18. Effect of bowl storage depth at Holden South on the water balance with various underlying soil infiltration rates.

Ponding Depth (in)	Underlying Soil Infiltration Rate (in/hr)	Annual Fate of Runoff: (in per bioretention surface area per year [percent of annual runoff])				
		Runoff	*Drainage*	*Overflow*	*Exfiltration*	*ET*
9	0.02	522	358 [68.5]	57 [10.9]	81 [15.4]	27 [5.2]
12		522	369 [70.7]	45 [8.7]	81 [15.5]	27 [5.2]
15		522	378 [72.3]	36 [7]	81 [15.5]	27 [5.2]
18		522	384 [73.4]	31 [5.8]	81 [15.5]	27 [5.2]
24		522	392 [75.1]	22 [4.1]	81 [15.6]	27 [5.2]
9	0.05	522	290 [55.5]	49 [9.4]	156 [29.9]	27 [5.2]
12		522	299 [57.2]	40 [7.6]	157 [30]	27 [5.2]
15		522	306 [58.6]	32 [6.1]	157 [30.1]	27 [5.2]
18		522	311 [59.5]	27 [5.1]	158 [30.2]	27 [5.2]
24		522	319 [61]	19 [3.6]	158 [30.2]	27 [5.2]
9	0.2	522	164 [31.4]	38 [7.3]	294 [56.2]	27 [5.2]
12		522	170 [32.5]	31 [5.8]	295 [56.5]	27 [5.2]
15		522	174 [33.3]	25 [4.7]	297 [56.8]	27 [5.2]
18		522	177 [33.9]	21 [4]	297 [56.9]	27 [5.2]
24		522	182 [34.9]	14 [2.7]	299 [57.2]	27 [5.2]
9	0.5	522	99 [19]	28 [5.4]	368 [70.4]	27 [5.2]
12		522	102 [19.6]	23 [4.4]	370 [70.9]	27 [5.2]
15		522	105 [20]	19 [3.6]	372 [71.2]	27 [5.2]
18		522	106 [20.3]	16 [3]	374 [71.5]	27 [5.2]
24		522	109 [20.9]	10 [2]	376 [72]	27 [5.2]

3.2.3.5 Watershed Area to Bioretention Surface Area Ratio

To determine the effects of under- or over-sizing bioretention filter bed area on long-term performance, the field ratio in the DRAINMOD was varied to simulate changes in watershed area to bioretention surface area ratio. The percentage imperviousness of the watersheds was not modified, nor was the surface area of the bioretention cell.

As the hydraulic loading ratio (HLR) increased, the amount of inflow to the bioretention cell increased due to the change in watershed size. Substantial differences in drainage, overflow, exfiltration, and ET existed across the various HLRs and underlying soil infiltration rates. The fraction of drainage increased rapidly as an oversized system approached the standard 20:1 design scenario used in Ohio. When HLR was greater than 20:1, the fraction of overflow increased substantially, moderating or halting further increases in percentage of drainage. As additional inflow was added to the bioretention cell through increases in HLR, the proportion of exfiltration decreases by as much as 35% for a given underlying soil infiltration rate. HLR was the one factor that substantially affected the long-term percentage of ET, with the lowest loading ratio having 6-7% and the highest 2-3% ET. Since the same amount of plants and media are present (i.e. bioretention size is not changing), the volume of ET stays constant, but the percentage varies based on the inflow volume. The results for each underlying soil infiltration rate suggested undersized bioretention cells provide at most only 20% less treated outflow (i.e. the sum of underdrain flow, exfiltration, and ET) than the standard 20:1 design. This suggested undersized systems might deserve proportionally more credit. This is further supported by the field research on undersized bioretention cells in Luell et al. (2011). The long-term fraction of overflow declines in undersized systems as the underlying soil infiltration rate increases; thus, undersized systems situated over sandy soils might be particularly good retrofits. However, it should be noted maintenance frequency and effort for pre-treatment devices will increase as the bioretention cell becomes increasingly undersized.

Table 19. Effect of hydraulic loading ratio at the Ursuline College bioretention cell on the water balance with various underlying soil infiltration rates.

HLR	Underlying Soil Infiltration Rate (in/hr)	Annual Fate of Runoff: (in per bioretention surface area per year [percent of annual runoff])				
		Runoff	*Drainage*	*Overflow*	*Exfiltration*	*ET*
10:1	0.02	429	226 [51.8]	7 [1.7]	176 [40.2]	27 [6.2]
15:1		583	344 [58]	30 [5]	192 [32.4]	27 [4.6]
20:1		719	446 [61.1]	55 [7.6]	202 [27.6]	27 [3.8]
35:1		1152	709 [60.6]	214 [18.3]	220 [18.8]	27 [2.3]
50:1		1589	907 [56.2]	449 [27.8]	231 [14.3]	27 [1.7]
10:1	0.05	429	156 [35.8]	7 [1.5]	246 [56.5]	27 [6.2]
15:1		583	257 [43.5]	23 [3.9]	285 [48.1]	27 [4.6]
20:1		719	344 [47.2]	49 [6.7]	310 [42.4]	27 [3.7]
35:1		1152	588 [50.2]	194 [16.5]	362 [30.9]	27 [2.3]
50:1		1589	780 [48.3]	413 [25.6]	394 [24.4]	27 [1.7]
10:1	0.2	429	77 [17.7]	4 [1]	328 [75.1]	27 [6.2]
15:1		583	141 [23.8]	16 [2.7]	408 [68.8]	27 [4.6]
20:1		719	201 [27.6]	34 [4.7]	467 [64]	27 [3.7]
35:1		1152	381 [32.5]	152 [13]	611 [52.1]	27 [2.3]
50:1		1589	534 [33.1]	342 [21.2]	711 [44]	27 [1.7]
10:1	0.5	429	40 [9.2]	3 [0.7]	366 [83.9]	27 [6.2]
15:1		583	79 [13.4]	10 [1.7]	475 [80.3]	27 [4.6]
20:1		719	119 [16.3]	23 [3.1]	562 [76.9]	27 [3.7]
35:1		1152	244 [20.9]	112 [9.6]	787 [67.2]	27 [2.3]
50:1		1589	358 [22.2]	267 [16.5]	962 [59.6]	27 [1.7]

Table 20. Effect of hydraulic loading ratio at Holden South on the water balance with various underlying soil infiltration rates.

HLR	Underlying Soil Infiltration Rate (in/hr)	Annual Fate of Runoff: (in per bioretention surface area per year [percent of annual runoff])				
		Runoff	*Drainage*	*Overflow*	*Exfiltration*	*ET*
10:1	0.02	371	256 [69.2]	10 [2.7]	77 [20.8]	27 [7.3]
15:1		447	320 [71.6]	21 [4.6]	79 [17.7]	27 [6.1]
20:1		522	378 [72.3]	36 [7]	81 [15.5]	27 [5.2]
35:1		750	532 [71]	105 [14.1]	85 [11.3]	27 [3.6]
50:1		977	651 [66.6]	211 [21.6]	88 [9]	27 [2.8]
10:1	0.05	371	192 [51.8]	9 [2.3]	143 [38.7]	27 [7.3]
15:1		447	250 [56]	18 [4.1]	151 [33.8]	27 [6]
20:1		522	306 [58.6]	32 [6.1]	157 [30.1]	27 [5.2]
35:1		750	457 [60.9]	95 [12.7]	171 [22.8]	27 [3.6]
50:1		977	578 [59.1]	191 [19.6]	181 [18.5]	27 [2.8]
10:1	0.2	371	95 [25.6]	7 [1.8]	242 [65.4]	27 [7.3]
15:1		447	134 [30.1]	14 [3.1]	271 [60.8]	27 [6]
20:1		522	174 [33.3]	25 [4.7]	297 [56.8]	27 [5.2]
35:1		750	286 [38.1]	81 [10.8]	356 [47.5]	27 [3.6]
50:1		977	386 [39.5]	165 [16.9]	400 [40.9]	27 [2.8]
10:1	0.5	371	53 [14.4]	4 [1]	287 [77.4]	27 [7.3]
15:1		447	79 [17.6]	9 [2.1]	332 [74.3]	27 [6]
20:1		522	105 [20]	19 [3.6]	372 [71.2]	27 [5.2]
35:1		750	183 [24.4]	64 [8.5]	475 [63.4]	27 [3.6]
50:1		977	255 [26.1]	139 [14.2]	556 [56.9]	27 [2.8]

3.2.4 Bioretention Performance under Climate Change Scenarios

3.2.4.1 Climate Data Summary

In order to frame the hydrologic modeling, temperature, and rainfall data were summarized in Table 21 for the Ursuline College and Holden Arboretum sites under both current (2001-2004, baseline) and mid-century (2055-2059, RCP4.5 and RCP8.5) scenarios. Discrete hydrologic storm events were identified by an antecedent dry period of at minimum six hours and an event depth of at least 0.1 inches (Driscoll, 1989). Average annual precipitation was highest during the current climate, and mean and median event depth tended to decrease in the mid-century data. At Holden Arboretum, the extreme rainfall events, represented by the 90th percentile and maximum storm depths, tended to moderate in the future. At Ursuline College, maximum rainfall depths increased in the future climate scenarios; these differences in extreme rainfall show how spatially varied future climate predictions are, as the two sites are 25 km apart.

Consecutive dry days also tended to increase in future climate scenarios for measures of central tendency and extreme cases at both Ursuline College and Holden Arboretum. Longer dry periods and moderating rainfall depths are consistent with future climate data presented for this region in Gao et al. (2012). Mean and median daily temperature was predicted to increase by 3-5˚F for this region, and maximum and minimum average daily temperatures were exacerbated under future climate scenarios, warming by 3-10˚F. In combination with decreased annual precipitation depths, these data suggested a hotter, drier, and more drought-prone climate for this region of the Lake Erie shoreline.

Table 21. Precipitation and temperature summary statistics for Ursuline College and Holden Arboretum under all climate scenarios.

Parameter	Statistic	Ursuline College			Holden Arboretum		
		Baseline	RCP 4.5	RCP 8.5	Baseline	RCP 4.5	RCP 8.5
Consecutive Dry Days	Maximum	35.7	43.3	31.8	36.3	51.3	39.8
	90th percentile	9.5	11.3	11.4	10.0	11.6	11.9
	Mean	4.4	5.0	5.1	4.8	5.1	5.2
	Median	3.4	3.3	3.4	3.3	3.4	3.4
	St. Dev	4.3	5.3	4.9	5.3	5.7	5.6
Storm Event Summary	Annual average rainfall (in)	37.85	33.24	36.60	37.94	31.64	32.40
	Max (in)	3.14	3.57	5.33	4.12	3.73	3.97
	90th percentile (in)	1.37	1.20	1.40	1.39	1.11	1.16
	Mean (in)	0.56	0.55	0.60	0.60	0.53	0.54
	Median (in)	0.40	0.36	0.33	0.41	0.35	0.34
	St. Dev. (in)	0.52	0.57	0.66	0.59	0.56	0.58
Temperature	Mean (F)	54.0	57.2	58.3	51.9	55.1	56.1
	Median (F)	55.7	59.1	60.8	53.8	57.3	58.7
	St. Dev (F)	19.7	19.8	21.0	19.1	19.2	20.3
	Maximum daily average (F)	91.2	93.3	97.9	86.2	89.9	93.6
	Minimum daily average (F)	-3.5	-7.5	0.2	-12.7	-10.6	-1.8

3.2.4.1 Hydrologic Balance under Climate Change Scenarios

Calibrated and validated DRAINMOD models for Ursuline College, Holden South, and Holden North were utilized in the climate change scenarios without modification, similar to methods in Hathaway et al. (2014). Current, RCP 4.5, and RCP 8.5 rainfall and temperature data were input into DRAINMOD, contributing runoff files were created, and the bioretention models were simulated. Summary statistics are presented in Table 22. The percent difference in depth of each hydrologic fate was calculated as:

$$\frac{Depth_{RCP} - Depth_{Base}}{Depth_{Base}} * 100 \tag{3.3}$$

Differences in the water balance among the baseline and future climate scenarios were calculated as (with the given example for drainage):

$$\%Drain_{RCP} - \%Drain_{Base} \tag{3.4}$$

Because of the generally decreasing future annual rainfall totals, the inflow to the Holden Arboretum bioretention cells was less under the future climate scenarios than under the current climate. While average and extreme event rainfall depth tended to decrease with time at Holden Arboretum, overflow volume and percentage of the water balance actually increased. This could be related to back-to-back large storm events. Drainage volume was in most cases unchanged or up to 37% less, although one future scenario at Ursuline resulted in a 31% increase in drainage, resulting in 6% increase in drainage in the overall water balance. Exfiltration volumes were around 10-20% less under future climate scenarios based on depth, but only modestly changed as a percentage of the water balance. Due to the warmer air temperatures, longer dry periods, and low exfiltration rates resulting in long-term storage of water in the IWS zone, evaporation increased by 5-34%, depending on the future climate scenario. For the Holden Arboretum bioretention cells, the percentage of runoff volume abstracted (i.e. the sum of exfiltration and

ET) increased by 4-8%; however, the percentage of total inflow that overflowed the Holden Arboretum bioretention cells was the same or higher under future climate scenarios, resulting from smaller inflow but similar overflow volumes. The future performance of the Holden Arboretum was expected to be better for volume reduction, but up to 24% more untreated overflow could occur.

At Ursuline College, the DRAINMOD model predicted a decrease (RCP 4.5) or modest increase (RCP 8.5) in surface runoff. This factor combined with higher average and extreme rainfall depths resulted in 2-6% greater drainage fraction of the water balance under future climate. Drainage depth was either unchanged or increased by 30% from the base case. Overflow depth increased by 5-66% under future climate scenarios, representing a 1-2% increase in the overall water balance under RCP 4.5 and 8.5, respectively. Exfiltration depth decreased by 10-20% from the base case; this decreased abstraction was partially offset by a smaller volume but similar percentage increase in ET. Overall, volume reduction as a percentage of inflow was 72% under the base climate scenario; this decreased to 69% and 64% under RCP 4.5 and 8.5, respectively. The bioretention cell at Ursuline College is thus expected to perform worse for volume reduction and treated percentage of the water balance under future climate conditions.

Taken together, the future climate modeling suggests that volume mitigation provided by bioretention SCMs in Northeast Ohio will in some cases be slightly better than current performance (by 4-8% at Holden Arboretum) and in some cases suffer (by 3-8% at Ursuline College). This is due to the spatially diverse rainfall and temperature data under future climate scenarios, and suggests the need for additional resolution both spatially and temporally to effectively model site scale, small watershed hydrology. Overflow as a percentage of total inflow to the bioretention cells increased under most future climate scenarios. Total outflow decreased under all but one of the future climate scenario and bioretention cell combinations, owing to the decreased inflow caused by lower annual rainfall depths and generally smaller median and mean rainfall depths. Evaporation increased in all modeled bioretention cells under future climate due to elevated temperatures and elongated dry periods.

Table 22. Average annual water balances for each site and climate profile. Depths are in terms of inches per bioretention surface area.

Site	**Climate Scenario**	**Runoff**	**Drainage**				**Overflow**				**Exfiltration**				**Evaporation**			
		Depth (in)	Depth (in)	% Difference Depth	% of Runoff	Difference Water Balance	Depth (in)	% Difference Depth	% of Runoff	% Difference Water Balance	Depth (in)	% Difference Depth	% of Runoff	% Difference Water Balance	Depth (in)	% Difference Depth	% of Runoff	% Difference Water Balance
Ursuline College	Base	549	129	-	23	-	20	-	4	-	365	-	67	-	32	-	6	-
	RCP 4.5	486	126	-2	26	2	21	5	4	1	303	-17	62	-4	34	5	7	1
	RCP 8.5	567	169	31	30	6	32	66	6	2	325	-11	57	-9	38	19	7	1
Holden South	Base	539	278	-	52	-	28	-	5	-	203	-	38	-	27	-	5	-
	RCP 4.5	421	185	-33	44	-8	35	24	8	3	167	-18	40	2	34	23	8	3
	RCP 8.5	422	175	-37	41	-10	32	13	8	2	178	-12	42	4	37	35	9	4
Holden North	Base	538	293	-	55	-	33	-	6	-	184	-	34	-	26	-	5	-
	RCP 4.5	421	197	-33	47	-8	38	17	9	3	154	-16	37	2	32	22	8	3
	RCP 8.5	432	212	-28	49	-5	33	0	8	1	156	-15	36	2	30	16	7	2

3.4 Conclusions

Hydrologic data were collected for a period of at least one year for three bioretention cells in northeast Ohio. These data were used to calibrate and validate the agricultural drainage model DRAINMOD, which can model an IWS zone drainage configuration and accounts for soil water content using the soil-water characteristic curve. The calibrated models were utilized to conduct sensitivity analyses on five parameters: media depth, IWS zone depth, rooting depth, bowl storage depth, and hydraulic loading ratio. Additionally, future climate data were utilized in the calibrated models to predict future performance of bioretention cells in northeast Ohio. The following conclusions can be derived from this work:

1. DRAINMOD accurately predicted runoff volume from drainage areas with a mixture of pervious and impervious surfaces. Nash-Sutcliffe efficiencies and coefficients of determination for runoff volume at the three sites were all greater than 0.98. Because the watersheds were at minimum 20% pervious, the watershed modeling was broken into two sub-watershed models, one apiece for the impervious and pervious drainage areas. This allowed for "fine tuning" of the Green-Ampt infiltration parameters separately, which improved the representativeness of the inflow volume predictions. As watershed imperviousness decreased, the goodness-of-fit statistics diverged from 1.0.

2. Bioretention models were built in DRAINMOD based on field-measured and as-built design parameters. Model fit was best for the Ursuline College site, which had Nash-Sutcliffe efficiencies for drainage and exfiltration/ET that were greater than 0.94. Overflow was the most difficult parameter to predict in DRAINMOD, with validation period Nash-Sutcliffe efficiencies of 0.73, 0.74, and 0.71 for Ursuline, Holden South, and Holden North, respectively. The Holden Arboretum site also had good agreement between measured and modeled data, with validation

period Nash-Sutcliffe efficiencies of 0.98 and 0.95 for drainage and 0.75 and 0.71 for exfiltration/ET. Over the entire monitoring period at each site, the monitored and modeled percentage of the water balance never diverged by more than 3%, suggesting DRAINMOD provided reliable predictions of long-term bioretention hydrology.

3. A sensitivity analysis was performed using two calibrated and validated DRAINMOD models to determine bioretention cell performance over various underlying soil types. The models were most sensitive to hydraulic loading ratio and IWS zone depth, which modified the fraction of drainage and exfiltration by 20% or more regardless of underlying soil type. DRAINMOD was moderately sensitive to bowl storage depth. The model was least sensitive to rooting depth and media depth. The latter conclusion is a bit surprising in light of the recommendations provided in previous research.

4. A baseline scenario and two future climate scenarios were analyzed in three calibrated DRAINMOD models by modifying the temperature and rainfall input files. Generally, the future climate data resulted in less rainfall and longer dry periods than present climate. Due to warmer air temperatures in the future, ET depth increased by 5-35% from the bioretention cells and its percentage of the water balance by 1-4%. The future climate data did not substantially affect the overall water balance for each bioretention cell, with drainage, overflow, exfiltration, and ET each varying by 10% or less from the current climate under RCP 4.5 and RCP 8.5. Modeling of the three bioretention cells suggested that volume reductions under future climate would remain in a similar range to present climate model runs, with a range of -8% to +8% change. In each future climate scenario, the fraction of the overall water balance represented by overflow was predict to at least stay the same (1 case) or increase by up to 3% (5 cases).

3.5 References

Amatya, D.M., Skaggs, R.W., & Gregory, J.D. (1995). “Comparison of methods for estimating REF-ET.” *Journal of Irrigation and Drainage Engineering*. 121(6), 427-435.

Brown, R.A. (2011). *Evaluation of bioretention hydrology and pollutant removal in the upper coastal plain of North Carolina with development of a bioretention modeling application in DRAINMOD*. Ph.D. Dissertation, North Carolina State University, Raleigh, NC. <http://repository.lib.ncsu.edu/ir/bitstream/1840.16/6783/1/etd.pdf>.

Brown, R. A., & Hunt III, W. F. (2011a). “Impacts of media depth on effluent water quality and hydrologic performance of undersized bioretention cells.” *Journal of Irrigation and Drainage Engineering*. 137(3), 132-143.

Brown, R. A. and Hunt, W. F. (2011b). “Underdrain configuration to enhance bioretention exfiltration to reduce pollutant loads.” *Journal of Environmental Engineering*. 137(11), 1082-1091.

Brown, R.A., R.W. Skaggs, and W.F. Hunt. (2013). “Calibration and validation of DRAINMOD to model bioretention hydrology.” *Journal of Hydrology*. 486, 430-442.

Browne, D., Deletic, A., Mudd, G.M., & Fletcher, T.D. (2008). “A new saturated/unsaturated model for stormwater infiltration systems.” *Hydrological Processes*, 22(25), 4838-4849.

Davis, A.P., Traver, R.G., Hunt, W.F., Lee, R., Brown, R.A., & Olszewski, J.M. (2012). “Hydrologic performance of bioretention storm-water control measures.” *Journal of Hydrologic Engineering*, *17*(5), 604-614.

Driscoll, E. (1989). *Analysis of Storm Event Characteristics for Selected Rainfall Gages Throughout the United States: Draft.* US Environmental Protection Agency, 1989.

Emerson, C.H., and Traver, R.G. (2008). “Multiyear and seasonal variation of infiltration from storm-water best management practices.” *Journal of Irrigation and Drainage Engineering*, 134(5), 598-605.

Gao, Y., Fu, J.S., Drake, J.B., Liu, Y., & Lamarque, J.F. (2012). “Projected changes of extreme weather events in the eastern United States based on a high resolution climate modeling system.” *Environmental Research Letters*. 7(4), 044025.

Gee, G.W., and Bauder, J.W. (1986). “Particle-size analysis.” *Methods of soil analysis. Part 1: Physical and mineralogical methods*, A. Klute, ed., Soil Science Society of America, Madison, Wis., 383-411.

Hathaway, J.M., Brown, R.A., Fu, J.S., & Hunt, W.F. (2014). “Bioretention function under climate change scenarios in North Carolina, USA.” *Journal of Hydrology*, *519*, 503-511.

Heasom, W., Traver, R.G., & Welker, A. (2006). “Hydrologic modeling of a bioinfiltration best management practice.” *Journal of the American Water Resources Association*. 42(5), 1329-1347.

Hunt, W.F., Davis, A.P., & Traver, R.G. (2012). “Meeting hydrologic and water quality goals through targeted bioretention design.” *Journal of Environmental Engineering*. 138(6), 698-707.

Jones, M.P. and Hunt, W.F. (2009). “Bioretention impact on runoff temperature in trout sensitive waters.” *Journal of Environmental Engineering*. 135(8), 577-585.

Klute, A., and Dirksen, C. (1986). “Hydraulic conductivity and diffusivity: Laboratory methods.” *Methods of soil analysis. Part 1: Physical and mineralogical methods*, A. Klute, ed., Soil Science Society of America, Madison, Wis.697-732

Klute, A. (1986). “Water retention: Laboratory methods.” *Methods of soil analysis. Part 1: Physical and mineralogical methods*, A. Klute, ed., Soil Science Society of America, Madison, Wis., 635–662.

LeFevre, G.H., Paus, K.H., Natarajan, P., Gulliver, J.S., Novak, P.J., & Hozalski, R.M. (2014). “Review of dissolved pollutants in urban storm water and their removal and fate in bioretention cells.” *Journal of Environmental Engineering*. 141(1), 04014050.

Li, H., Sharkey, L.J., Hunt, W.F., & Davis, A.P. (2009). “Mitigation of impervious surface hydrology using bioretention in North Carolina and Maryland.” *Journal of Hydrologic Engineering*. 14(4), 407-415.

Lucas, W.C., & Greenway, M. (2011). “Hydraulic response and nitrogen retention in bioretention mesocosms with regulated outlets: Part I—hydraulic response.” *Water Environment Research*. 83(8), 692-702.

Luell, S.K., Hunt, W.F., & Winston, R.J. (2011). “Evaluation of undersized bioretention stormwater control measures for treatment of highway bridge deck runoff.” *Water Science & Technology*. 64(4), 974-979.

Muthanna, T.M., Viklander, M., & Thorolfsson, S.T. (2008). “Seasonal climatic effects on the hydrology of a rain garden.” *Hydrological Processes*. 22(11), 1640-1649.

Nash, J.E., and Sutcliffe, J.V. (1970). “River flow forecasting through conceptual models part 1 – A discussion of principles.” *Journal of Hydrology*, 10(3), 282-290.

National Oceanic and Atmospheric Administration (NOAA). (2015). *National climatic data center, U.S. local climatological data*. Cleveland, OH airport. Available: http://www.ncdc.noaa.gov/

Ohio Department of Natural Resources (ODNR), Division of Soil and Water Conservation. (2006). *Rainwater and land development: Ohio’s standards for stormwater management, low impact development, and urban stream protection*. 3rd edition. Ed: John Mathews.

R Core Team. (2015). *A language and environment for statistical computing*. R Foundation for Statistical Computing. Vienna, Austria.

Saltelli, A. (2002). "Sensitivity analysis for importance assessment." *Risk Analysis.* 22(3), 579-590.

United States Department of Agriculture (USDA). (1986). *Urban hydrology for small watersheds*. Technical Release 55 (TR-55). 2nd edition. Natural Resources Conservation Service, Conservation Engineering Division.

Winston, R.J., Dorsey, J.D. and Hunt, W.F. (2015). *Monitoring the performance of bioretention and permeable pavement stormwater controls in Northern Ohio: Hydrology, water quality, and maintenance needs*. Final Report Submitted to the University of New Hampshire and the Chagrin River Watershed Partners. In Fulfilment of NOAA Award number NA09NOS4190153.

4. PERMEABLE PAVEMENT HYDROLOGIC MODELING USING DRAINMOD

The agricultural water balance model DRAINMOD was used to simulate long-term permeable pavement performance for three field-monitored permeable pavement applications in northern Ohio. The model was calibrated and validated against the field collected data using separate DRAINMOD models for each site. Sensitivity analyses were completed to determine the response of the water balance to the many different design configurations that are possible in a permeable pavement system. Finally, future climate data for the mid-twenty-first century were used to model permeable pavement performance under predicted changing temperature and rainfall patterns in northern Ohio.

4.1 Site Descriptions

DRAINMOD was calibrated and validated for three permeable pavement applications at two sites in northern Ohio (Winston et al. 2015). Underlying soil, watershed, and design characteristics for each permeable pavement are shown in Table 23 and Table 24. All the permeable pavements incorporated an elevated or upturned elbow in the underdrain to create a 6 inch internal water storage (IWS) zone within the aggregate subbase. The two applications in Willoughby Hills (WH), Ohio were constructed with permeable interlocking concrete pavement (PICP) and received runoff from entirely impervious watersheds. The third site in Perkins Township (PT), Ohio, was constructed as pervious concrete (PC). The PT system received from both an impermeable watershed (0.32 ac) and a pervious watershed (0.1 ac). Detailed site descriptions can be found in Chapter 1 of Winston et al. (2015). Data collection was suspended from December 2013 to March 2014 due to below freezing temperatures.

Table 23. Characteristics of each monitored permeable pavement site.

Location	Mapped Soil Series	Soil Type	Pavement Type	Average Measured Drawdown Rate (in/hr)	Data Collection Period
Perkins Township	Bennington	Silty Clay Loam	Permeable Concrete	0.013	Apr. 2013-Nov. 2014
Willoughby Hills	Mahoning	Fill	PICP	0.002 – 0.008	Oct. 2013-Nov. 2014

Equation 4.1 was used to calculate the ratio of drainage area to the infiltrative surface area of the permeable pavement, referred to as the "field ratio" in DRAINMOD:

$$Field\ Ratio = \frac{A_{WS}}{A_{PP}} \tag{4.1}$$

Where A_{PP} is the infiltrative surface area of the permeable pavement and A_{WS} is the surface area of the contributing watershed. The permeable pavement applications varied in underlying soil type, aggregate depth, and drainage area to permeable pavement surface area ratios. Design characteristics remained unchanged throughout the course of the monitoring period.

Table 24. Design characteristics of each monitored permeable pavement application.

Location	Contributing Watershed Area **(ac)**	Pavement Surface Area **(ft^2)**	Infiltrative Surface Area **(ft^2)**	Field Ratio	Pavement Thickness **(in)**	Aggregate Depth **(in)**
Perkins Township	0.42	2592	4818	3.8:1	6	15 - 18
Willoughby Hills Large	0.22	4420	2200[a]	2.2:1[b]	4	20
Willoughby Hills Small	0.08	482	482	7.2:1	4	20

[a]A stepped subgrade at WH Large forced ponding over only a portion of the pavement subgrade.
[b]Six inches of ponding occurred over appx. 2200 ft^2 of the subgrade, the remainder was raked for minimal storage (appx. 0.5 inches). To account for this, an effective IWS depth was calculated for this site (see section 4.3.1) and the field ratio was based on the pavement surface area.

4.2 Methods

4.2.1 Field Monitoring

The hydrologic monitoring methods are described in detail for each site in Chapter 1 of Winston et al. (2015). In general, runoff, drainage, and overflow volumes were measured or estimated for each site. Runoff from the contributing watershed was estimated using the NRCS Curve Number (CN) method (NRCS 1986). Runoff generated from impermeable (CN = 98) and permeable (CN = 80) watershed areas were computed discretely and summed. Antecedent moisture corrections were applied as described in NRCS (2004). Underdrain flow from each permeable pavement site was routed into a sharp crested, v-notch weir equipped with a HOBO U20 pressure transducer which measured flow depth on a 2-minute interval (Onset Computer Corporation, Bourne, MA). While surface runoff was not observed at the PT site during the course of the study, surface runoff was observed at the WH Large bay in July 2014 due to localized clogging. Subsequently, flow diverters were installed on August 5, 2014 at both the WH Small and WH Large catch basins to route any surface runoff into the existing weir box. For the remainder of the study, the volume of surface runoff was determined by separation of the outflow hydrograph.

To determine the inter-event drawdown rate within the IWS, water level within the aggregate subbase of each permeable pavement application was measured using a HOBO U20 pressure transducer housed within a 1” diameter water table well. The change in stage during each dry period was multiplied by the effective porosity of the aggregate (0.40) and divided by drawdown time to characterize the overall rate of exfiltration and evaporation occurring in the system. The average drawdown rate was used as the initial input for the deep seepage parameter in DRAINMOD.

The surface infiltration rate of the pavement was measured throughout the course of the study using both a single ring, constant head test (ASTM 2009 for PICP; ASTM 2013 for PC) and the simple infiltration test (see Chapter 6 of Winston et al. 2015). For the PT and WH Small applications, measured pavement infiltration rates were high enough that they were not a limiting parameter for modeling infiltration and drainage through the system. For these sites, the average measured surface infiltration rate was used as the hydraulic conductivity input in DRAINMOD's soil preparation program. At the WH Large application, localized clogging at the permeable-impermeable interface and along curblines reduced surface infiltration rates such that surface runoff occurred. Since DRAINMOD does not have a mechanism to model localized clogging, this site was modeled by considering only the permeable pavement surface area where infiltration rates remained high enough to infiltrate runoff (see Section 4.3.1).

At each site, the drainage area, permeable pavement area, aggregate depth, drain depth and depth of the IWS zone were determined from construction plans and confirmed via visual inspection. These design specifications were entered into the model to simulate the hydrologic response of the systems.

4.2.2 Drainage Inputs

DRAINMOD requires several drainage inputs for simulation including the drain spacing, drainage coefficient, and drainage configuration. Since a single underdrain was used at all three sites, an effective drain spacing for each application was estimated by dividing the infiltrative surface area of the permeable pavement by the total length of the underdrain (Brown 2011). The drainage coefficient characterizes the maximum drainage capacity of the system in inches/day; if the drainage flux calculated by the model using Kirkham's or Hooughoudt's equations exceeds the maximum drainage capacity, the daily drainage rate predicted by the model will be restricted to the drainage coefficient. Due to the size of the underdrains (and high drainable porosity of the aggregate), it was rare the drainage rate was limited by the drainage configuration and fully saturated conditions were not observed. Because of this, the parameter was calibrated for each site, to 30 in/day for PT, 40 in/day for the WH Small bay, and 20 in/day for the WH Large bay, using the largest measured daily drainage as a guideline.

For the PT application, internal water storage was created by an elevated underdrain. Thus, for this site, conventional drainage was modeled and the depth to drain and aggregate depth were entered according to design specifications (Figure 12). To model internal water storage for the WH locations, where IWS was created by an upturned underdrain, a controlled drainage configuration was used (Figure 13). The input for depth to weir was set to equal the depth from the pavement surface to the invert of the upturned elbow of the underdrain such that 6 inches of IWS was created.

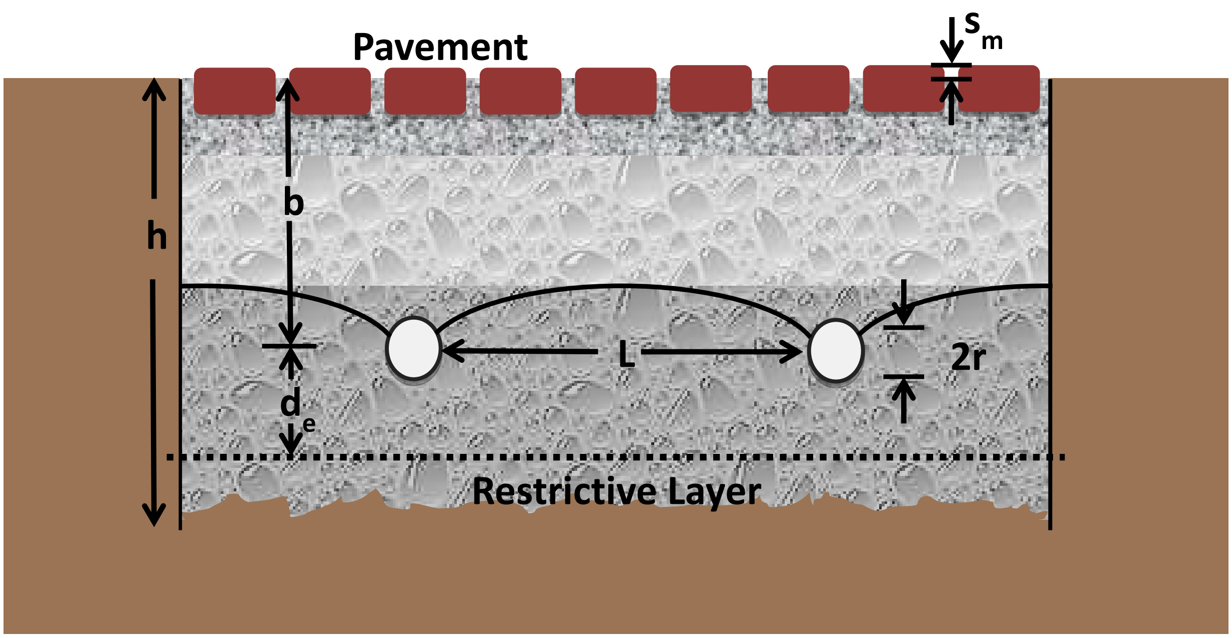

Figure 12. Elevated underdrain creating internal water storage, which was modeled using conventional drainage in DRAINMOD.

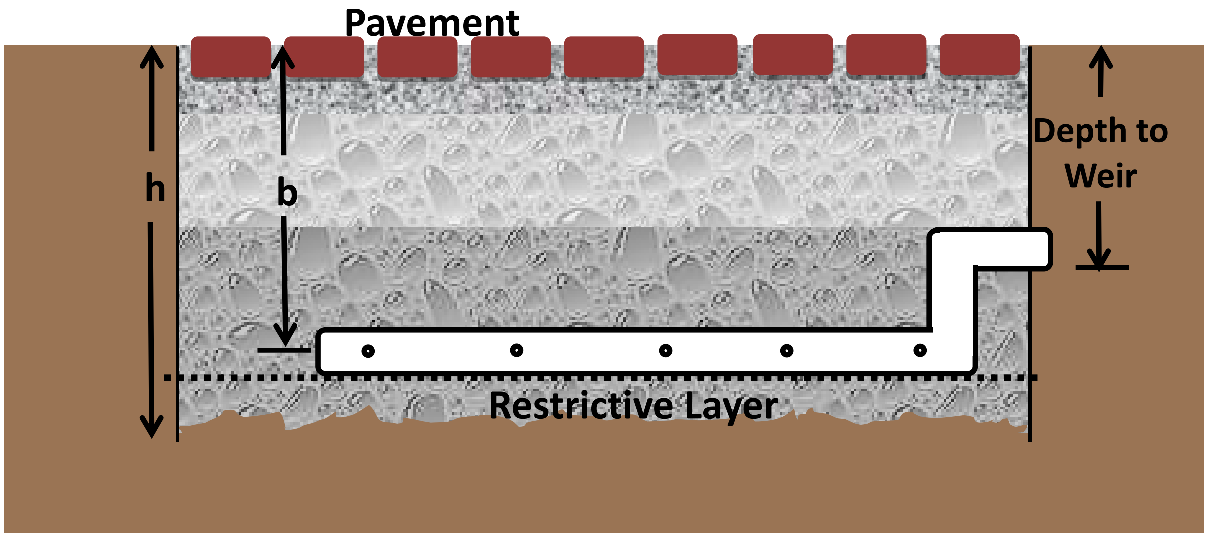

Figure 13. Upturned elbow on underdrain creating internal water storage, which was modeled with controlled drainage in DRAINMOD.

4.2.3 Soil Inputs

The soil preparation program in DRAINMOD was used to develop Green-Ampt infiltration coefficients, water table depth-volume drained relationships and water table depth-upward flux relationships for each site. This program requires the saturated hydraulic conductivity and water retention curve of the aggregate media. As described in Section 4.2.1, saturated hydraulic conductivity was estimated by infiltration testing; these values were in the range of measured hydraulic conductivities for other permeable pavements (Starke et al. 2010, Montes and Haselbach 2006) (Table 25).

Table 25. Average measured surface infiltration rate for Perkins Township and Willoughby Hills with comparison to measured hydraulic conductivities of permeable pavements.

Location	Surface Infiltration Rate **(in/hr)**	Hydraulic Conductivity **(in/hr)**
Perkins Township	1247	-
Willoughby Hills	294	-
Starke et al. 2010	-	480 - 1100
Montes and Haselbach 2006	-	20 - 1600

One challenge in using DRAINMOD to predict permeable pavement hydrology is determining a water retention curve representative of its highly porous aggregate media, which has a greater drainable porosity than the typical agricultural soil for which the model was developed. Brown (2011) developed a reasonable estimation for an aggregate media by modifying the water retention curve for a very sandy soil (Table 26). This water retention curve was used for all aggregate layers beneath the permeable pavements.

Table 26**.** Water retention curve for aggregate (Brown 2011).

Soil Water Content **(in^3/in^3)**	Pressure Head **(in)**
0.300	0
0.100	-1
0.050	-4
0.050	-12
0.045	-15
0.044	-20
0.044	-40
0.044	-80
0.044	-160
0.044	-240
0.010	-5900

Other required soil parameters include the lateral saturated hydraulic conductivity and vertical seepage rate. Given the high drainable porosity of the aggregate, flow within the aggregate was assumed to be non-limiting; the lateral saturated conductivity for the aggregate was calibrated to 80 in/hr. The measured drawdown rate was assumed equivalent to the sum of lateral and vertical exfiltration and was adequately modeled in the vertical dimension. As described in Section 4.2.1, the average measured exfiltration rate was used as a guideline for the vertical conductivity input for deep seepage.

4.2.4 Climatic Inputs

4.2.4.1 Temperature

DRAINMOD requires maximum and minimum daily air temperatures as climatic inputs. During the calibration and validation periods, temperature was measured at both sites using a 6-ft tall HOBO weather station (Onset Computer Corporation, Bourne, MA). All rainfall and climatic parameters were recorded on a 1-minute interval. The weather stations were located in open areas free from overhanging trees. Long-term weather files were created for the Cleveland area using minimum and maximum temperature data obtained from the National Climatic Data Center at the Cleveland-Hopkins Airport station [COOP:331657] (NOAA 2015a). These 30-year weather files (from 1983 – 2012) were used as inputs for the sensitivity analysis (see Section 4.3.3.).

4.2.4.2 Precipitation

Precipitation depths were measured on site using a tipping bucket rain gauge with a 0.01-in resolution. All precipitation data were stored in the data logger attached to the nearby weather station (Davis Instruments, Hayward, California). The minimum resolution for precipitation entered into DRAINMOD is hourly, thus all rainfall data were summed on an hourly basis. As with temperature, 30-year precipitation files were created for the Cleveland area using hourly rainfall obtained from the National Climatic Data Center at the Cleveland-Hopkins Airport (NOAA 2015a).

4.2.4.3 Potential Evapotranspiration (PET)

DRAINMOD has the option to input potential evapotranspiration on a daily basis using any desired PET calculation method. Alternatively, the Thornthwaite method can be used to calculate PET based on the provided minimum and maximum daily air temperatures. The Thornthwaite method only requires mean monthly air temperature, which is used to calculate the heat index for the site. The calculated heat indices for PT and WH were 48.7 and 49.0, respectively. While monthly correction factors can be used to increase accuracy of the Thornthwaite method, none were available specific to northern Ohio. In order to simulate evaporation only, rooting depths were set to the minimum allowable value (appx. 0.4 in).

4.2.5 Data Analysis

The average drawdown rates at all three sites were very low (less than 0.02 in/hr); because of this, exfiltration and evaporation occurred slowly over the course of the dry period. To compare modeled and monitored exfiltration/evaporation on a storm-by-storm basis, runoff that did not exit the system via overflow or drainage was assumed to be lost via exfiltration or evaporation using the water balance in equation 4.2. Occasionally, two or more storm events occurred during the same day. DRAINMOD's minimum output resolution is daily; thus separation of these events was not feasible. For these situations, runoff and drainage volumes were lumped together and analyzed as a combined event.

$$V_{EE} = V_{in} - V_O - V_D \quad (4.2)$$

Where V_{EE} is the total volume of exfiltration and evaporation, V_{in} is the runoff volume from the watershed, V_O is the volume of bypass or overflow, and V_D is the drainage volume.

Since the average period of data collection was approximately 12 months, to ensure the calibration of the model represented the entire year's data, storm events occurring during even months were used for model calibration. Calibration of the contributing area runoff was conducted first. Once modeled runoff was in acceptable agreement with the estimated runoff, the model was calibrated for the various forms of outflow (drainage, exfiltration/ET and overflow). Nash-Sutcliffe Efficiencies (NSEs) for inflow, drainage, and exfiltration/evaporation were calculated to measure model fit (eq. 4.3, Nash and Sutcliffe 1970). An NSE of 1.0 represents perfect agreement between measured and modeled data; a model with an NSE of 0.0 or lower is no more accurate than predicting the mean value.

$$NSE = 1 - \frac{\sum_{i=1}^{N}\left(Q_{i,measured} - Q_{i,modeled}\right)^2}{\sum_{i=1}^{N}\left(Q_{i,measured} - Q_{average}\right)^2} \quad (4.3)$$

where $Q_{i,measured}$ is measured volume for event *i*, $Q_{i,modeled}$ is modeled volume for event *i*, and $Q_{average}$ is the average measured volume for *N* events.

Upon calibration of the model, the model was validated by assessing model performance against measured data from odd months. Given the NSE can be sensitive to sample size, outlier values and bias, (McCuen et al. 2006, Jain and Sudheer 2008), additional calculations of the coefficients of determination (R^2) and percent error of measured and predicted volumes were used to assess the goodness-of-fit for runoff and outflow variables holistically. Additionally, at the PT site, measured and predicted water table depths were compared.

4.2.6 Sensitivity Analysis

A sensitivity analysis was performed to analyze the overall impact of different design features on the performance of permeable pavements. 30-year weather files (1983 – 2012) for precipitation and temperature were created for the Cleveland area using data recorded at the Cleveland-Hopkins Airport. Using the existing design specifications, baseline models were established for each site given different underlying soil infiltration rates: 0.02 in/hr, 0.05 in/hr, 0.20 in/hr and 0.50 in/hr. Design features including aggregate depth, IWS zone depth, and the ratio of the watershed area to permeable pavement surface area, were then varied to assess the implications of design parameters on performance. For each sensitivity analysis, one design variable was modified at a time and all other design variables were held constant at their base levels to reduce modeling error (Saltelli 2002).

4.2.7 Climate Change Modeling

The use of DRAINMOD to simulate SCM performance under future climate scenarios has been shown to be an effective tool for analyzing changes in the SCM water balance (Hathaway et al. 2014). To predict hydrologic response of permeable pavements given future climate scenarios, calibrated models were simulated with site specific data from Gao et al. (2012). Gao et al. (2012) generated high resolution climate projection data for the eastern United States using dynamic downscaling of the Weather Research and Forecasting model (WRF). Modeling was performed on a 4 km x 4 km high resolution scale with the Community Earth System Model version 1.0 (CESM v1.0) serving to establish boundary conditions for the WRF model. A full description of the dynamic downscaling methodology is available in Gao et al. (2012).

Three climate scenarios were developed for this work, each containing 4 or 5 years of data. The baseline model was created based on modeled 2001-2004 data for each location. The other two climate scenarios were developed using data from two of the Intergovernmental Panel on Climate Change (IPCC) Representative Concentration Pathways (RCP 4.5 and RCP 8.5). Permeable pavement performance was analyzed under two fossil fuel usage scenarios, one moderate (RCP 4.5) and one intensive (RCP 8.5). Predictions from 2055 to 2059 (5 years) were used for both climate change scenarios. The results for each future scenario were compared to performance for the baseline scenario (2001-2004); differences among performance between the two climate scenarios were not compared.

4.3 Results and Discussion

4.3.1 Contributing Area Runoff

The contributing area runoff was the first parameter calibrated. Separate runoff files were created to represent inflow volume from each drainage area. The PT site required the development of two contributing runoff files – one for the pervious drainage area and a second for the impervious drainage area. Since the drainage areas for the WH sites were 100% impervious, only one contributing runoff file was needed. Contributing runoff was modeled in DRAINMOD using a low surface infiltration rate (typically between 0.0 and 0.005 in/hr for impervious surfaces) and wide drain spacing. Depending on the amount of perviousness in the contributing drainage area, available surface storage and infiltration rate of the surface were adjusted until the model adequately represented the estimated inflow from the contributing drainage area. The field ratio (drainage area to permeable pavement area) was then set to equal the values in Table 24. Inflow was predicted well at both the PT and WH Small applications, with a Nash-Sutcliffe Efficiency of 0.96 and 0.99 during the calibration periods, respectively (Figure 14, Figure 15). The lower NSE for the PT application is attributed to the pervious portion of its contributing area, which generates more variable runoff as a function of soil moisture and antecedent dry period. Given that DRAINMOD was not developed to estimate runoff from urbanized watersheds, with increasing perviousness it is more difficult to "trick" the model into accurately predicting the surface runoff estimated by widely-used empirical methods (e.g., Curve Number method). Despite this, during the validation period, NSEs were 0.99 for both the PT and WH Small sites.

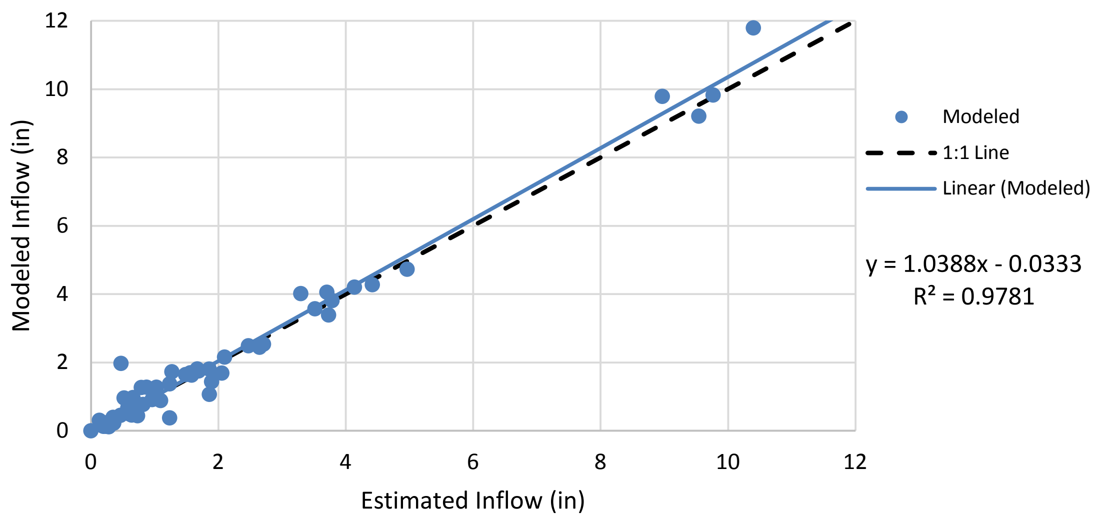

Figure 14. Modeled (predicted) vs. estimated runoff volume from the Perkins Township watershed for 69 modeled storm events. Also presented are the linear trendline with equation, the Coefficient of Determination (R^2), and the 1:1 line. All units are in inches per permeable pavement surface area.

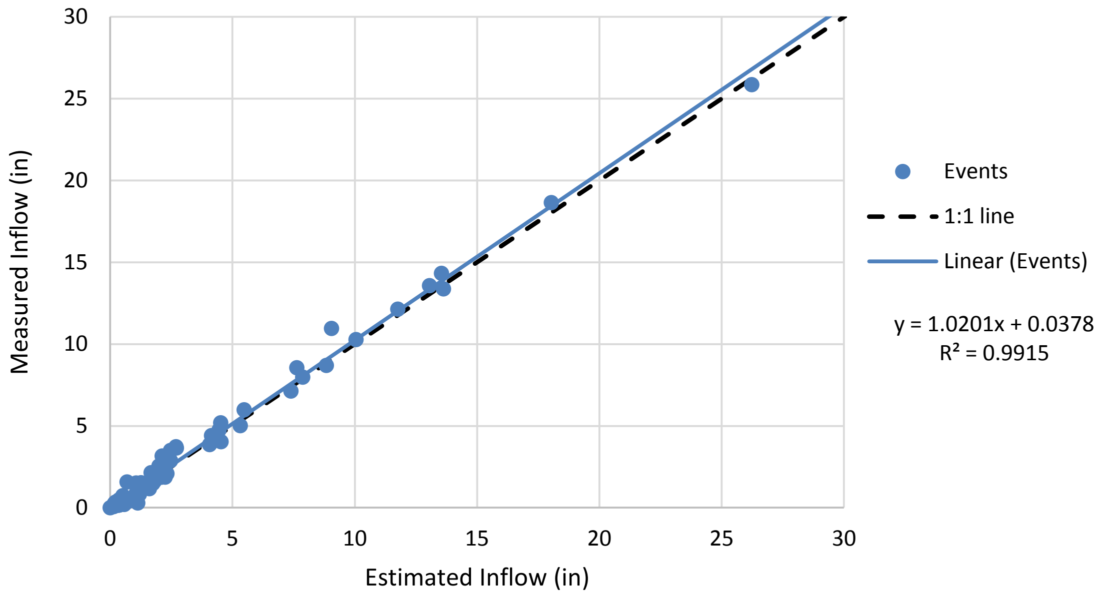

Figure 15. Modeled (predicted) vs. estimated runoff volume from the Willoughby Hills Small watershed for all 72 modeled storm events. Also presented are the linear trendline with equation, Coefficient of Determination (R^2), and the 1:1 line. All units are in inches per permeable pavement surface area.

For the WH Large bay, a different approach to modeling inflow was required due to two factors: (1) a stepped subgrade was utilized to make up for the 1-2% surface slope; this resulted in four steps in the subgrade with the underdrain at the bottom of the cross-section and thus no IWS in this portion of the subgrade, and (2) localized surface clogging of the permeable pavement, which affected up to 30% of the watershed area (Figure 15). As the PICP surface clogged over time, inflow from this portion of the drainage area bypassed the system as surface runoff.

To account for the first factor, a weighted IWS depth was calculated based on the estimated ponded area of the subgrade (appx. 2200 ft^2 with 6 inches of IWS) and non-ponded area of the subgrade (appx. 2200 ft^2 with soil storage up to 0.5 inches). The average IWS depth over the entire subgrade was 3.3 inches; this was used as the input parameter for controlled drainage.

Since surface runoff was not monitored prior to August 2014, it was difficult to determine what portion of the inflow bypassed, and in turn accurately model drainage and exfiltration from the system (this was further compounded by the stepped subgrade). DRAINMOD does not have a method to incorporate progressive clogging of the infiltrative surface, so an "effective drainage area" was determined based on visual inspection of the site and the estimated surface runoff from the measured water balance. The contributing drainage area was adjusted based on the surface runoff from the measured water balance; from this analysis, approximately 16% of the PICP was determined to be clogged (700 ft^2). The clogged portion represented 4000 ft^2 of the 9600 ft^2 drainage area and resulted in surface runoff equivalent to 24% of the overall water balance for the permeable pavement (Figure 16). Because of clogging, the ratio of drainage area to permeable pavement area was reduced from 2.2:1 to 1.3:1. Using the contributing runoff file created for the WH Small site, the field ratio was calibrated to 1.1 to best represent the effective inflow to the WH Large system. This represented error between the modeled and measured data that was unable to be reconciled.

DRAINMOD requires surface infiltration rate to be held constant for the entire period of simulation; in reality, there was temporal variation of surface clogging and thus any initial assumptions of an unclogged surface could not be represented in the model. Because of this, inflow was slightly under predicted for the WH Large Bay, but was adequate given the circumstances and assumptions required (Figure 17).

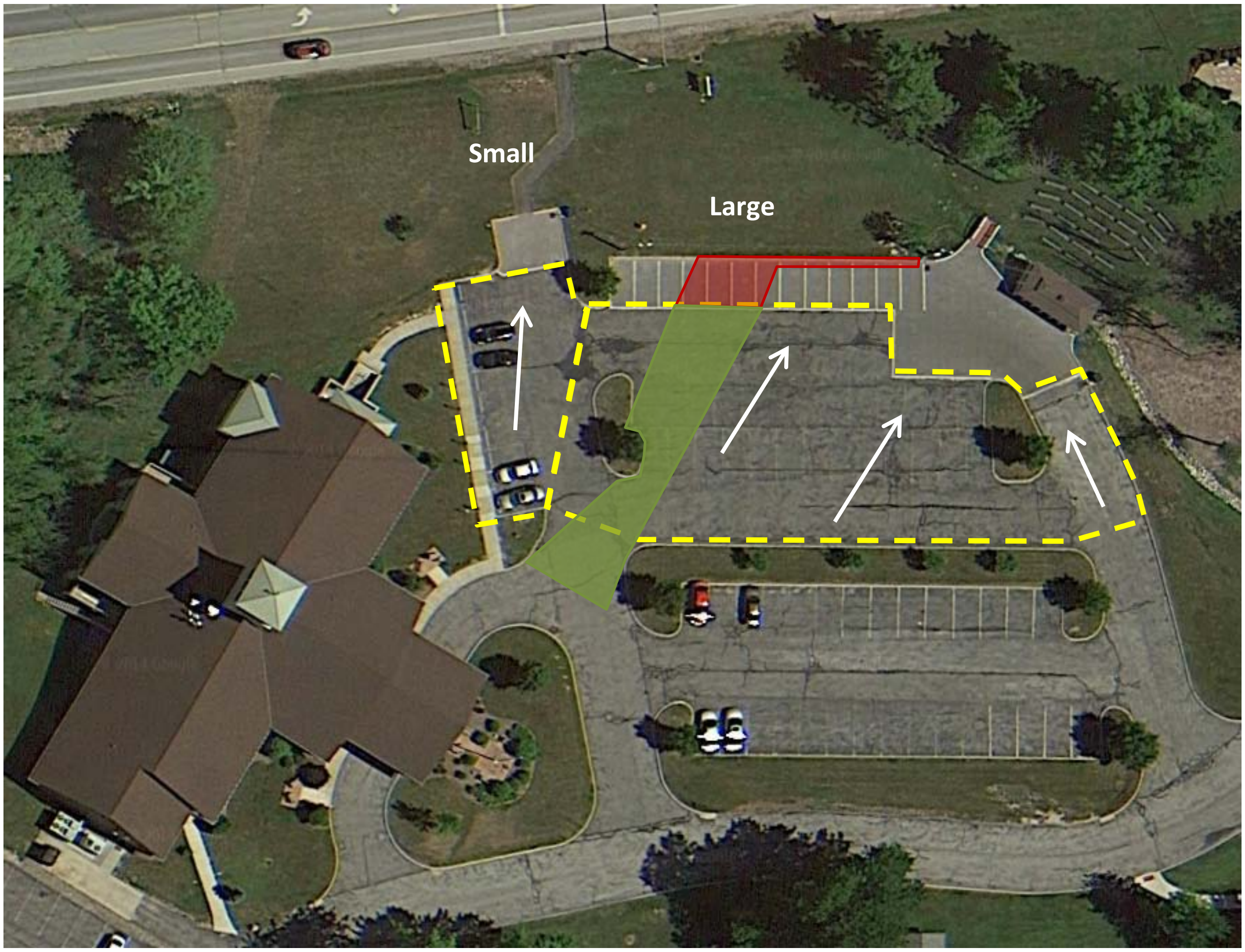

Figure 16. Estimated clogged PICP surface (red) and contributing drainage area received by this surface (green).

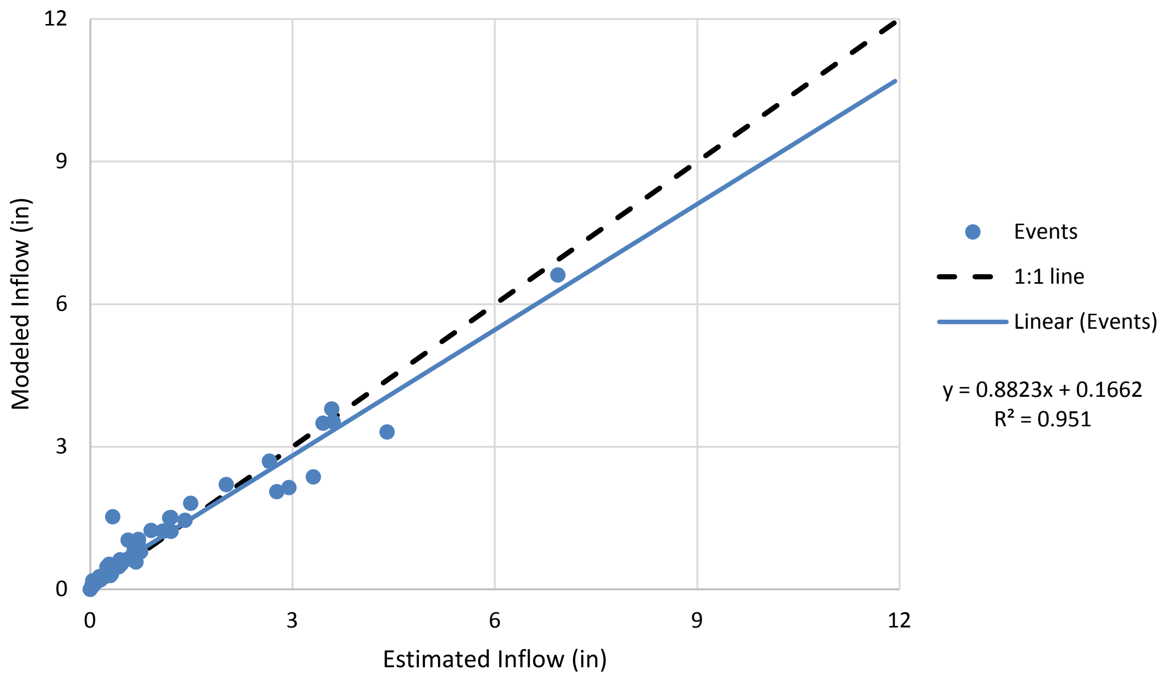

Figure 17. Modeled (predicted) vs. estimated runoff volume from the Willoughby Hills Large watershed for all 55 monitored storm events. Also presented are the linear trendline with equation, Coefficient of Determination (R^2), and the 1:1 line. All units are in inches per permeable pavement surface area.

4.3.2 DRAINMOD Calibration and Validation

4.3.2.1 Perkins Township

As shown in Figure 18 and Table 27, the modeled data at the PT site were in good agreement with measured and estimated data during the calibration and validation periods. Drainage had the strongest agreement, with computed NSEs exceeding 0.85, and the cumulative percent error less than 5% during both periods. NSEs for exfiltration/evaporation were slightly lower at 0.77 and 0.58 during the calibration and validation periods, respectively. Despite this, the error between predicted and measured cumulative exfiltration/ET volumes was only 2.5% and 14% during calibration and validation. While the model predicted 2 overflow events during the validation period, comparison among measured and modeled overflow statistics could not be computed since overflow did not occur at this location. The extraneous overflow events predicted by the model are likely a function of the hourly rainfall resolution employed by DRAINMOD. Zhang and Guo (2014) found a minimum time step of 30 minutes is required for accurate representation of infiltration using the LID module in SWMM 5.0. While the hourly time step still resulted in excellent agreement of the cumulative fate of runoff during the study period (Figure 18), this is a feature of DRAINMOD that potentially limits its utility in assessing permeable pavement performance during individual storm events.

The PT site differed from the WH applications because it was constructed using an elevated underdrain to create the IWS zone as opposed to an upturned elbow (see Section 4.2.2). Because of this, the PT site was modeled using conventional drainage (and the corresponding inputs); this did not affect the calibration and validation process, but would affect the model inputs if instead the controlled drainage method was used. For a conventionally drained system, the model calculates outflow when the water table is greater than the midpoint of the drain; for a system where the underdrain lies on the subgrade and drainage is controlled by an upturned elbow, the model calculates outflow as soon as the water level exceeds the invert of the upturned elbow. Because of this, to accurately model the IWS zone as controlled drainage when an elevated underdrain is constructed, the depth to the weir should be set to the midpoint of the drain as opposed to the invert.

Table 27. Comparison of measured/estimated and modeled results for the Perkins Township permeable pavement.

Monitoring Period	Method of Comparison	Fate of Runoff: (inches per permeable pavement surface area over the monitoring period [percent of annual runoff])			
		Runoff	Drainage	Overflow	Exfiltration/Evap.
Calibration (April 2013, June 2013, August 2013, October 2013, April 2014, June 2014, August 2014, October 2014)	Measured/estimated volume	63	24 [38.1%]	0 [0%]	39 [61.9%)
	Modeled volume	65	25 [35.8%]	0 [0%]	40 [61.5%]
	Difference between modeled and measured	-2	-1	0	-1
	Percent difference between modeled and measured	3%	4%	0%	2.5%
	Nash-Sutcliffe Coefficient	0.96	0.87	-	0.78
	Coefficient of Determination (r^2)	0.97	0.88	-	0.81

Monitoring Period	Method of Comparison	Fate of Runoff: (inches per permeable pavement surface area over the monitoring period [percent of annual runoff])			
		Runoff	Drainage	Overflow	Exfiltration/Evap.
Validation (May 2013, July 2013, September 2013, November 2013, July 2014, September 2014, November 2014)	Measured/estimated volume	64	36 [56.3%]	0 [0%]	28 [58%]
	Modeled volume	62	36 [58.1%]	2 [3.2%]	24 [57.5%]
	Difference between modeled and measured	2	0	-2	4
	Percent difference between modeled and measured	-3%	0%	-	14%
	Nash-Sutcliffe Coefficient	0.99	0.85	-	0.58
	Coefficient of Determination (r^2)	0.99	0.85	-	0.61

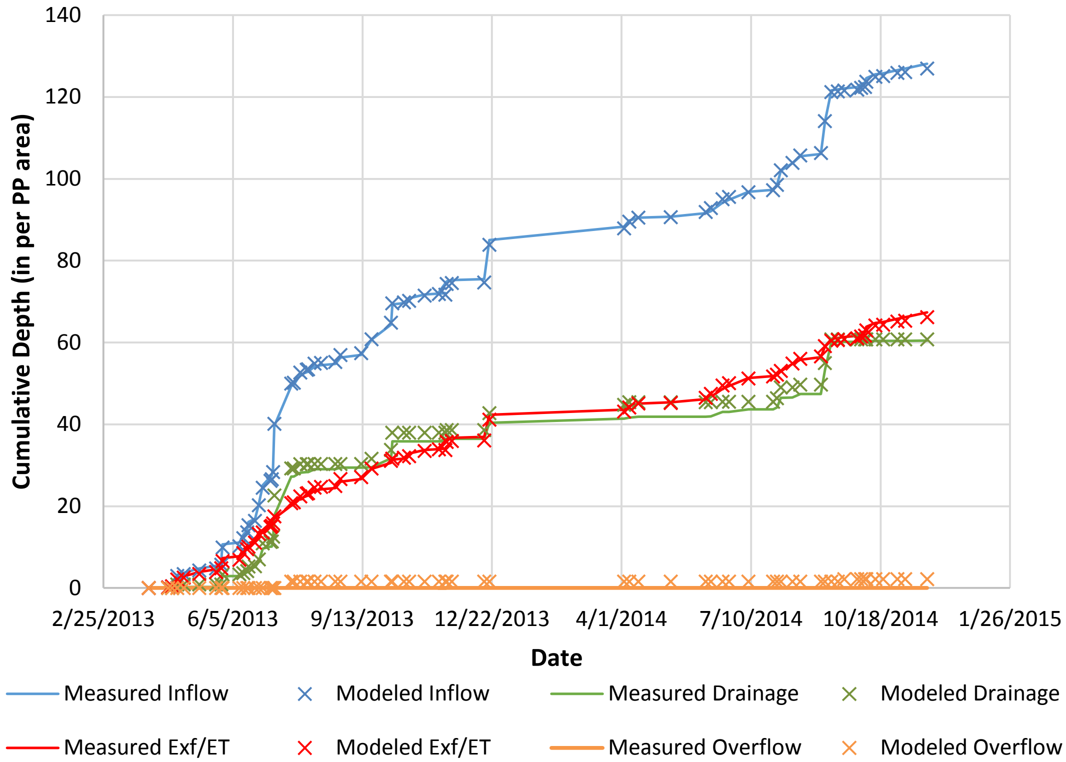

Figure 18. Cumulative fate of runoff for the Perkins Township permeable pavement, with field-measured depths shown as lines and modeled depth shown as symbols.

Figure 19 shows examples of the modeled and measured water table depth over the course of a 5-month period. In general, model prediction matched the peaks during storm events, and drawdown was accurately modeled within the IWS zone. The average absolute error (AAE) between the daily predicted and measured water table depths (WTD) over the first year of monitoring was 0.8 inches, where N = number of daily WTD measurements (eq. 4.4). WTDs were only compared once daily based on the maximum measured water level in the subbase, which did cause some skew from outliers (Figure 20). The coefficient of determination over the first year of monitoring was 0.81.

$$AAE = \frac{\sum_{i=1}^{N} \left| WTD_{predicted} - WTD_{modeled} \right|}{N} \tag{4.4}$$

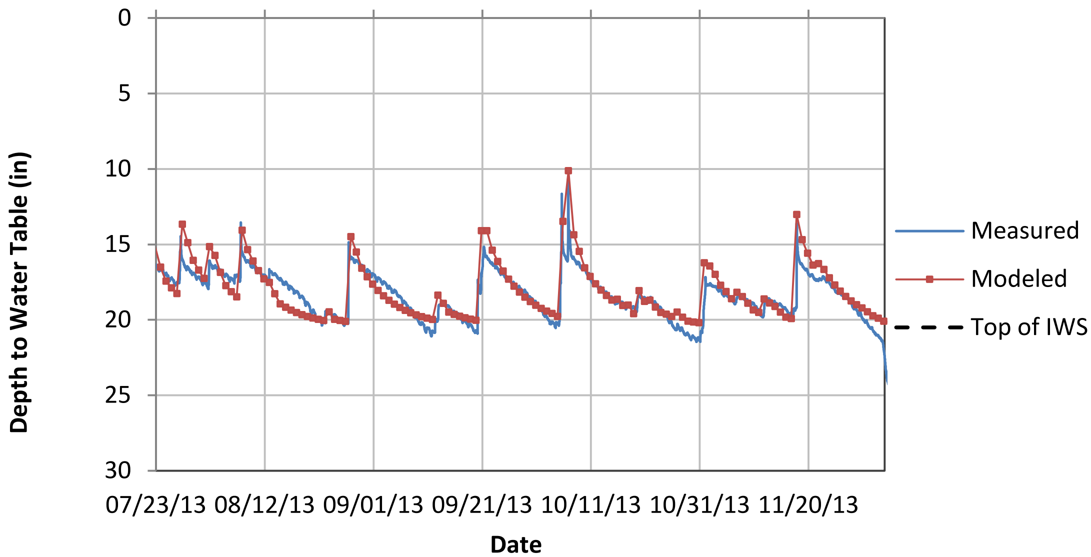

Figure 19. Modeled and measured water table depth at Perkins Township for a five-month period from July 2013 to November 2013.

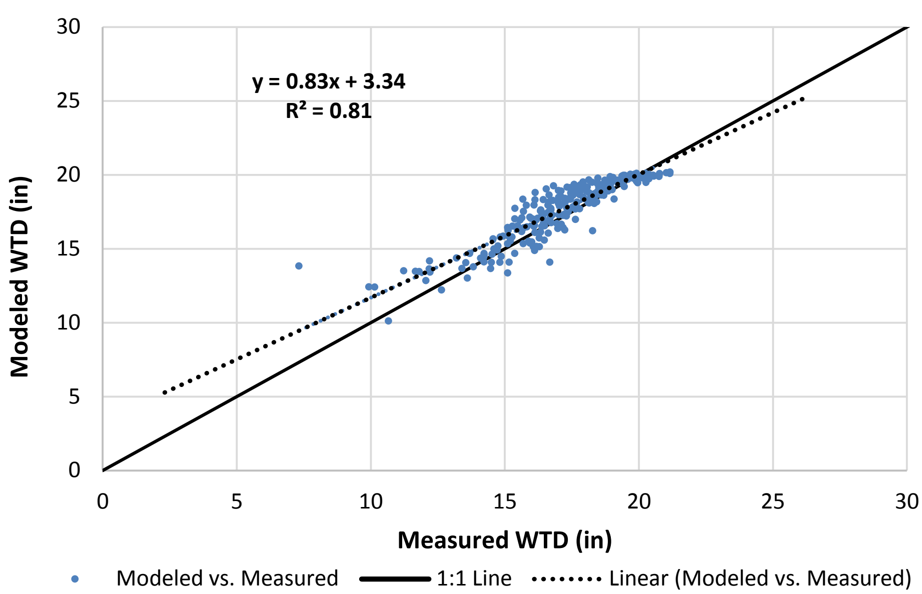

Figure 20. Modeled versus measured water table depth at Perkins Township from April 2013 to December 2014.

4.3.2.2 Willoughby Hills Small

The WH Small application had excellent agreement between predicted and measured inflow and drainage volumes (Table 28, Figure 21). NSEs exceeded 0.90 for these parameters during both the calibration and validation periods, and cumulative volume was predicted within 2-7%. Exfiltration and evaporation were not predicted well on an event-by-event basis, with computed NSEs of 0.35 and 0.19 during calibration and validation, respectively. This is partially due to the very low exfiltration rates (less than 0.01 in/hr) and subsequently minimal amount of runoff volume lost via exfiltration. Measured exfiltration/evaporation volumes were so small in magnitude any predicted deviation from the measured value resulted in a considerable percent error. Additionally, because storm-by-storm overflow events were unable to be separated from drainage for this site, any events where the model predicted overflow were not considered in the analysis, reducing the number of analyzed events and thus increasing variability. Despite this, cumulative exfiltration/evaporation was still predicted well for the entire monitoring period (within 10% error), indicating that long-term estimation of exfiltration/evaporation is viable despite inaccurate storm-by-storm prediction (Figure 21). While storm-by-storm comparisons of modeled and measured overflow were unable to be made due to lack of overflow monitoring prior to August 5, 2014, the portion of the water balance predicted to overflow by the model was within 2% of what was estimated (Winston et al. 2015).

Table 28. Comparison of measured/estimated and modeled results for the Willoughby Hills Small permeable pavement application.

Monitoring Period	Method of Comparison	**Fate of Runoff**: (inches per permeable pavement surface area over the monitoring period [percent of annual runoff])			
		Runoff	Drainage	Overflow	Exfiltration/Evap.*
Calibration (Even Months)	Measured/estimated volume	133	100 [71.9%]	- [-%]	22 [11.5%]
	Modeled volume	137	107 [78.1%]	10 [9.8%]	17 [9.5%]
	Difference between modeled and measured	4	7	-	-5
	Percent difference between modeled and measured	3%	7%	-	-23%
	Nash-Sutcliffe Coefficient	0.99	0.92	-	0.35
	Coefficient of Determination (r^2)	0.99	0.94	-	0.49
Monitoring Period	**Method of Comparison**	**Fate of Runoff**: (inches per bioretention surface area over the monitoring period [percent of annual runoff])			
		Runoff	Drainage	Overflow	Exfiltration/Evap.
Validation (Odd Months)	Measured/estimated volume	90	66 [73.3%]	- [-%]	11 [12.2%]
	Modeled volume	92	67 [72.8%]	9 [9.8%]	14 [15.2%]
	Difference between modeled and measured	2	1	-	3
	Percent difference between modeled and measured	2%	1.5%	-	27%
	Nash-Sutcliffe Coefficient	0.99	0.94	-	0.19
	Coefficient of Determination (r^2)	0.99	0.96	-	0.37

*Does not include exfiltration from events where the modeled predicted overflow.

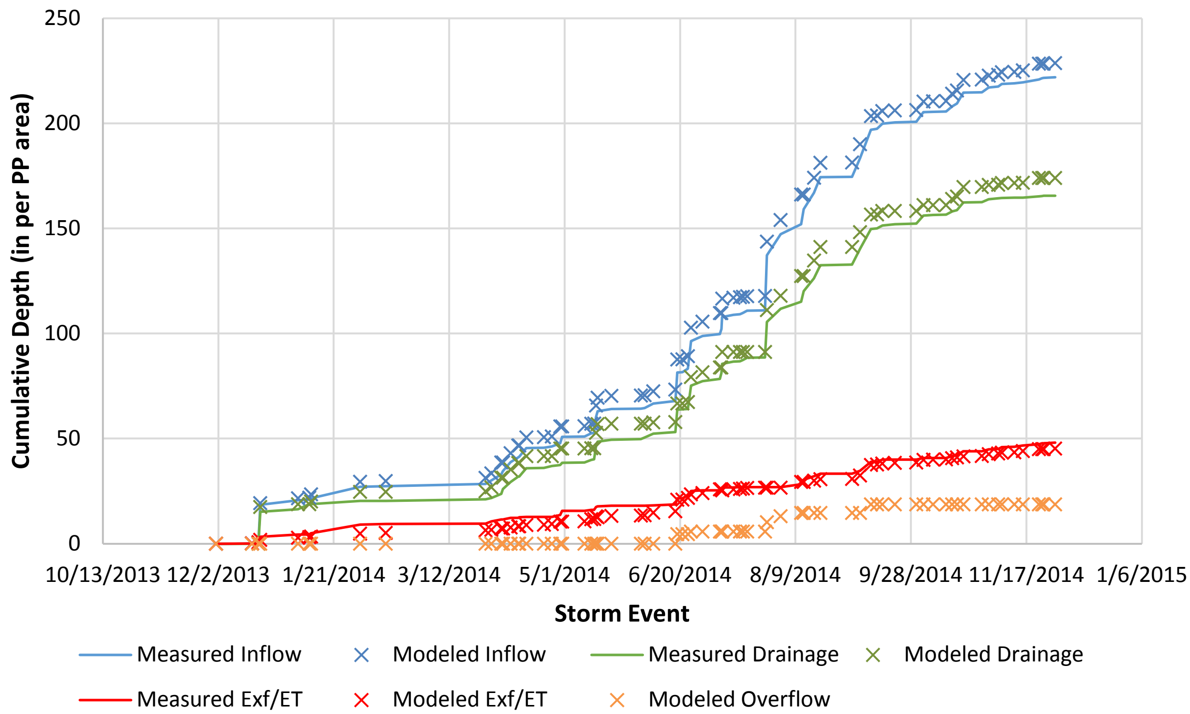

Figure 21. Cumulative fate of runoff for the Willoughby Hills Small permeable pavement application, with field-measured depths shown as lines and modeled depth shown as symbols.

4.3.2.3 Willoughby Hills Large

The unique approach utilized to model inflow volume at the WH Large application (explained in Section 4.3.1) resulted in acceptable agreement between predicted and measured runoff volumes over the course of the monitoring period, with calibration and validation NSEs of 0.94 and 0.97, respectively (Table 29). Unfortunately, at this site, some events were invalidated due to unreliable drainage data, which increased variability in prediction of outflow. Because of this, only 55 storms were used for calibration (n = 23 storms) and validation (n = 32 storms) compared to 69 storms at PT and 72 storms at the WH Small application. Despite this, the model was effectively used as a tool to confirm what portion of the PICP surface was clogged and therefore generating surface runoff. Drainage was predicted to NSEs of 0.82 and 0.94 for the calibration and validation periods, respectively. Similar to the WH Small site, low exfiltration rates (and subsequently low exfiltration volumes) deemed the prediction of storm-by-storm events to be somewhat variable, with NSEs of 0.34 and 0.32 during the calibration and validation periods, respectively. Cumulative drainage and exfiltration/evaporation volumes were predicted well over the course of the monitoring period (Figure 22). Given that the NSE is sensitive to sample size and outlier events (McCuen et al. 2006), slightly better performance was observed in the validation period due to a larger number of analyzed storm events and one storm event in the validation period exceeding 3 inches. The WH Large application had the highest variability between predicted and measured data, but valuable insight was still gained by applying the model as a tool to verify the percentage of the permeable pavement surface that was clogged.

Table 29. Comparison of measured/estimated and modeled results for the Willoughby Hills Large permeable pavement application.

Monitoring Period	Method of Comparison	**Fate of Runoff**: (inches per permeable pavement surface area over the monitoring period [percent of annual runoff])				
		Runoff	Inflow	Drainage	Overflow	Exfiltration/Evap.
Calibration (Even Months)	Measured/estimated volume	32	25	14 [43.8%]	7 [21.0%]	11 [35.2%]
	Modeled volume	-	25	15 [45.3%]	- [-%]	10 [31.8%]
	Difference between modeled and measured	-	0	1	-	-1
	Percent difference between modeled and measured	-	-2%	3%	-	-10%
	Nash-Sutcliffe Coefficient	-	0.94	0.82	-	0.34
	Coefficient of Determination (r^2)	-	0.95	0.83	-	0.35
Monitoring Period	**Method of Comparison**	**Fate of Runoff**: (inches per permeable pavement surface area over the monitoring period [percent of annual runoff])				
		Runoff	Inflow	Drainage	Overflow	Exfiltration/Evap.
Validation (Odd Months)	Measured/estimated volume	33	24	15 [44.9%]	9 [26.3%]	9 [31.0%]
	Modeled volume	-	26	14 [41.5%]	- [-%]	13 [40.1%]
	Difference between modeled and measured	-	2	-2	-	4
	Percent difference between modeled and measured	-	10%	-8%	-	37%
	Nash-Sutcliffe Coefficient	-	0.97	0.94	-	0.32
	Coefficient of Determination (r^2)	-	0.98	0.95	-	0.50

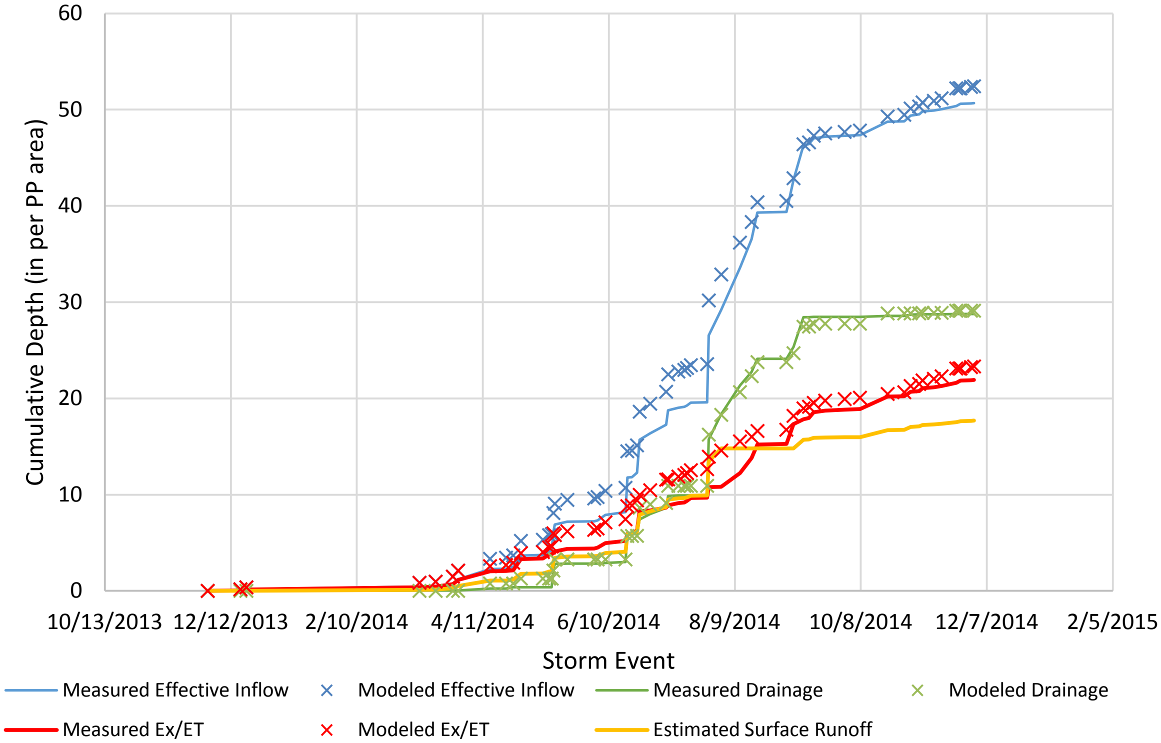

Figure 22. Cumulative fate of runoff for 56 storm events at the Willoughby Hills Large permeable pavement application, with field-measured depths shown as lines and modeled depth shown as symbols.

The DRAINMOD models developed for each of three permeable pavement applications field monitored in Northern Ohio were calibrated and validated, with reliable agreement between measured and modeled data. This is further supported by the measured versus modeled hydrology in Table 30, which shows excellent agreement for the percentage of the cumulative water balance (monitored versus modeled) over the entire monitoring period for each permeable pavement. The overall water balance was predicted to within 1% – 4% of the measured water balance for drainage, overflow, and exfiltration/evaporation.

Table 30. Monitored versus modeled water balance over the entire monitoring period for each of the permeable pavement applications in northern Ohio. All numbers are percentages.

Type of Data	Hydrologic Fate	Perkins Township	Willoughby Hills Small	Willoughby Hills Large
Monitored	Drainage	53	76	44
Modeled	Drainage	49	75	42
Monitored	Overflow	0	8	24*
Modeled	Overflow	1	6	
Monitored	Exfiltration/ET	47	17	32
Modeled	Exfiltration/ET	50	18	34

*Overflow was not modeled for the Willoughby Hills Large site due to localized surface clogging. See section 4.3.1 for more details.

4.3.3 Sensitivity Analysis

A sensitivity analysis was performed to analyze the overall impact of different design features on the performance of permeable pavements. The annual water balance of the baseline models developed for each underlying soil infiltration rate at PT, WH Small and WH Large are displayed below (Figure 23, Figure 24, and Figure 25). The WH Large site was modeled such that the pavement was unclogged, fully functioning, and had a 6 inch IWS zone across the entire subgrade. This gives greater insight on the performance of the "typical" application constructed in northern Ohio, which has a 2:1 run-on ratio (defined as the ratio of impermeable drainage area to permeable pavement surface area). Compared to the WH Small bay, the WH Large bay exhibited lower outflow volumes (drainage + overflow) and a larger amount of volume reduction via exfiltration and evaporation; this is a function of the WH Large bay's larger footprint (and thus increased available area for exfiltration and evaporation) and lower loading ratio. Overflow decreased with increasing underlying soil infiltration rate, with at maximum 5.7% overflow in the 0.02 in/hr underlying soil infiltration rate case for WH Small. For all cases, the portion attributed to evaporation was between 5% - 12%, which is in agreement with a recent study quantifying evaporation from permeable pavement (Brown and Borst 2015).

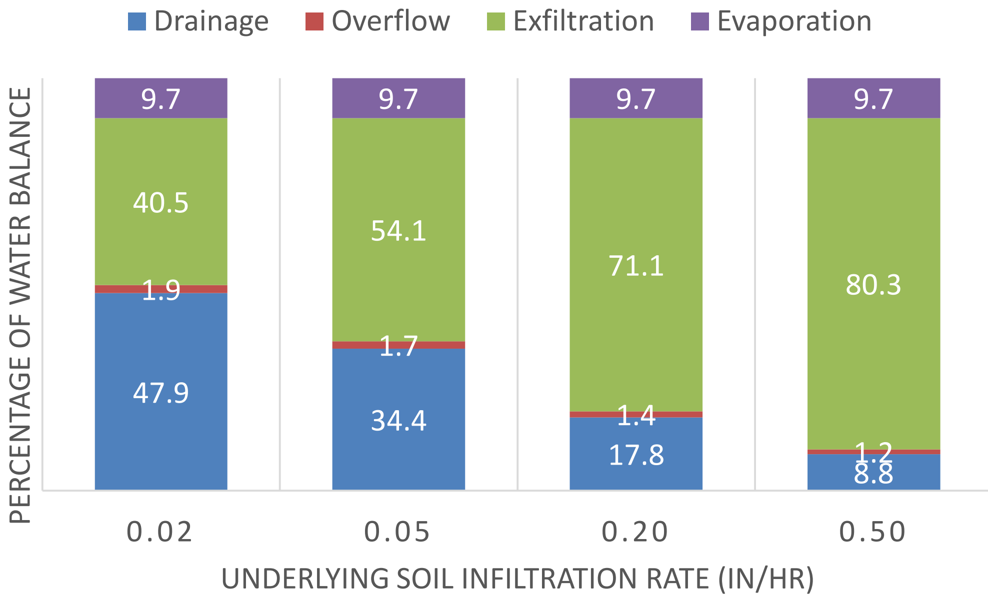

Figure 23. Modeled water balance given different underlying soil infiltration rates for Perkins Township.

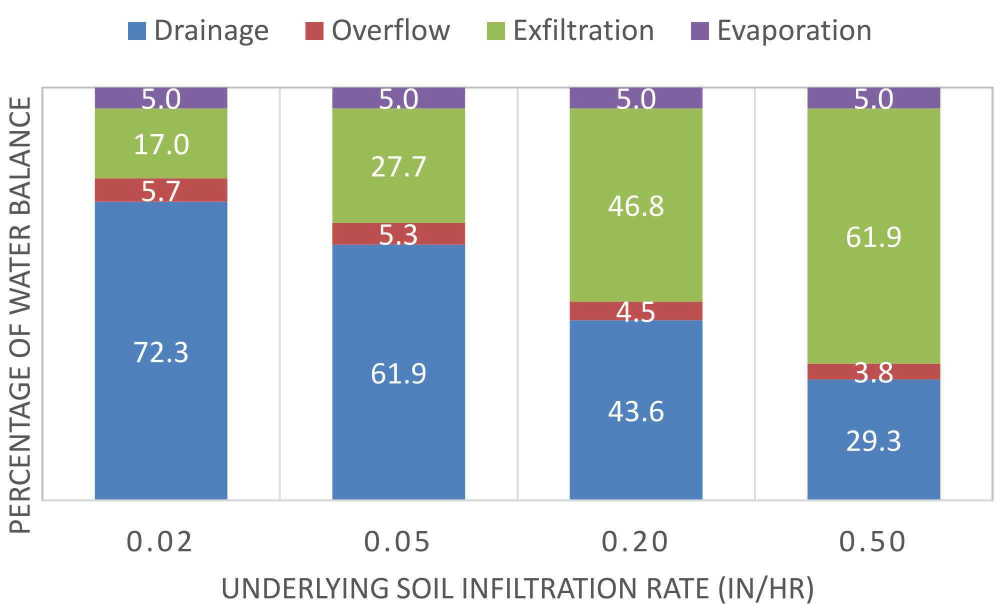

Figure 24. Modeled water balance given different underlying soil infiltration rates for the Willoughby Hills Small application.

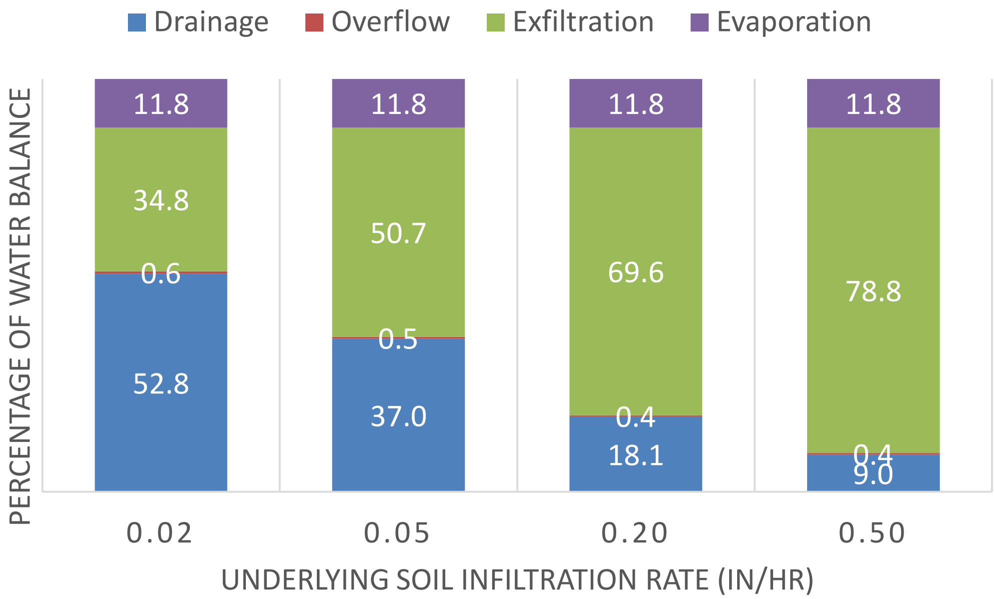

Figure 25. Modeled water balance given different underlying soil infiltration rates for the Willoughby Hills Large application.

4.3.3.1 Pavement + Aggregate Depth

To determine the effect of the aggregate depth on annual hydrology, the total depth of the pavement and aggregate was varied from 9 inches to 36 inches. A minimum depth of 12 inches from the top of the pavement to the top of the internal water storage zone was required as a stipulation for simulations.

The total pavement and aggregate depth had little effect on performance of the systems when the depth of internal water storage remained as designed at 6 inches (Table 31, Table 32, and Table 33). In general, as pavement and aggregate depth increased, overflow decreased and drainage increased, but these effects were not substantial. For typical 2:1 loading ratios used in Ohio, varying aggregate depth changed drainage, overflow, and exfiltration long-term fate by less than 5%. Treating 90% of annual runoff (and thus limiting overflow to 10%) is a common water quality goal for several state-mandated stormwater programs (NCDENR 2009, MDE 2009, PADEP 2006). Overflow was limited to less than 10% for all scenarios except the WH Small site, which had the largest ratio of watershed area to permeable pavement area (7.2:1), which is well above the 2:1 recommended ratio in Ohio (ODNR 2006). When the underlying soil infiltration rate was 0.02 in/hr and aggregate depth was 18 inches, overflow for WH Small was 11%; overflow decreased below the 10% threshold as either infiltration rate or aggregate depth increased. For the WH Large Bay, an 18 inch pavement and aggregate depth limited overflow to less than 1.5% for all soil types. This indicates that an aggregate depth of 18 inches sufficiently treats 90% of annual runoff for the typical Ohio permeable pavement design with 6 inches of internal water storage. While aggregate depth does not affect the long-term water balance appreciably, permeable pavement designs often must consider peak flow mitigation for infrequent storm events, which will be easier to accomplish with additional aggregate depth for water storage.

Table 31. Effect of aggregate depth at Perkins Township for different underlying soil infiltration rates. Watershed area to permeable pavement area remained as designed (3.8:1), and internal water storage was 6 inches.

Pavement + Aggregate Depth (in)	Underlying Soil Infiltration Rate (in/hr)	Annual Fate of Runoff: (in per permeable pavement surface area per year [percent of annual runoff])				
		Runoff	Drainage	Overflow	Exfiltration	Evap.
18	0.02	110	49 [45%]	5 [4.5%]	45 [41%]	11 [9.7%]
24	0.02	110	53 [48%]	2.1 [1.9%]	44 [40%]	11 [9.7%]
36	0.02	110	54 [48%]	0.5 [0.5%]	45 [41%]	11 [9.7%]
18	0.05	110	35 [32%]	4.2 [3.8%]	60 [55%]	11 [9.7%]
24	0.05	110	38 [34%]	1.9 [1.7%]	59 [54%]	11 [9.7%]
36	0.05	110	38 [35%]	0.5 [0.5%]	60 [55%]	11 [9.7%]
18	0.20	110	18 [16%]	3.2 [2.8%]	78 [71%]	11 [9.7%]
24	0.20	110	20 [18%]	1.6 [1.4%]	78 [71%]	11 [9.7%]
36	0.20	110	20 [18%]	0.4 [0.3%]	79 [72%]	11 [9.7%]
18	0.50	110	8.6 [7.8%]	2.4 [2.2%]	88 [80%]	11 [9.7%]
24	0.50	110	9.7 [8.8%]	1.3 [1.2%]	88 [80%]	11 [9.7%]
36	0.50	110	9.9 [9.0%]	0.4 [0.3%]	89 [81%]	11 [9.7%]

Table 32. Effect of aggregate depth at the Willoughby Hills Small Bay for different underlying soil infiltration rates. Watershed area to permeable pavement area remained as designed (7.2:1), and internal water storage was 6 inches.

Aggregate Depth (in)	Underlying Soil Infiltration Rate (in/hr)	Annual Fate of Runoff: (in per permeable pavement surface area per year [percent of annual runoff])				
		Runoff	Drainage	Overflow	Exfiltration	Evap.
18	0.02	213	144 [68%]	23 [11%]	35 [17%]	11 [5%]
24	0.02	213	154 [73%]	12 [5.7%]	36 [17%]	11 [5%]
36	0.02	213	165 [77%]	4.1 [2%]	33 [16%]	11 [5%]
18	0.05	213	124 [58%]	22 [10%]	56 [27%]	11 [5%]
24	0.05	213	132 [62%]	11 [5.3%]	59 [28%]	11 [5%]
36	0.05	213	143 [67%]	3.8 [1.8%]	55 [26%]	11 [5%]
18	0.20	213	88 [41%]	18 [8.5%]	96 [45%]	11 [5%]
24	0.20	213	93 [44%]	9.5 [4.5%]	100 [47%]	11 [5%]
36	0.20	213	103 [49%]	3.4 [1.6%]	96 [45%]	11 [5%]
18	0.50	213	60 [28%]	15 [7.3%]	127 [60%]	11 [5%]
24	0.50	213	63 [29%]	8.0 [3.8%]	131 [62%]	11 [5%]
36	0.50	213	70 [33%]	2.9 [1.3%]	129 [61%]	11 [5%]

Table 33. Effect of aggregate depth at the Willoughby Hills Large Bay for different underlying soil infiltration rates. Watershed area to permeable pavement area remained as designed (2.2:1), and internal water storage was 6 inches.

Aggregate Depth (in)	**Underlying Soil Infiltration Rate (in/hr)**	**Annual Fate of Runoff: (in per permeable pavement surface area per year [percent of annual runoff])**				
		Runoff	**Drainage**	**Overflow**	**Exfiltration**	**Evap.**
18	0.02	91	48 [53%]	1.3 [1.4%]	31 [34%]	11 [12%]
24	0.02	91	48 [53%]	0.5 [0.6%]	31 [35%]	11 [12%]
36	0.02	91	51 [56%]	0.1 [0.1%]	29 [32%]	11 [12%]
18	0.05	91	34 [38%]	1.1 [1.2%]	45 [49%]	11 [12%]
24	0.05	91	34 [37%]	0.4 [0.5%]	46 [51%]	11 [12%]
36	0.05	91	37 [41%]	0.0 [0.0%]	43 [47%]	11 [12%]
18	0.20	91	17 [19%]	0.9 [1.0%]	62 [68%]	11 [12%]
24	0.20	91	16 [18%]	0.4 [0.4%]	64 [70%]	11 [12%]
36	0.20	91	19 [21%]	0.0 [0.0%]	61 [67%]	11 [12%]
18	0.50	91	8.9 [9.8%]	0.8 [0.9%]	70 [78%]	11 [12%]
24	0.50	91	8.1 [9.0%]	0.4 [0.4%]	72 [79%]	11 [12%]
36	0.50	91	10 [11%]	0.0 [0.0%]	70 [77%]	11 [12%]

Total pavement and aggregate depths of 9 inches, 12 inches and 18 inches were also modeled without the inclusion of an IWS zone (Table 34, Table 35, and Table 36). When compared to the IWS zone results, the standard drainage configuration exhibited far more variability in performance as a function of aggregate depth, especially with regard to overflow and drainage. Additionally, the inclusion of an IWS zone in an 18” aggregate depth system increased exfiltration by 9-21% under a 2:1 field ratio. Thus, the inclusion of an IWS zone both improves overall performance and reduces its variability as a function of aggregate depth. At the PT and WH Small applications, a total pavement and aggregate depth of 9 inches (PT and WH Small) and 12 inches (WH Small only) caused overflow to exceed 10% of the long-term water balance regardless of underlying soil infiltration rate. These sites had substantially higher watershed area to permeable pavement area ratios than the 2:1 ratio recommended by the Ohio Rainwater and Land Development Manual (ODNR 2006). For the WH Large site, which has a more typical design of 2.2:1, overflow only exceeded the 10% threshold for an aggregate depth of 9 inches when infiltration rates were less than 0.05 in/hr.

Table 34. Effect of aggregate depth at Perkins Township for different underlying soil infiltration rates. Watershed area to permeable pavement area remained as designed (3.8:1), and there was no internal water storage.

Aggregate Depth (in)	Underlying Soil Infiltration Rate (in/hr)	Annual Fate of Runoff: (in per permeable pavement surface area per year [percent of annual runoff])				
		Runoff	Drainage	Overflow	Exfiltration	Evap.
9	0.02	110	66 [60%]	22 [20%]	11 [10 %]	11 [9.7%]
12	0.02	110	78 [71%]	9.7 [8.8%]	11 [11%]	11 [9.7%]
18	0.02	110	85 [77%]	2.8 [2.6%]	11 [11%]	11 [9.7%]
9	0.05	110	58 [53%]	21 [19%]	20 [19%]	11 [9.7%]
12	0.05	110	69 [62%]	9.3 [8.4%]	21 [19%]	11 [9.7%]
18	0.05	110	75 [68%]	2.7 [2.5%]	21 [20%]	11 [9.7%]
9	0.20	110	40 [37%]	18 [16%]	41 [38%]	11 [9.7%]
12	0.20	110	48 [44%]	7.9 [7.2%]	43 [39%]	11 [9.7%]
18	0.20	110	53 [48%]	2.4 [2.2%]	44 [40%]	11 [9.7%]
9	0.50	110	26 [24%]	14 [13%]	59 [54%]	11 [9.7%]
12	0.50	110	31 [28%]	6.4 [5.8%]	62 [57%]	11 [9.7%]
18	0.50	110	34 [21%]	2.1 [1.9%]	63 [58%]	11 [9.7%]

Table 35. Effect of aggregate depth at the Willoughby Hills Small Bay for different underlying soil infiltration rates. Watershed area to permeable pavement area remained as designed (7.2:1), and there was no internal water storage.

Aggregate Depth (in)	Underlying Soil Infiltration Rate (in/hr)	Annual Fate of Runoff: (in per permeable pavement surface area per year [percent of annual runoff])				
		Runoff	Drainage	Overflow	Exfiltration	Evap.
9	0.02	213	110 [52%]	80 [37%]	12 [5.6%]	11 [5%]
12	0.02	213	143 [67%]	47 [22%]	12 [5.9%]	11 [5%]
18	0.02	213	170 [80%]	19 [9.1%]	13 [6.1%]	11 [5%]
9	0.05	213	102 [49%]	77 [36%]	23 [10%]	11 [5%]
12	0.05	213	133 [62%]	46 [22%]	23 [11%]	11 [5%]
18	0.05	213	159 [75%]	19 [8.9%]	24 [12%]	11 [5%]
9	0.20	213	81 [38%]	72 [34%]	49 [23%]	11 [5%]
12	0.20	213	106 [50%]	42 [20%]	54 [25%]	11 [5%]
18	0.20	213	128 [60%]	17 [8.2%]	57 [27%]	11 [5%]
9	0.50	213	59 [28%]	63 [30%]	80 [37%]	11 [5%]
12	0.50	213	78 [37%]	37 [17%]	87 [41%]	11 [5%]
18	0.50	213	95 [44%]	16 [7.3%]	91 [43%]	11 [5%]

Table 36. Effect of aggregate depth at the Willoughby Hills Large Bay for different underlying soil infiltration rates. Watershed area to permeable pavement area remained as designed (2.2:1), and there was no internal water storage.

Aggregate Depth (in)	Underlying Soil Infiltration Rate (in/hr)	Annual Fate of Runoff: (in per permeable pavement surface area per year [percent of annual runoff])				
		Runoff	Drainage	Overflow	Exfiltration	Evap.
9	0.02	91	58 [64%]	11 [12%]	11 [12%]	11 [12%]
12	0.02	91	65 [71%]	3.9 [4.3%]	11 [13%]	11 [12%]
18	0.02	91	67 [74%]	1.0 [1.1%]	12 [13%]	11 [12%]
9	0.05	91	50 [55%]	10 [11%]	20 [22%]	11 [12%]
12	0.05	91	56 [62%]	3.7 [4.1%]	20 [22%]	11 [12%]
18	0.05	91	59 [65%]	0.9 [1.0%]	20 [23%]	11 [12%]
9	0.20	91	33 [37%]	8.3 [9.1%]	39 [42%]	11 [12%]
12	0.20	91	38 [41%]	3.2 [3.5%]	39 [43%]	11 [12%]
18	0.20	91	39 [43%]	0.9 [0.9%]	40 [44%]	11 [12%]
9	0.50	91	20 [22%]	6.5 [7.2%]	54 [59%]	11 [12%]
12	0.50	91	23 [25%]	2.5 [2.8%]	55 [60%]	11 [12%]
18	0.50	91	24 [26%]	0.8 [0.9%]	55 [61%]	11 [12%]

In all scenarios, aggregate depth had minimal effect on exfiltration and evaporation; however, inclusion of an IWS zone made a substantial impact on exfiltration and evaporation. While a 12 inch pavement depth may be adequate to meet maximum overflow treatment goals for pavements with a low hydraulic loading ratio, structural needs and/or inclusion of an IWS zone can dictate a total pavement and aggregate thickness greater than this (Eisenberg et al. 2015). The differences between different aggregate depths were minimal enough such that there appears to be no substantial hydrologic benefit for aggregate depth to exceed 24 inches, and in most cases, 18 inches of pavement and aggregate will sufficiently meet water quality design goals; greater depths may be needed for peak flow mitigation.

4.3.3.2 Internal Water Storage Zone Depth

It has been shown that increasing IWS zone depth can substantially increase volume reduction in permeable pavements (Wardynski et al. 2012). To quantify this effect for applications typical of northern Ohio, the IWS zone depth was varied between 0, 6, and 12 inches at each location, with the existing pavement + aggregate depth held constant (approximately 24 inches for all three locations). Not unexpectedly, the depth of the internal water storage zone had a substantial effect on the annual hydrology of all three pavements, even though they were located in poorly draining soils, with the most affected forms of outflow being drainage and exfiltration (Table 37, Table 38, and Table 39). Generally, implementing a 12” IWS zone versus a standard drainage configuration increased long-term exfiltration by 25-50%, with greater improvement in poorer soils.

Without an IWS zone, when the underlying soil infiltration rate is 0.02 in/hr, the percent of runoff attributed to exfiltration is less than 15% for all three applications. Increasing the internal water storage to just 6 inches more than doubled the proportion of exfiltration at this low underlying soil infiltration rate. Increasing it further to 12 inches quadrupled the fate of runoff to exfiltration (and consequently reduced drainage volume by at least one-third).

Twelve inch IWS zones maximized volume reduction (combined exfiltration and evaporation) while minimizing drainage and overflow for all three sites and all underlying soil types. However, diminishing marginal returns are observed as underlying infiltration rate increases. An illustration of this at the PT location is given in Figure 26. As infiltration rate increases, the effect of a deeper IWS zone is dampened. Because of this, the greatest impact on increasing IWS depth is in the HSG C infiltration rates (0.05 in/hr, 0.2 in/hr).

Variation in the water balance among the three applications also was a function of the field ratio. Generally, the percentage of exfiltration increased as the permeable pavement surface area increased, due to a larger available footprint for exfiltration. For identical drainage configurations, exfiltration was lowest for the WH Small site when compared to the other two practices due to its augmented hydrologic loading ratio. Despite having different field ratios, the PT and WH Large systems performed similarly, due to the PT site having a greater watershed perviousness, larger effective drain spacing (slower drainage, more exfiltration) as well as an elevated underdrain versus an upturned elbow. The depth of internal water storage had little effect on overflow and evaporation; for all scenarios, overflow remained less than 10%.

Table 37. Effect of IWS zone depth at Perkins Township for different underlying soil infiltration rates. Watershed area to permeable pavement area remained as designed (3.8:1) and aggregate depth was 24 inches.

Internal Water Storage Zone (in)	Underlying Soil Infiltration Rate (in/hr)	Annual Fate of Runoff: (in per permeable pavement surface area per year [percent of annual runoff])				
		Runoff	Drainage	Overflow	Exfiltration	Evap.
0	0.02	110	86 [78%]	1.5 [1.3%]	12 [11%]	11 [9.7%]
6	0.02	110	53 [48%]	2.1 [1.9%]	44 [40%]	11 [9.7%]
12	0.02	110	29 [27%]	4.2 [3.8%]	66 [60%]	11 [9.7%]
0	0.05	110	76 [69%]	1.4 [1.3%]	22 [20%]	11 [9.7%]
6	0.05	110	38 [34%]	1.9 [1.7%]	59 [54%]	11 [9.7%]
12	0.05	110	17 [16%]	3.1 [2.8%]	79 [72%]	11 [9.7%]
0	0.20	110	54 [49%]	1.3 [1.2%]	44 [40%]	11 [9.7%]
6	0.20	110	20 [18%]	1.6 [1.4%]	77 [71%]	11 [9.7%]
12	0.20	110	6.7 [6.1%]	2.1 [1.9%]	80 [82%]	11 [9.7%]
0	0.50	110	34 [31%]	1.2 [1.1%]	64 [58%]	11 [9.7%]
6	0.50	110	9.7 [8.9%]	1.3 [1.2%]	88 [80%]	11 [9.7%]
12	0.50	110	2.6 [2.4%]	1.6 [1.4%]	95 [86%]	11 [9.7%]

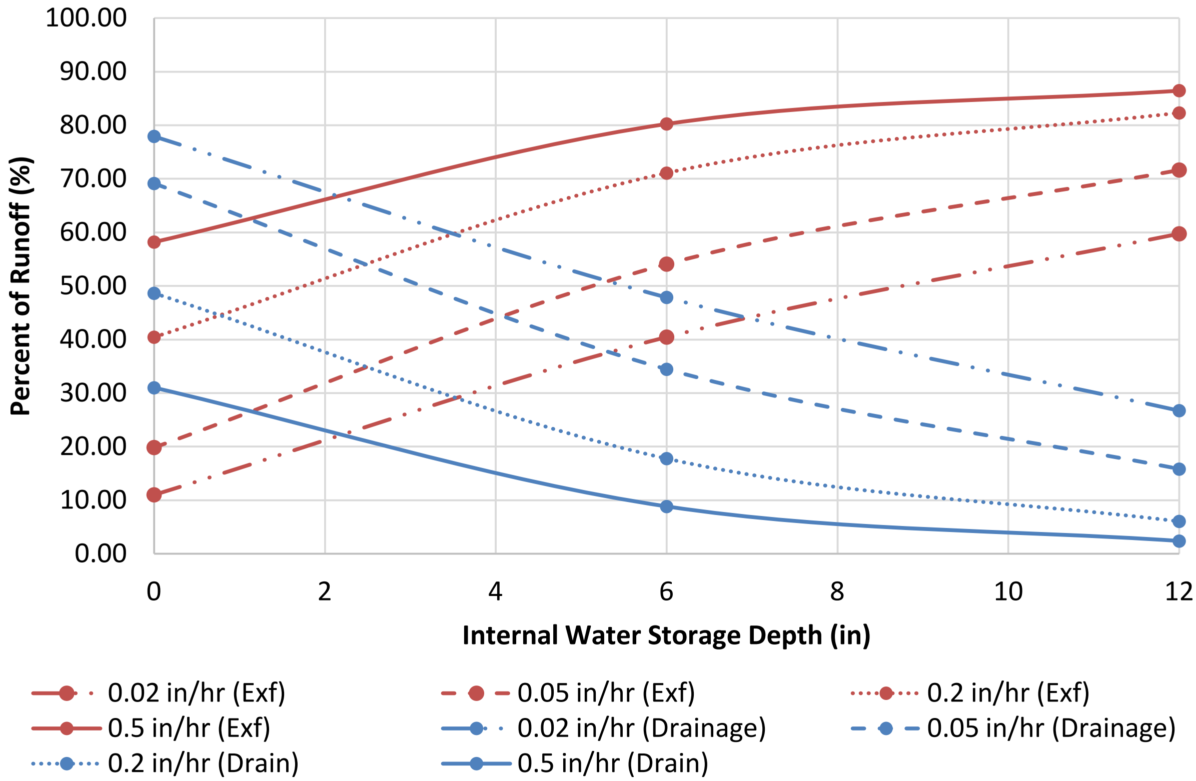

Figure 26. Effect of IWS zone depth on annual hydrology for Perkins Township. Watershed area to permeable pavement area remained as designed (3.8:1) and aggregate depth was 24 inches.

Table 38. Effect of IWS zone depth at Willoughby Hills Small Bay for different underlying soil infiltration rates. Watershed area to permeable pavement area remained as designed (7.2:1) and aggregate depth was 24 inches.

Internal Water Storage Zone (in)	**Underlying Soil Infiltration Rate (in/hr)**	**Annual Fate of Runoff: (in per permeable pavement surface area per year [percent of annual runoff])**				
		Runoff	**Drainage**	**Overflow**	**Exfiltration**	**Evap.**
0	0.02	213	175 [82%]	11 [5.0%]	16 [7.6%]	11 [5%]
6	0.02	213	154 [73%]	12 [5.7%]	36 [17%]	11 [5%]
12	0.02	213	117 [55%]	17 [7.8%]	68 [32%]	11 [5%]
0	0.05	213	163 [76%]	10 [4.9%]	29 [14%]	11 [5%]
6	0.05	213	132 [62%]	11 [5.3%]	59 [28%]	11 [5%]
12	0.05	213	91 [43%]	14 [6.6%]	97 [45%]	11 [5%]
0	0.20	213	129 [61%]	9.5 [4.4%]	64 [30%]	11 [5%]
6	0.20	213	93 [44%]	9.5 [4.5%]	100 [47%]	11 [5%]
12	0.20	213	57 [27%]	11 [5.1%]	134 [63%]	11 [5%]
0	0.50	213	94 [44%]	8.3 [3.8%]	100 [47%]	11 [5%]
6	0.50	213	63 [29%]	8.0 [3.8%]	131 [62%]	11 [5%]
12	0.50	213	36 [17%]	8.6 [4.0%]	157 [74%]	11 [5%]

Table 39. Effect of IWS zone depth at the Willoughby Hills Large Bay for different underlying soil infiltration rates. Watershed area to permeable pavement area remained as designed (2.2:1) and aggregate depth was 24 inches.

Internal Water Storage Zone (in)	Underlying Soil Infiltration Rate (in/hr)	Annual Fate of Runoff: (in per permeable pavement surface area per year [percent of annual runoff])				
		Runoff	Drainage	Overflow	Exfiltration	Evap.
0	0.02	91	65 [72%]	0.4 [0.5%]	15 [15%]	11 [12%]
6	0.02	91	48 [53%]	0.5 [0.6%]	31 [35%]	11 [12%]
12	0.02	91	26 [29%]	0.7 [0.8%]	53 [59%]	11 [12%]
0	0.05	91	55 [61%]	0.4 [0.5%]	25 [27%]	11 [12%]
6	0.05	91	34 [37%]	0.4 [0.5%]	46 [51%]	11 [12%]
12	0.05	91	15 [16%]	0.5 [0.6%]	65 [71%]	11 [12%]
0	0.20	91	36 [39%]	0.4 [0.4%]	44 [48%]	11 [12%]
6	0.20	91	16 [18%]	0.4 [0.4%]	64 [70%]	11 [12%]
12	0.20	91	6.0 [6.6%]	0.4 [0.5%]	74 [81%]	11 [12%]
0	0.50	91	21 [23%]	0.4 [0.4%]	59 [65%]	11 [12%]
6	0.50	91	8.1 [9.0%]	0.4 [0.4%]	72 [79%]	11 [12%]
12	0.50	91	2.8 [3.1%]	0.4 [0.4%]	77 [85%]	11 [12%]

Based on the findings from this portion of the sensitivity analysis, it is recommended at least 6 inches (and preferably 12 inches) of internal water storage be incorporated into permeable pavements to improve volume reduction, even when constructed over poorly-infiltrating soils. Increasing IWS zone depth did marginally increase overflow, especially in the worst soil infiltration rates.

4.3.3.3 Watershed Area to Permeable Pavement Infiltrative Surface Area Ratio

The final variable considered was the ratio of watershed area to permeable pavement infiltrative surface area, or "field ratio." This ratio was varied between 0, 1, 2, and 3, and compared to the existing watershed area to permeable pavement area ratio, while internal water storage remained at the designed 6 inches (Table 40, Table 41, and Table 42). As the field ratio increases, the relative footprint of the permeable pavement compared to its watershed decreases. However the actual footprint, and consequently, the evaporative surface of the pavement, remained the same. Because of this, for systems modeled to receive less run-on, evaporation was a much higher portion of the water balance. The magnitude of evaporation hardly varied between scenarios, but with less runoff being received by the system, its effect on the water balance was larger for lower field ratios. For all three practices, drainage and overflow increased substantially as the field ratio increased and subsequently, exfiltration and evaporation decreased. Higher field ratios also lead to quicker clogging of the pavement surface, which may lead to surface bypass (Winston et al. 2015).

Similarly, it is important to consider the overall interpretation of the water balance when comparing the effect of different field ratios. As the modeled field ratio increased, the percentage of the water balance lost to exfiltration decreased, but the actual *volume* of exfiltration still continued to increase, as did the total treatment area. A careful balance must be struck between maximizing performance while cost-effectively treating a substantial portion of the watershed. For example, at the WH Small application, doubling the field ratio from 1 to 2 only increases drainage by 13% while managing stormwater from twice the area. Depending on the desired volume reduction, engineers and regulators can interpret these results to cost-effectively size permeable pavement systems while maximizing the treated watershed, with consideration that increased watershed size will increase maintenance frequency.

The maximum recommended run-on ratio for Ohio is 2:1 (ODNR 2006). For the WH Small site (which grossly exceeded the recommended Ohio guidelines), reducing the field ratio from 7.2:1 to 2:1 decreased total outflow (drainage + overflow) from 79% to 52% under the most restrictive modeled soil (0.02 in/hr). As the underlying soil infiltration rate increases, increasing and/or decreasing the field ratio is less impactful on the water balance. For example, at the PT site, tripling the field ratio from 1:1 to 3:1 when the underlying soils are more restrictive (0.02 in/hr) resulted in an increase in total outflow of 23%; for an underlying soil with high infiltration rates (0.50 in/hr), total outflow only increased by 6%. This indicates permeable pavement applications constructed over native soils with higher infiltration rates can still provide adequate hydrologic mitigation for field ratios greater than 2:1 if the pavement is maintained accordingly.

Any increase in run-on ratio, however, necessarily increases permeable pavement susceptibility to clogging. This is augmented when the pavement receives shallow concentrated flow due to parking lot islands, speed bumps, etc. (See Chapter 6 of Winston et al. 2015). For these reasons, any increase in run-on ratio from the current 2:1 design guidance should be designed to minimize these impacts. Shorter maintenance intervals and increased maintenance intensity will accompany increasing run-on ratios.

Table 40. Effect of watershed area to permeable pavement surface area ratio at Perkins Township for different underlying soil infiltration rates. Baseline watershed area to permeable pavement area remained as designed (3.8:1) and aggregate depth was 24 inches with a 6 inch internal water storage zone.

Watershed Area to PP Infiltrative Surface Area Ratio	Underlying Soil Infiltration Rate (in/hr)	Annual Fate of Runoff: (in per permeable pavement surface area per year [percent of annual runoff])				
		Runoff	Drainage	Overflow	Exfiltration	Evap.
0	0.02	39	2.2 [5.6%]	0.0 [0.0%]	26 [67%]	11 [28%]
1	0.02	58	12 [21%]	0.1 [0.1%]	35 [60%]	11 [19%]
2	0.02	76	26 [34%]	0.5 [0.6%]	39 [52%]	11 [14%]
3	0.02	94	41 [43%]	1.2 [1.2%]	41 [45%]	11 [11%]
3.8	0.02	110	53 [48%]	2.1 [1.9%]	44 [40%]	11 [9.7%]
0	0.05	39	0.8 [2.0%]	0.0 [0.0%]	27 [70%]	11 [28%]
1	0.05	58	6.4 [11%]	0.0 [0.0%]	41 [70%]	11 [19%]
2	0.05	76	16 [21%]	0.4 [0.5%]	49 [64%]	11 [14%]
3	0.05	94	28 [29%]	1.1 [1.1%]	54 [58%]	11 [11%]
3.8	0.05	110	38 [34%]	1.9 [1.7%]	59 [54%]	11 [9.7%]
0	0.20	39	0.2 [0.5%]	0.0 [0.0%]	28 [72%]	11 [28%]
1	0.20	58	2.1 [3.6%]	0.0 [0.0%]	45 [78%]	11 [19%]
2	0.20	76	6.6 [8.6%]	0.4 [0.5%]	58 [77%]	11 [14%]
3	0.20	94	13 [14%]	0.9 [0.9%]	69 [74%]	11 [11%]
3.8	0.20	110	20 [18%]	1.6 [1.4%]	77 [71%]	11 [9.7%]
0	0.50	39	0.0 [0.2%]	0.0 [0.0%]	28 [72%]	11 [28%]
1	0.50	58	0.8 [1.4%]	0.0 [0.0%]	46 [80%]	11 [19%]
2	0.50	76	2.7 [3.6%]	0.3 [0.4%]	62 [82%]	11 [14%]
3	0.50	94	6.1 [6.4%]	0.8 [0.8%]	76 [82%]	11 [11%]
3.8	0.50	110	9.7 [8.9%]	1.3 [1.2%]	88 [80%]	11 [9.7%]

Table 41. Effect of watershed area to permeable pavement surface area ratio at Willoughby Hills Small Bay for different underlying soil infiltration rates. Baseline watershed area to permeable pavement area remained as designed (7.2:1) and aggregate depth was 24 inches with a 6 inch internal water storage zone.

Watershed Area to PP Infiltrative Surface Area Ratio	**Underlying Soil Infiltration Rate (in/hr)**	**Annual Fate of Runoff: (in per permeable pavement surface area per year [percent of annual runoff])**				
		Runoff	**Drainage**	**Overflow**	**Exfiltration**	**Evap**
0	0.02	39	6.1 [16%]	0.0 [0.0%]	22 [57%]	11 [28%]
1	0.02	63	24 [39%]	0.1 [0.1%]	28 [44%]	11 [17%]
2	0.02	87	45 [52%]	0.4 [0.5%]	31 [35%]	11 [12%]
3	0.02	111	67 [60%]	1.1 [1.0%]	32 [29%]	11 [9.6%]
7.2	0.02	213	154 [73%]	12 [5.7%]	36 [17%]	11 [5.0%]
0	0.05	39	2.4 [6.1%]	0.0 [0.0%]	26 [66%]	11 [28%]
1	0.05	63	15 [23%]	0.0 [0.0%]	37 [60%]	11 [17%]
2	0.05	87	32 [37%]	0.4 [0.4%]	44 [51%]	11 [12%]
3	0.05	111	51 [46%]	0.9 [0.8%]	48 [44%]	11 [9.6%]
7.2	0.05	213	132 [62%]	11 [5.3%]	59 [28%]	11 [5.0%]
0	0.20	39	0.6 [1.5%]	0.0 [0.0%]	27 [71%]	11 [28%]
1	0.20	63	5.9 [9.4%]	0.0 [0.0%]	46 [74%]	11 [17%]
2	0.20	87	16 [18%]	0.3 [0.4%]	60 [69%]	11 [12%]
3	0.20	111	29 [26%]	0.8 [0.7%]	81 [63%]	11 [9.6%]
7.2	0.20	213	93 [44%]	9.5 [4.5%]	100 [47%]	11 [5.0%]
0	0.50	39	0.2 [0.6%]	0.0 [0.0%]	28 [72%]	11 [28%]
1	0.50	63	2.6 [4.2%]	0.0 [0.0%]	49 [79%]	11 [17%]
2	0.50	87	8.2 [9.4%]	0.3 [0.3%]	68 [78%]	11 [12%]
3	0.50	111	16 [15%]	0.7 [0.7%]	83 [75%]	11 [9.6%]
7.2	0.50	213	63 [29%]	8.0 [3.8%]	131 [62%]	11 [5.0%]

Table 42. Effect of watershed area to permeable pavement surface area ratio at Willoughby Hills Large Bay for different underlying soil infiltration rates. Baseline watershed area to permeable pavement area remained as designed (2.2:1) and aggregate depth was 24 inches with a 6 inch internal water storage zone.

Watershed Area to PP Infiltrative Surface Area Ratio	Underlying Soil Infiltration Rate (in/hr)	Annual Fate of Runoff: (in per permeable pavement surface area per year [percent of annual runoff])				
		Runoff	Drainage	Overflow	Exfiltration	Evap.
0	0.02	39	5.9 [15%]	0.0 [0.0%]	22 [57%]	11 [28%]
1	0.02	63	24 [38%]	0.1 [0.1%]	28 [44%]	11 [17%]
2	0.02	87	45 [51%]	0.5 [0.5%]	31 [36%]	11 [12%]
2.2	0.02	91	48 [53%]	0.5 [0.6%]	32 [35%]	11 [12%]
3	0.02	111	66 [59%]	1.2 [1.0%]	33 [30%]	11 [9.6%]
0	0.05	39	2.2 [5.8%]	0.0 [0.0%]	26 [67%]	11 [28%]
1	0.05	63	14 [23%]	0.0 [0.0%]	38 [60%]	11 [17%]
2	0.05	87	31 [35%]	0.4 [0.4%]	45 [52%]	11 [12%]
2.2	0.05	91	34 [37%]	0.4 [0.5%]	46 [51%]	11 [12%]
3	0.05	111	50 [45%]	1.0 [0.9%]	49 [45%]	11 [9.6%]
0	0.20	39	0.5 [1.4%]	0.0 [0.0%]	28 [71%]	11 [28%]
1	0.20	63	5.4 [8.6%]	0.0 [0.0%]	47 [74%]	11 [17%]
2	0.20	87	15 [17%]	0.3 [0.4%]	61 [70%]	11 [12%]
2.2	0.20	91	16 [18%]	0.4 [0.4%]	64 [70%]	11 [12%]
3	0.20	111	27 [24%]	0.9 [0.8%]	72 [65%]	11 [9.6%]
0	0.50	39	0.2 [0.5%]	0.0 [0.0%]	28 [72%]	11 [28%]
1	0.50	63	2.3 [3.6%]	0.0 [0.0%]	50 [79%]	11 [17%]
2	0.50	87	7.2 [8.2%]	0.3 [0.3%]	69 [79%]	11 [12%]
2.2	0.50	91	8.1 [9.0%]	0.4 [0.4%]	72 [79%]	11 [12%]
3	0.50	111	14 [13%]	0.8 [0.7%]	85 [77%]	11 [9.6%]

By far, the infiltration rate of the native soil had the greatest effect on annual hydrology and largely controlled the water balance. For the state standard design of a 2:1 run-on ratio, total volume reduction via exfiltration and evaporation varied from 47-96% depending on the hydraulic conductivity of the underlying soil, and overflow was limited to less than 1%. The inclusion of an IWS zone also was shown to substantially increase exfiltration, sometimes by as much as 50% of the overall water balance. Results from this sensitivity analysis can be used by engineers to cater design specifications to reach a desired goal (e.g., targeted volume reduction, limit surface runoff, minimize drainage, etc.).

4.3.4 Permeable Pavement Performance under Climate Change Scenarios

4.3.4.1 Climate Data Summary

Three climate scenarios were developed for this work, each containing 4 or 5 years of data. The baseline model was created based on modeled 2001-2004 data for each location. The other two climate scenarios were developed from 2055-2059 using data from two of the Intergovernmental Panel on Climate Change (IPCC) Representative Concentration Pathways (RCP 4.5 and RCP 8.5). For comparison of measured and modeled baseline data, precipitation data were obtained from Old Woman Creek National Estuarine Research Reserve [12 miles from PT] (NOAA 2015b) and Cleveland Hopkins airport [31 miles from WH] (NOAA 2015a) over this time period, similar to the approach taken in Gao et al. (2012). For the baseline scenario, the average modeled annual rainfall for 2001-2004 was 34.1 inches (range 29.3-38.0) at PT and 40.4 inches (range 34.5-45.5) at WH. During the same time period, Old Woman Creek recorded an average of 33.1 inches (range 30.4-35.0) and Cleveland Hopkins airport recorded on average 38.2 inches (range 34.4-42.5) of rainfall per year (NOAA 2015a, NOAA 2015b) (Table 43). The model overestimated average yearly rainfall for the two sites by less than 2.2 inches, but had comparable median and 90th percentile event depths. The median and 90th percentile consecutive dry days were also similar between the modeled and observed data. From this analysis, the modeled baseline climate data was judged comparable to observed data.

Table 43. Comparison of modeled (Perkins Township, Willoughby Hills) and measured annual rainfall (Old Woman Creek, Cleveland Hopkins).

Year	Perkins Township	Old Woman Creek	Willoughby Hills	Cleveland Hopkins
	Modeled	Measured[a]	Modeled	Measured
2001	37.7	-	42.3	34.4
2002	31.5	30.4	34.5	36.4
2003	29.3	-	39.2	42.5
2004	38.0	35.8	45.5	39.4
Average	34.1	33.1	40.4	38.2

[a]Data unavailable for 2001 and 2003.

Summary statistics of the climate change scenarios (RCP 4.5 and RCP 8.5) are displayed in Table 44. Discrete hydrologic storm events were identified by a gap in precipitation exceeding six hours and a minimum rainfall depth of 0.1 inches (Driscoll, 1989). At both locations, the baseline model had higher annual precipitation and lower mean daily temperatures (by 3 – 5 °F) than the future climate scenarios. At PT, the mean precipitation depth, maximum precipitation depth, and 90th percentile storm event under RCP 4.5 and RCP 8.5 increased from the baseline. At WH, the mean, maximum and 90th percentile precipitation depths decreased, demonstrating the geographical variability of future climate predictions between the two sites. Consecutive dry days statistics increased in future climate scenarios for both measures of central tendency and extreme cases at both sites.

Table 44. Precipitation and temperature summary statistics for Perkins Township and Willoughby Hills under all climate scenarios.

Parameter	Statistic	Perkins Township			Willoughby Hills		
		Baseline	RCP 4.5	RCP 8.5	Baseline	RCP 4.5	RCP 8.5
Consecutive dry days	Maximum	33.1	53.7	36.8	35.7	51.4	32.4
	90th percentile	11.7	12.5	13.7	10.7	12.1	12.1
	Mean	5.4	6.0	5.9	4.8	5.2	5.2
	Median	4.0	4.1	3.7	3.4	3.4	3.5
	St. Dev	5.1	7.1	6.2	5.1	6.0	5.5
Storm Event Summary	Annual avg. rainfall (in)	34.13	33.86	33.46	40.39	34.25	35.43
	Max (in)	3.29	5.65	5.92	4.45	4.37	4.10
	90th percentile (in)	1.28	1.47	1.39	1.37	1.26	1.27
	Mean (in)	0.57	0.62	0.60	0.60	0.56	0.58
	Median (in)	0.40	0.38	0.33	0.43	0.35	0.34
	St. Dev. (in)	0.52	0.73	0.73	0.60	0.59	0.64
Temperature	Mean (°F)	51.9	55.2	56.3	52.2	55.4	56.5
	Median (°F)	54.7	58.2	59.1	54.0	57.4	59.0
	St. Dev (°F)	20.1	19.8	20.8	19.1	19.2	20.3
	Max. daily average (°F)	86.9	88.9	91.1	87.5	90.4	94.0
	Min. daily average (°F)	-16.6	-19.4	-13.0	-5.5	-9.4	-1.9

4.3.4.2 Hydrologic Balance Summary

DRAINMOD generated a complete water balance for each climate scenario, including stormwater runoff entering the permeable pavement (runoff), stormwater bypassing the permeable pavement as surface runoff (overflow), stormwater infiltrating into the native soils (exfiltration) and runoff removed via evaporation (evaporation). These are presented for both sites in Table 45. The depth percent difference for each hydrologic fate was calculated as:

$$\frac{Depth_{RCP} - Depth_{Base}}{Depth_{Base}} * 100 \tag{4.5}$$

Differences in the water balance among the baseline and future climate scenarios were calculated as (with the given example for drainage):

$$\%Drain_{RCP} - \%Drain_{Base} \tag{4.6}$$

At PT, the changes in the overall water balance between the baseline and climate change scenarios were relatively modest. No water fate (e.g., drainage, evaporation) varied by more than 10 percent from baseline to climate change scenario. Climate change caused a slight increase in annual runoff depths and a substantial increase in mean daily temperature. This in turn caused an increase in drainage, overflow and evaporation depths. Comparing the climate change scenario water balances to the baseline, a slight increase in the percentage of runoff leaving as drainage and evaporation was modeled (1%), whereas overflow more substantially increased (5-6%) and exfiltration decreased (8-9%). Increases of the maximum and 90th percentile storm event from the baseline likely overwhelmed the storage capacity and drainage rate of the permeable pavement during large, infrequent events, causing more overflow; increases in overflow combined with increased evaporation caused the marked decrease in exfiltration. Increases in overflow are of most concern, as this runoff bypasses treatment by the permeable pavement. Under the climate change scenarios analyzed, overflow depths increased by 254-352% but were still relatively low and less than 10% of the overall water balance. Overall, volume reduction as a percentage of inflow was 52.4% under the base case scenario, this decreased to 45.1% and 46.1% under RCP 4.5 and 8.5 respectively. These results are a function of the change in extreme rainfall depths (maximum, 90th percentile), as the future climate change scenarios had similar measures of annual rainfall and central tendency from the baseline.

At the WH location, climate change caused a decrease in annual runoff depths of approximately 15-20%, which in turn caused decreases in runoff depths for drainage (16-25%), overflow (13-64%), and exfiltration (9-14%). Evaporation depths increased 4-12% due to the increase in mean daily temperature. Changes in the overall water balance between the baseline and climate change scenarios at WH were relatively moderate, with no water fate varying by more than 6 percent. Comparing the climate change scenario water balances to the baseline, a decrease in the percentage of runoff leaving as drainage was modeled (1-6%); overflow decreased or stayed the same (0-1%), exfiltration increased or stayed the same (0-1%), and evaporation increased (1-4%). Because average and extreme precipitation depths remained similar between baseline and climate change scenarios the effect on the water balance (specifically overflow and exfiltration) was not as pronounced as at PT. Overall, volume reduction as a percentage of inflow was 13.3% and 30.6% under the base case scenario for the WH Small and Large applications, respectively; this increased to 14.8 – 16.0% and 33.2 – 35.9% under future climate scenarios. This is attributed to the expected increase in evaporation volumes and decrease in overflow volumes due to diminished maximum and 90th percentile event depths.

The future climate modeling suggested volume mitigation provided by permeable pavements in northern Ohio will in some cases be slightly better than current performance (by 2-5% at WH) and in some cases be slightly worse (by 6-7% at PT). Overflow as a percentage of total inflow to the permeable pavement cells increased at PT and decreased at WH, as did total outflow. This is due to the spatial variability of rainfall and temperature data under future climate scenarios for the two sites; PT is expected to see increased extreme precipitation, whereas WH is expected to see lower annual rainfall depths and generally smaller median and extreme rainfall depths. Evaporation increased in all modeled permeable pavements under future climate due to elevated temperatures and protracted periods of consecutive dry days.

Table 45. Average annual water balances for each site scenario and climate profile – depths in terms of inches over the permeable pavement area.

Site	Climate Scenario	Runoff	Drainage				Overflow				Exfiltration				Evaporation			
		Depth (in)	Depth (in)	% diff. Depth	% of Runoff	diff. Water Balance	Depth (in)	% diff. Depth	% of Runoff	diff. Water Balance	Depth (in)	diff. Water Balance	% of Runoff	% diff. Depth	Depth (in)	diff. Water Balance	% of Runoff	% diff. Depth
Perkins Township	Base	94.8	43.3	-	46	-	1.8	-	2	-	39.5	-	42	-	10.2	-	11	-
	RCP 4.5	97.9	45.6	5	47	1	8.1	352	8	6	32	-9	33	-19	12.2	1	12	19
	RCP 8.5	95.8	45.2	4	47	1	6.4	254	7	5	33	-8	34	-16	11.1	1	12	9
Willoughby Hills Small	Base	224.6	174	-	77	-	20.7	-	9	-	18.9	-	8	-	11	-	5	-
	RCP 4.5	180.1	135.9	-22	75	-2	15.4	-26	9	0	16.5	1	9	-12	12.3	2	7	12
	RCP 8.5	193.3	146.4	-16	76	-1	18.3	-12	9	0	17.1	1	9	-9	11.4	1	6	4
Willoughby Hills Large	Base	94.7	65.1	-	69	-	0.7	-	1	-	17.9	-	19	-	11	-	12	-
	RCP 4.5	77.2	48.9	-25	63	-6	0.6	-13	1	0	15.4	1	20	-14	12.3	4	16	12
	RCP 8.5	81.9	54.5	-16	67	-2	0.2	-64	0	-1	15.8	0	19	-12	11.4	2	14	4

4.4 Conclusions

Permeable pavements are one of the most popular SCMs implemented for hydrologic mitigation, but their performance is highly dependent on underlying soil type and design specifications. DRAINMOD was used to simulate hydrologic performance of three permeable pavement systems in northern Ohio. Each of the sites was monitored for at least one year. Results indicate DRAINMOD can be applied to predict the water balance of permeable pavements on a long-term, continuous basis. Outputs included volumes of groundwater recharge (exfiltration), treated outflow (drainage), untreated bypass (overflow), and volume reduction through exfiltration and evaporation. The results are valuable for estimating pollutant loads to meet Total Maximum Daily Load (TMDL) requirements. Long-term volume mitigation can also be used to evaluate whether a site meets the pre-development hydrologic condition.

DRAINMOD accurately predicted runoff volumes from drainage areas that varied both in percent imperviousness and field ratio. Nash-Sutcliffe efficiencies exceeded 0.94 for the prediction of inflow during calibration and validation of all three sites, including when an innovative method was used to account for surface runoff (i.e. runoff bypassing the permeable pavement due to clogging) occurring at the WH Large application. Excellent agreement between predicted and measured drainage was observed, with Nash-Sutcliffe efficiencies ranging from 0.82-0.95. Modeled and measured agreement of exfiltration and evaporation volumes was more varied, with NSE ranging from 0.15-0.77; this is partially due to the low exfiltration rates and therefore very small magnitude of exfiltration volumes that occurred. Despite this event-by-event variability, the total volumes of exfiltration and evaporation were predicted to within 6% of the measured volumes at both the PT and WH Small applications. For the WH Large application, the cumulative exfiltration and evaporation volume was within 20% of what was measured; this greater error was due to greater pavement surface clogging (Winston et al. 2015), a factor which DRAINMOD is unable to account for. During the calibration and validation periods, cumulative predicted drainage volume was within 5% for PT, and 11% for both WH applications.

The benefit of a calibrated, continuous, long-term model is the opportunity for designers and regulators to establish performance expectations for permeable pavements given site-specific characteristics. By modeling a variety of different drainage configurations, aggregate depths, and field ratios, DRAINMOD can be used to evaluate the hydrologic performance of a variety of permeable pavement design configurations. The model can also be used by designers and regulators to target a desired hydrologic goal (e.g., 80% volume reduction, 10% overflow, pre-development hydrology, etc.).

Results from the sensitivity analysis show for permeable pavements with field ratios greater than 2:1, more than 10% of the water balance will overflow and remain untreated when the total cross-section depth is less than 12 inches. Increasing this depth to 18 or 24 inches limited overflow while maximizing other hydrologic benefits; increasing aggregate depth further to 36 inches created little appreciable volume reduction benefit. Including an IWS zone substantially reduced total outflow for all soil types. The impact was greatest when underlying soils had lower hydraulic conductivities, but even the highest underlying soil infiltration rate modeled (0.5 in/hr) saw marked improvement in volume reduction as IWS zone depth increased. Current Ohio design standards restrict the run-on ratio to 2:1; for scenarios with less restrictive soils, increasing the run-on ratio provided adequate (and potentially more cost-effective) hydrologic mitigation, but this is at the risk of increased likelihood of clogging. Designers and regulators must weigh this decreased cost with the long-term cost of increased frequency and difficulty of maintenance. Results from the sensitivity analysis will best be utilized to evaluate volume reduction for various permeable pavements applications and thus move away from a "one size fits all" design and crediting approach.

Permeable pavement performance for baseline and future climate scenarios were analyzed by simulating the three calibrated models with high-resolution dynamically downscaled climate data. For PT, the future climate data resulted in similar annual rainfall with greater mean, median, and extreme rainfall depths. At WH, the future climate data resulted in less rainfall and longer periods of consecutive dry days. Because of this, the fraction of the overall water balance represented by overflow was predicted to increase by up to 6% for PT and stay the same or decrease for Willoughby Hills. Due to warmer air temperatures predicted for the future, evaporation volumes increased by 4-19% from the permeable pavements. Otherwise, future climate scenarios did not substantially affect the overall water balance, with drainage, overflow, exfiltration, and evaporation each varying by less than 10% from the current climate under RCP 4.5 and 8.5. The fraction of volume reduction is expected to remain similar to the present climate, with a range of -7% to 5% change.

4.5 References

American Society for Testing and Materials (ASTM). (2009). *Standard test method for infiltration rate of in place pervious concrete*. ASTM C1701/C1701M-09.

American Society for Testing and Materials (ASTM). (2013). *Standard test method for surface infiltration rate of permeable unit pavement systems.* C1781/C1781M-13.

Brown, R.A. (2011). *Evaluation of bioretention hydrology and pollutant removal in the upper coastal plain of North Carolina with development of a bioretention modeling application in DRAINMOD*. Ph.D. Dissertation, North Carolina State University, Raleigh, NC. <http:// repository.lib.ncsu.edu/ir/bitstream/1840.16/6783/1/etd.pdf>.

Brown, R. A., and Borst, M. (2015). "Quantifying evaporation in a permeable pavement system." *Hydrological Processes*, 29(9), 2100-2011.

Driscoll, E. (1989). *Analysis of Storm Event Characteristics for Selected Rainfall Gages Throughout the United States: Draft.* US Environmental Protection Agency, 1989.

Eisenberg, B.E., Lindow, K.C., Smith, D.R. (2015). *Permeable Pavements*, 1st Ed., American Society of Engineers, Reston, VA.

Gao, Y., Fu, J.S., Drake, J.B., Liu, Y., & Lamarque, J.F. (2012). "Projected changes of extreme weather events in the eastern United States based on a high resolution climate modeling system." *Environmental Research Letters*. 7(4), 044025.

Hathaway, J.M., Brown, R.A., Fu, J.S., & Hunt, W.F. (2014). "Bioretention function under climate change scenarios in North Carolina, USA." *Journal of Hydrology*, *519*, 503-511.

Jain, S.K., and Sudheer, K.P. (2008). "Fitting of hydrologic models: a close look at the Nash-Sutcliffe Index." *Journal of Hydrologic Engineering*, 13(10), 981-986

MDE (Maryland Department of the Environment) (2009). *Maryland stormwater design manual*,.Water Management Administration, Baltimore, MD.

McCuen, R.H., Knight, Z., Cutter, A.G. (2006). "Evaluation of the Nash-Sutcliffe Efficiency Index." *Journal of Hydrologic Engineering*, 11(6), 597-602.

Montes, F., and Haselbach, L. (2006). "Measuring hydraulic conductivity in pervious concrete." *Environmental Engineering Science*, 23(6), 960-969.

Nash, J.E., and Sutcliffe, J.V. (1970). "River flow forecasting through conceptual models part 1 – A discussion of principles." *Journal of Hydrology*, 10(3), 282-290.

National Oceanic and Atmospheric Administration (NOAA). (2015a). *National climatic data center, U.S. local climatological data*. Cleveland, OH airport. Available: http://www.ncdc.noaa.gov/

National Oceanic and Atmospheric Administration (NOAA). (2015b). *National estuarine research reserve system, Centralized data management office*. Old Woman Creek National Estuarine Research Reserve. Available: http://cdmo.baruch.sc.edu/

Natural Resources Conservation Service (NRCS). (1986). *Urban hydrology for small watersheds*. Technical Release 55 (TR-55). 2nd edition. United States Department of Agriculture (USDA), Natural Resources Conservation Service, Conservation Engineering Division.

Natural Resource Conservation Service (NCRS). (2004). "Estimation of direct runoff from storm rainfall." *Hydrology: National engineering handbook*, Chapter 10, Part 360, Washington, DC.

NCDENR (North Carolina Department of Environment and Natural Resources) (2009). *Stormwater best management practices manual*. Div. of Water Quality, Raleigh, NC.

Ohio Department of Natural Resources (ODNR), Division of Soil and Water Conservation. (2006). *Rainwater and land development: Ohio's standards for stormwater management, low impact development, and urban stream protection*. 3rd edition. Ed: John Mathews.

PADEP (Pennsylvania Department of Environmental Protection) (2006). *Pennsylvania stormwater best management practices manual*. Bureau of Waterways Engineering and Wetlands, Harrisburg, PA.

Saltelli, A. (2002). "Sensitivity analysis for importance assessment." *Risk Analysis.* 22(3), 579-590.

Starke, P., Göbel, P., and Coldewey, W.G. (2010). "Urban evaporation rates from water-permeable pavements." *Water Science and Technology*, 62(5), 1161-1169.

Winston, R.J., Dorsey, J.D., and Hunt, W.F. (2015). *Monitoring the performance of bioretention and permeable pavement stormwater controls in Northern Ohio: Hydrology, water quality, and maintenance needs*. Final Report Submitted to the University of New Hampshire and the Chagrin River Watershed Partners. In Fulfilment of NOAA Award number NA09NOS4190153.

Wardynski, B. J., Winston, R. J., & Hunt, W. F. (2012). "Internal water storage enhances exfiltration and thermal load reduction from permeable pavement in the North Carolina mountains." *Journal of Environmental Engineering*, 139(2), 187-195.

Zhang, S. and Guo, Y. (2014). "SWMM Simulation of the Storm Water Volume Control Performance of Permeable Pavement Systems." *Journal of Hydrologic Engineering*, 06014010.

5 SUMMARY AND CONCLUSIONS

Design engineers and regulators currently work within a rigid framework for design and crediting of permeable pavements and bioretention cells. Designs must "fit the mold" and meet all technical specifications outlined in the state stormwater manual. There are many situations where this one-size-fits-all design may not produce the best results or may preclude the use of these SCMs, such as in design of SCM retrofits. A more flexible design and crediting mechanism is needed for these systems, so designers have the ability to choose from a menu of design parameters and receive appropriate credit.

To do so, long-term models are needed to simulate the hydrologic performance of bioretention and permeable pavement SCMs, as field-monitoring of every design scenario is not economically feasible. In this work, the agricultural drainage and water balance model DRAINMOD was adapted for use in modeling urban stormwater practices, namely bioretention and permeable pavement. Many inputs for agricultural drainage have counterparts in these SCMs – underdrains, soils, plants, surface storage, deep seepage (i.e. exfiltration), *et cetera*. The model was calibrated and validated against field-collected hydrologic data from three permeable pavements and three bioretention cells in Northern Ohio.

Excellent model fit to runoff from the mostly impervious watersheds was made possible by "tricking" the model through wide drain spacing, low infiltration parameters for Green & Ampt, and small surface storage. Nash-Sutcliffe efficiencies for inflow were in all cases 0.94 or greater. Uncertainty in modeled inflow increased with the percentage of pervious area. Following calibration of inflow, SCM simulations were run for both bioretention cells and permeable pavement, with generally good to excellent agreement between modeled and monitored hydrologic fate. Validation period NSEs varied from 0.86-0.98 for drainage, 0.73-

0.90 for overflow, and 0.71-0.96 for exfiltration/ET for the three modeled bioretention cells. Similarly, validation period NSEs varied from 0.82-0.95 for drainage and 0.19-0.78 for exfiltration/evaporation for the three modeled permeable pavements; individual storm event comparisons between modeled and measured overflow could not be made due to lack of observed or measured overflow. Over the period of data collection, the modeled and monitored percentage of drainage, overflow, and exfiltration/ET never diverged by more than 3% for the three bioretention cells. For the three monitored permeable pavements, the difference between the modeled and monitored water balance was within 4%. These results suggested DRAINMOD is an excellent tool for analysis of long-term bioretention and permeable pavement hydrology.

Sensitivity analyses were conducted using DRAINMOD by modifying design parameters one-at-a-time. The bioretention models were most sensitive to hydraulic loading ratio and IWS zone depth, which modified the fraction of drainage and exfiltration by 20% or more. DRAINMOD was moderately sensitive to bowl storage depth and was least sensitive to rooting depth and media depth. The permeable pavement models were also most sensitive to hydraulic loading ratio and IWS with wide variations in performance depending on underlying soil type; the model was less sensitive to aggregate depth. The results of the sensitivity analyses could be used to create a "sliding scale" crediting system for both bioretention cells and permeable pavments in Ohio based on the fractions of treated drainage and volume reduction through exfiltration and ET.

Rainfall and temperature data derived from dynamically downscaled future climate data were used to represent both existing (2001-2004) and future (2055-2059) climate scenarios for Northern Ohio. Generally, future climate scenarios suggested lower annual average rainfall depths, longer dry periods, and hotter temperatures for Northern Ohio. This resulted in increased in evapotranspiration in all bioretention and permeable pavement future climate modeling runs. For the three bioretention cells, the volume reductions provided by the SCMs changed from -6% to 8% under future climate conditions, suggesting that these systems will reduce runoff volume by about the same rate as under current climate scenarios. Similarly, for the permeable pavement applications, the volume reduction under future scenarios changed from -7% to 5% as compared to current climate scenarios. The fraction of overflow increased in nearly every bioretention future climate model as well as the Perkins Township permeable pavement future climate model, suggesting the fraction of untreated bypass could increase from SCM under mid-century climate. Overall, current designs may need to be modified only slightly to be resilient to climate change along the Northern Ohio Lake Erie shoreline.

6 ACKNOWLEDGEMENTS AND DISCLAIMER

This material is based upon work supported by the University of New Hampshire under Cooperative Agreement No. NA09NOS4190153 (CFDA No. 11.419) from the National Oceanic and Atmospheric Association. Financial assistance was also provided under award number DNRFP038 from the National Oceanic and Atmospheric Administration, U.S. Department of Commerce through the Old Woman Creek National Estuarine Research Reserve, administered by the Ohio Department of Natural Resources, Division of Wildlife. The Old Woman Creek National Estuarine Research Reserve is part of the National Estuarine Research Reserve System, (NERRS), established by Section 315 of the Coastal Zone Management Act, as amended. Additional information about the system can be obtained from the Estuarine Reserves Division, Office of Ocean and Coastal Resource Management, National Oceanic and Atmospheric Administration, US Department of Commerce, 1305 East West Highway – N/ORM5, Silver Spring, MD 20910. Any opinions, findings, and conclusions or recommendations expressed in this publication are those of the author(s) and do not necessarily reflect the views of the University of New Hampshire or the National Oceanic and Atmospheric Association.

The authors wish to thank the Chagrin River Watershed Partners, Ohio Department of Natural Resources (DNR), and the Old Woman Creek National Estuarine Research Reserve staff for their support throughout this modeling effort. The financial support of ODNR and OWC NERR grants to obtain the future climate data from the University of Tennessee/Oak Ridge National Laboratory is gratefully acknowledged. Drs. Jon Hathaway and Joshua Fu at the University of Tennessee are appreciated for coordination and provision of future climate data for this work.